

CHAPTER 36. SOLAR ENERGY USE

THE sun radiates considerable energy onto the earth. The desire to put that relatively low-intensity (rarely over 300 Btu/h · ft²) energy to work has led to the creation of many types of devices to convert that energy into useful forms, mainly heat and electricity. Economic valuing of that energy drives the ebb and flow of the global solar industry. This chapter discusses several different types of solar equipment and system designs for various HVAC applications, as well as methods to determine the availability of the solar resource. Further information such as solar radiation is included in [Chapters 14](#) and [15 of the 2021 ASHRAE Handbook—Fundamentals](#).

Worldwide, solar energy use varies in application and degree. In China and, to a lesser extent, Australasia, solar energy is widely used for electric power generation and solar thermal. Solar districts are also gaining popularity with the advent of 100% renewable heating and cooling (Lund 2014). In the Middle East, solar power is used for desalination and absorption air conditioning. In its earlier days, solar energy use in the United States was modest, mainly driven by tax policies and utility programs that generally react to energy shortages or oil prices. Today, however, many states are driving for solar power, solar heating, and sometimes solar cooling with the main motive of environmental concerns and global warming. For example, the state of California initiated the California Solar Initiative (CSI; CPUC 2020), which has a goal of transforming to 100 percent clean electric power by 2045. In 2020, solar PV and solar thermal power plants produced 29,440 GWh of energy or 15.42 percent of California's in-state generation portfolio. There are 770 operating solar power plants alone, with an installed capacity of about 13,989 MW.

In Europe, government incentives have fostered the use of photovoltaic and thermal systems for both domestic hot water and space heating (**solar combi systems**), which have a well-established market in several countries, and solar cooling is an emerging market with significant growth potential, driven by the fact that cooling loads will surpass the heating loads by 2070 (Hunt et al. 2020). Combined solar space heating/cooling and domestic hot water production (**solar combi-plus systems**) may lead to both high solar fractions and economic systems because of the continuous (annual) exploitation of the solar collector field and other system components.

Recent interest in sustainability, decarbonization, green buildings, passive buildings, nearly-zero carbon buildings, and net-zero energy buildings has led to an increased focus on solar energy systems and equipment, being free from direct emissions, renewable, and locally available, although interrupted (IPCC 2011). This interrupted nature often requires thermal and electrical storage of various forms. However, solar energy is considered one of the strongest instruments against global warming (IPCC 2012). Besides its embodied energy quantity and quality, embodied material, and production emissions, it offers clean power and heat and could largely replace fossil fuels. Solar energy is practically free from direct emissions, which lately has also shown a relationship between pandemics and air pollution (Kilkis 2021). However, like all other energy conversion systems, solar energy systems are still responsible for indirect emissions since they cannot utilize the entire quality of energy.

For more information on the use of solar and other energy sources, see the Energy Information Administration (EIA) of the U.S. Department of Energy (www.eia.gov) and the International Energy Agency (www.iea.org).

1. QUANTITY AND QUALITY OF SOLAR ENERGY

This section deals with the amount of solar energy, or solar intensity (solar power per unit area), according to the first law of thermodynamics. The second law of thermodynamics defines the **useful work potential (unit exergy)** or the quality of solar energy (ability to do useful work), which is a function of the solar intensity compared to the total solar intensity.

Total Solar Intensity TSI

This term, also known as the **solar constant**, is not a constant value, but changes seasonally or momentarily. Therefore, the scientific term is **total solar intensity**, defined by NASA (2022) as $1360.8 \pm 0.5 \text{ W/m}^2$. (Previous estimates in the 1990s put its value at $1365.4 \pm 1.3 \text{ W/m}^2$.) The earth maintains a thermal equilibrium between the annual input of shortwave radiation (0.3 to 2.0 μm) from the sun and the outward flux of longwave radiation (3.0 to 30 μm). Only a narrow band is considered in terrestrial applications because 99% of the sun's radiant energy has wavelengths between 0.28 and 4.96 μm .

Solar Declination Angle δ

The axis about which the earth rotates is tilted at 23.45° to the earth's orbital plane and the sun's equator. The earth's tilted axis results in a day-by-day variation of the angle between the earth-sun line and the earth's equatorial plane, called the **solar declination** δ . This angle varies with the date, as shown in [Figure 1](#), and may be estimated by the following equation:

$$\delta = 23.45 \sin \left[360^\circ \times \frac{284 + N}{365} \right] \quad (1)$$

where N = day of year, with January 1 = 1.

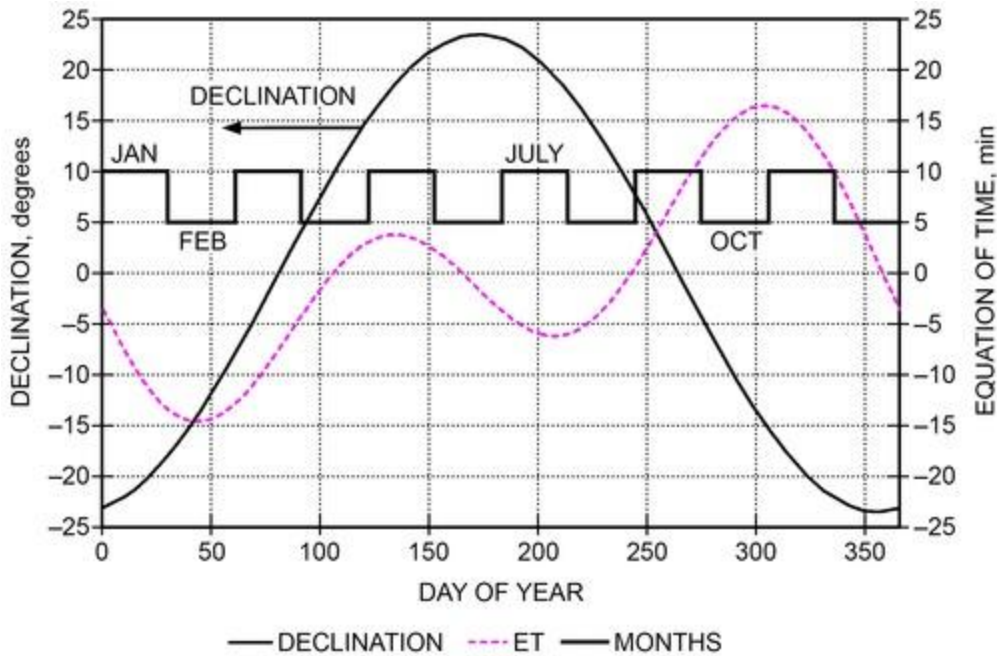


Figure 1. Variation of Declination δ (degrees) and Equation of Time ET as Function of Day of Year

The relationship between δ and the date from year to year varies to an insignificant degree. The daily change in the declination is the primary reason for the changing seasons, with their variation in the distribution of solar radiation over the earth's surface and the varying number of hours of daylight and darkness. Note that the following sections are based in the northern hemisphere; sites in the southern hemisphere will be 180° from the examples (e.g., a solar panel should face north).

The earth's rotation causes the sun's apparent motion ([Figure 2](#)). The sun's position can be defined by its altitude β above the horizon (angle HOQ) and its azimuth ϕ , measured as angle HOS in the horizontal plane.

At solar noon, the sun is exactly on the meridian, which contains the south-north line. Consequently, the solar azimuth ϕ is 0° . The noon altitude β_N is given by the following equation as

$$\beta_N = 90^\circ - \text{LAT} + \delta \quad (2)$$

where LAT = latitude.

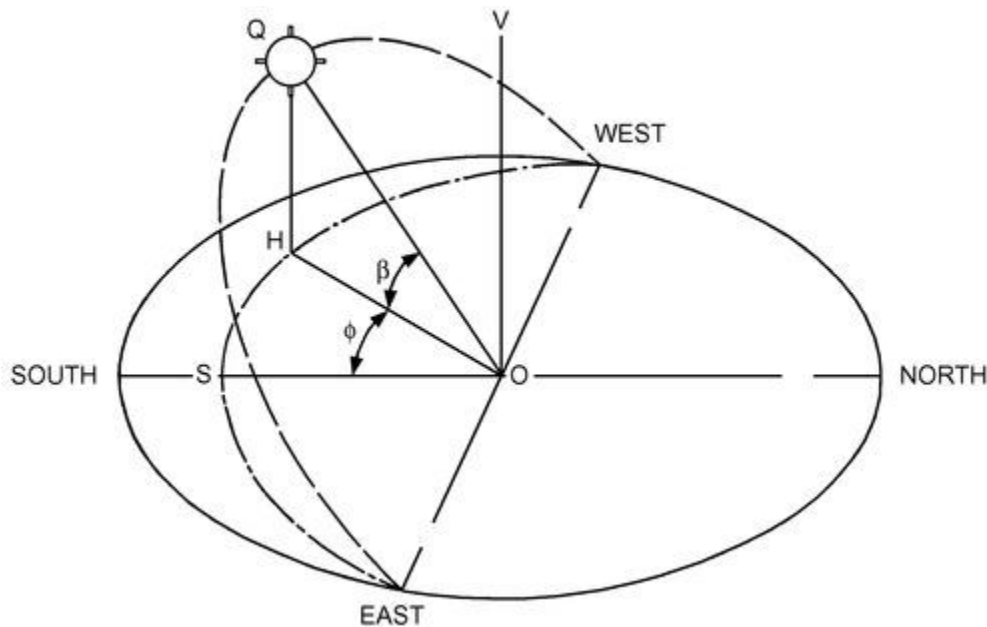


Figure 2. Apparent Daily Path of the Sun Showing Solar Altitude β and Solar Azimuth ϕ

Because the earth's daily rotation and its annual orbit around the sun are regular and predictable, the solar altitude and azimuth may be readily calculated for any desired time of day when the latitude, longitude, and date (declination) are specified. Apparent solar time (AST) must be used, expressed in terms of the hour angle H , where

$$\begin{aligned} H &= (\text{Number of hours from solar noon}) \times 15^\circ \\ &= \frac{\text{Number of minutes from solar noon}}{4} \end{aligned} \quad (3)$$

Solar Time AST

Apparent solar time (AST) generally differs from local standard time (LST) or daylight saving time (DST), and the difference can be significant, particularly when DST is in effect. (Note that some countries do not use LST.) Because the sun appears to move 360° in 24 h, its apparent rate of motion is 4 min per degree of longitude. The AST can be determined from the following equation:

$$\begin{aligned} \text{AST} &= \text{LST} + \text{ET} \\ &\quad + (4 \text{ min})(\text{LST meridian} - \text{Local longitude}) \end{aligned} \quad (4)$$

All standard meridians are multiples of 15° east or west of the prime meridian, which is at the Royal Observatory in Greenwich, U.K. The longitude correction is a positive value for the western hemisphere and a negative for the eastern hemisphere. The longitudes of the seven standard time meridians that affect North America are Atlantic ST, 60°W ; Eastern ST, 75°W ; Central ST, 90°W ; Mountain ST, 105°W ; Pacific ST, 120°W ; Alaska ST, 135°W ; and Hawaii-Aleutian ST, 150°W . Starting with the prime meridian through Greenwich, many European countries define their standard meridians based on legal, political, and economic, as well as purely physical or geographical, criteria. The longitudes of the three standard time meridians that affect Europe are western European ST (U.K., Ireland, and Portugal), 0° ; central European ST, 15°E [e.g., Spain (except for the Canary Islands) to the south, Serbia to the east, and Sweden to the north]; and eastern European ST, 30°E (e.g., Greece and Cyprus to the south, Turkey to the east, Finland to the north).

The equation of time (ET) is the measure, in minutes, of the extent to which solar time, as determined by a sundial, runs faster or slower than local standard time (LST), as determined by a clock that runs at a uniform rate. The following equation may estimate the equation of time:

$$\text{ET} = 9.87 \sin 2B - 7.53 \cos B - 1.5 \sin B \quad (5)$$

where $B = 0.989(N - 81)$.

Example 1. Find AST at noon DST on July 21 for Washington, D.C., longitude = 77°W ; for Chicago, longitude = 87.6°W ; for Athens, Greece, longitude = 23.75°E .

Solution: Noon DST is 11:00 am LST. Washington is in the eastern time zone, and the LST meridian is 75°W . From [Equation \(5\)](#), the equation of time for July 21 ($N = 202$) is -6.07 min. Thus, from [Equation \(4\)](#), noon DST for Washington is

$$\text{AST} = 11:00 - 6.07 + 4(75 - 77) = 10:45.93 \text{ AST} = 10.77 \text{ h}$$

Chicago is in the central time zone, and the LST meridian is 90°W. Thus, from [Equation \(4\)](#), noon central DST is

$$AST = 11:00 - 6.07 + 4(90 - 87.6) = 11:03.53 \text{ AST} = 11.06 \text{ h}$$

Athens is in the eastern European time zone, and the LST meridian is 30°E. Thus, from [Equation \(4\)](#), noon DST is

$$AST = 11:00 - 6.07 - 4(30 - 23.75) = 10:28.93 \text{ AST} = 10.48 \text{ h}$$

The hour angles H (see [Figure 3](#)) for these three examples are

$$\begin{aligned} \text{for Washington, } H &= (12.00 - 10.77)15^\circ = 18.6^\circ \text{ east} \\ \text{for Chicago, } H &= (12.00 - 11.06)15^\circ = 14.1^\circ \text{ east} \\ \text{for Athens, } H &= (12.00 - 10.48)15^\circ = 22.8^\circ \text{ east} \end{aligned}$$

To find the solar altitude β and the azimuth ϕ when the hour angle H , latitude LAT , and declination δ are known, the following equations may be used:

$$\sin \beta = \cos(LAT) \cos \delta \cos H + \sin(LAT) \sin \delta \quad (6)$$

$$\sin \phi = \cos \delta \sin H / \cos \beta \quad (7)$$

or

$$\cos \phi = (\cos H \cos \delta \sin LAT - \sin \delta \cos LAT) / \cos \beta \quad (8)$$

Incident Angle θ

The angle between the line normal to the irradiated surface (OP' in [Figure 3](#)) and the earth-sun line OQ is called the incident angle θ . It is important in solar technology because it affects the intensity of the direct component of solar radiation striking the surface and the surface's ability to absorb, transmit, or reflect the sun's rays.

The surface azimuth ψ and the surface-solar azimuth angle γ must be known to determine the angle θ . The surface azimuth (angle POS in [Figure 3](#)) is the angle between the south-north line SO and the normal PO to the intersection of the irradiated surface with the horizontal plane, shown as line OM . The surface-solar azimuth, angle HOP , is designated by γ and is the angular difference between the solar azimuth ϕ and the surface azimuth ψ . For surfaces facing east of south, $\gamma = \phi - \psi$ in the morning and $\gamma = \phi + \psi$ in the afternoon. For surfaces facing west of south, $\gamma = \phi + \psi$ in the morning and $\gamma = \phi - \psi$ in the afternoon. For south-facing surfaces, $\psi = 0^\circ$, so $\gamma = \phi$ for all conditions. Angles δ , β , and ϕ are always positive.

For a surface with a tilt angle Σ (measured from the horizontal), the angle of incidence θ between the direct solar beam and the normal to the surface (angle QOP' in [Figure 3](#)) is given by the following equation.

$$\cos \theta = \cos \beta \cos \gamma \sin \Sigma + \sin \beta \cos \Sigma \quad (9)$$

For vertical surfaces, $\Sigma = 90^\circ$, $\cos \Sigma = 0$, and $\sin \Sigma = 1.0$, so [Equation \(9\)](#) becomes

$$\cos \theta = \cos \beta \cos \gamma \quad (10)$$

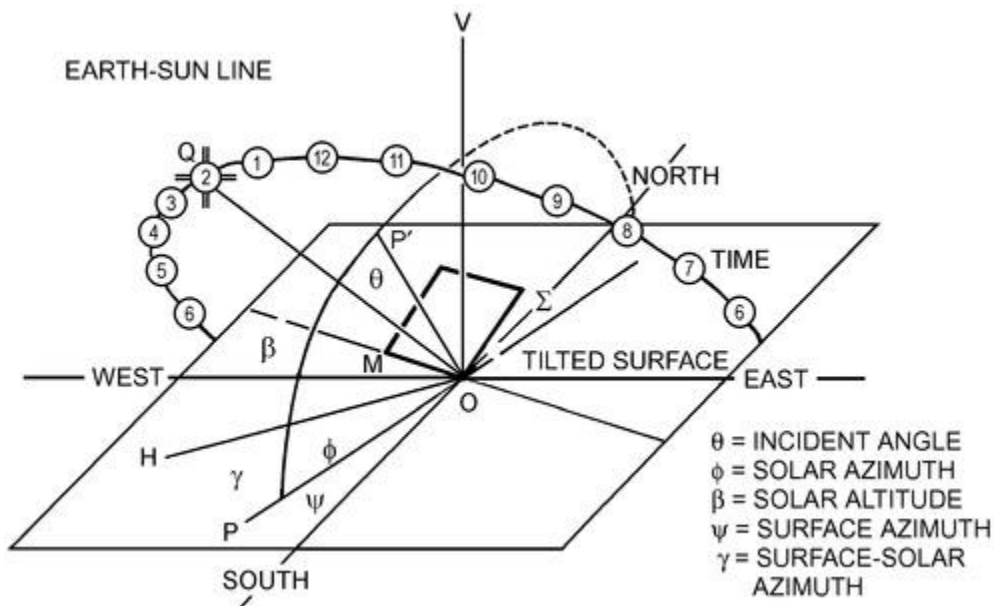


Figure 3. Solar Angles with Respect to a Tilted Surface

For horizontal surfaces, $\Sigma = 0^\circ$, $\sin \Sigma = 0$, and $\cos \Sigma = 1.0$, so [Equation \(9\)](#) leads to

$$\theta_H = 90^\circ - \beta \quad (11)$$

Example 2. Find θ for a south-facing surface tilted 30° upward from the horizontal at 40° north latitude at 4:00 pm, AST, on August 21.

Solution: From [Equation \(3\)](#), at 4:00 pm on August 21,

$$H = 4 \times 15^\circ = 60^\circ$$

From [Equation \(1\)](#) for August 21 ($N = 233$),

$$\delta = 11.8^\circ$$

From [Equation \(6\)](#),

$$\sin \beta = \cos 40^\circ \cos 11.8^\circ \cos 60^\circ + \sin 40^\circ \sin 11.8^\circ$$

$$\beta = 30.4^\circ$$

From [Equation \(7\)](#),

$$\begin{aligned} \sin \phi &= \cos 11.8^\circ \sin 60^\circ / \cos 30.4^\circ \\ \phi &= 79.4^\circ \end{aligned}$$

The surface faces south, so $\phi = \gamma$. From [Equation \(9\)](#),

$$\begin{aligned} \cos \theta &= \cos 30.4^\circ \cos 79.4^\circ \sin 30^\circ + \sin 30.4^\circ \cos 30^\circ \\ \theta &= 58.8^\circ \end{aligned}$$

Solar Spectrum

Beyond the earth's atmosphere, the effective blackbody temperature of the sun is $10,370^\circ\text{R}$. The maximum spectral intensity occurs at $0.48 \mu\text{m}$ in the green portion of the visible spectrum. Thekaekara (1973) presents tables and charts of the sun's extraterrestrial spectral irradiance from 0.120 to $100 \mu\text{m}$, the range in which most of the sun's radiant energy is contained. The ultraviolet section of the spectrum below $0.40 \mu\text{m}$ of wavelength contains 8.73% of the total. Another 38.15% is contained in the visible region between 0.40 and $0.70 \mu\text{m}$, and the infrared region contains the remaining 53.12%.

Solar Radiation at the Earth's Surface

In passing through the earth's atmosphere, some of the sun's direct radiation is scattered by nitrogen, oxygen, and other molecules, which are small compared to the wavelengths of the radiation; and by aerosols, water droplets, dust, and other particles with diameters comparable to the wavelengths (Gates 1966). This scattered radiation causes the sky to appear blue on clear days, and some of it reaches the earth as diffuse radiation.

Attenuation of the solar rays is also caused by absorption, first by the ozone in the outer atmosphere, which causes a sharp cutoff at $0.29 \mu\text{m}$ of the ultraviolet radiation reaching the earth's surface ([Figure 4](#)). In the longer wavelengths, there are a series of absorption bands caused by water vapor, carbon dioxide, and ozone. The total attenuation at any given location is determined by (1) the length of the atmospheric path through which the rays travel and (2) the atmosphere's composition. The path length is expressed in terms of the air mass m , which is the ratio of the mass of atmosphere in the actual earth-sun path to the mass that would exist if the sun were directly overhead at sea level ($m = 1.0$). For all practical purposes, at sea level, $m = 1.0/\sin \beta$. Beyond the earth's atmosphere, $m = 0$.

Before 1967, solar radiation data were based on an assumed solar constant of $419.7 \text{ Btu/h} \cdot \text{ft}^2$ and a standard sea-level atmosphere containing the equivalent depth of 2.8 mm of ozone, 20 mm of precipitable moisture, and 300 dust particles per cm^3 . Threlkeld and Jordan (1958) considered the wide variation of water vapor in the atmosphere above the United States at any given time, particularly the seasonal variation, which finds three times as much moisture in the atmosphere in midsummer as in December, January, and February. The basic atmosphere was assumed to be at sea-level barometric pressure, with 2.5 mm of ozone, 200 dust particles per cm^3 , and an actual precipitable moisture content that varied throughout the year from 8 mm in midwinter to 28 mm in mid-July. [Figure 5](#) shows the variation of

the direct normal irradiation I_{DN} with solar altitude, as estimated for clear atmospheres and an atmosphere with variable moisture content.

The ASHRAE clear-sky model described in previous editions of this chapter was tested and some initial limitations were identified: the clearness number was not universally available; its value varied between 0.85 and 1.20 according to location and season in the United States, and was often taken as unity for lack of better data in other countries. The model also lacked universal applicability and the values of its coefficients had to be altered according to location. In addition, the model was derived from a very limited number of measurements, and its applicability outside the United States had never been demonstrated. Finally, clear-sky diffuse irradiance was proportional to beam irradiance, which runs contrary to intuition (i.e., hazier skies should lead to less direct but more diffuse solar irradiation). To overcome these limitations, ASHRAE research projects RP-1363 and RP-1453 provided a significant update to the model (Thevenard and Gueymard 2010). The objectives were to obtain a more accurate model that could calculate clear-sky radiation for any location in the world for all 12 months of the year, while retaining a relatively simple formulation. The resulting model (Gueymard and Thevenard 2013) can be found in [Chapter 14 of the 2021 ASHRAE Handbook—Fundamentals](#), along with the tabulated parameters required at different locations.

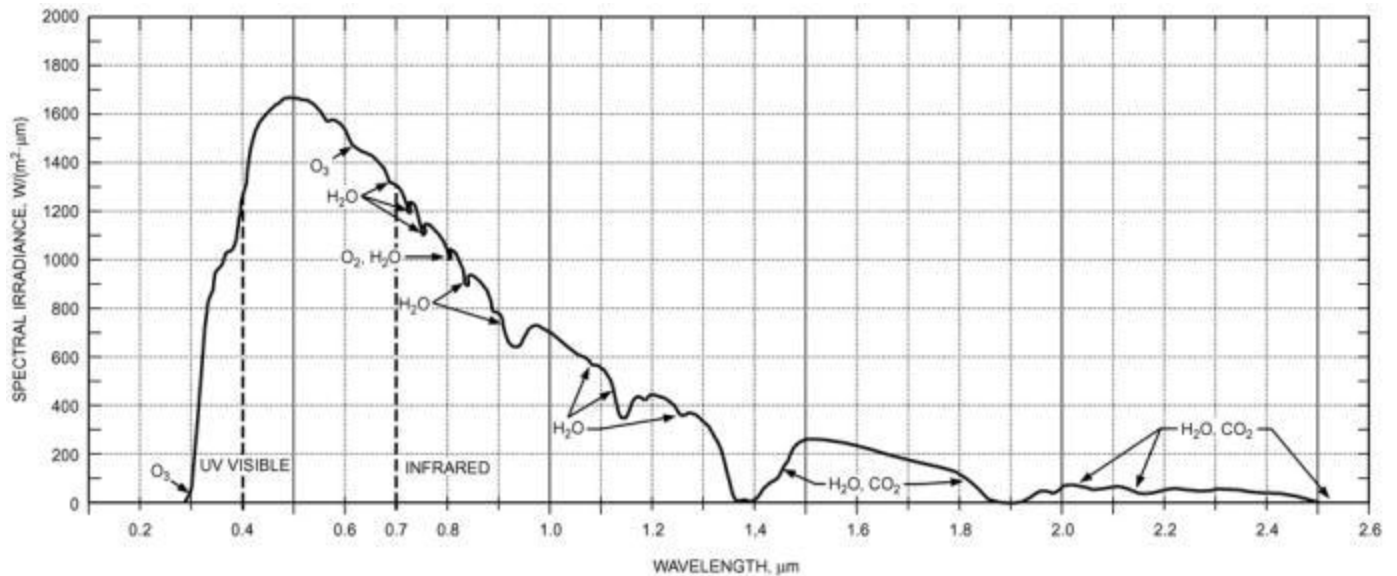


Figure 4. Spectral Solar Irradiation at Sea Level for Air Mass = 1.0

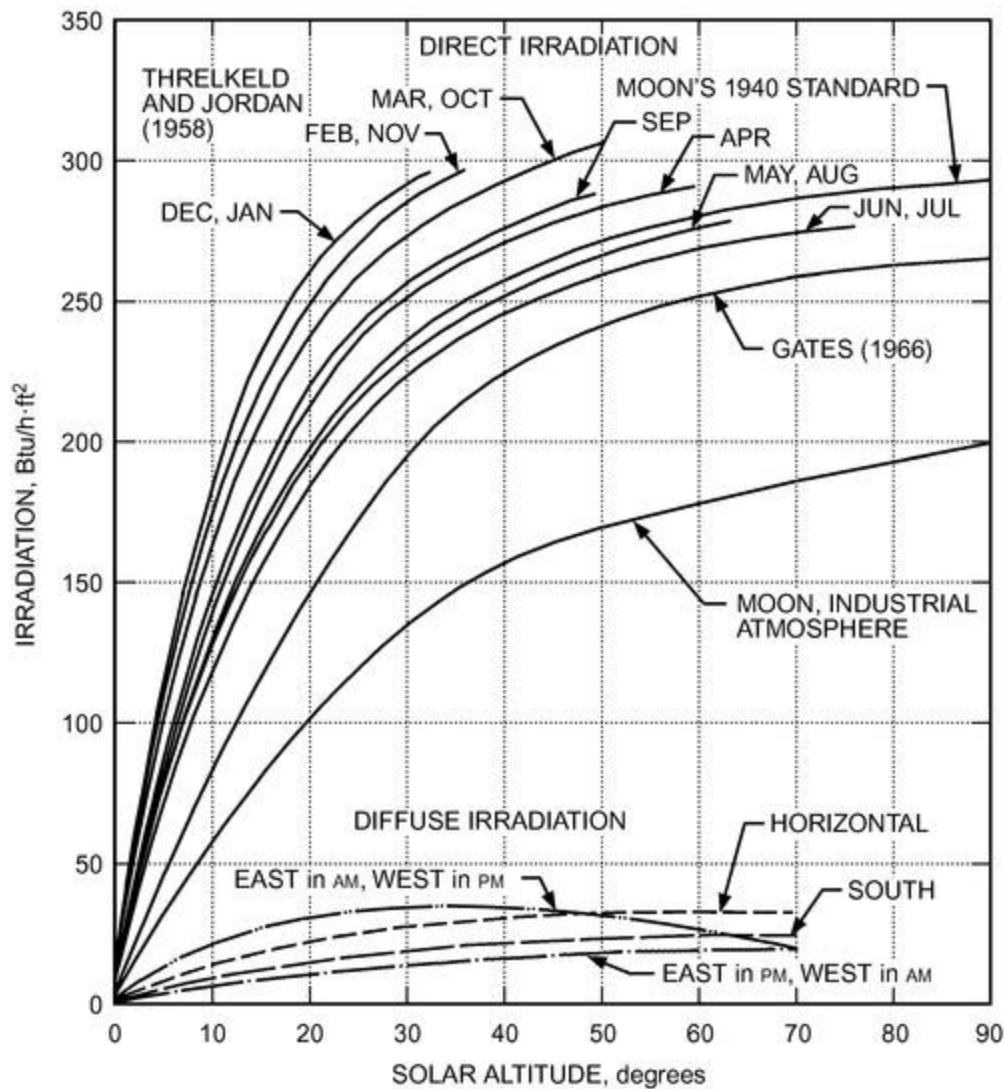


Figure 5. Variation with Solar Altitude and Time of Year for Direct Normal Irradiation

Design Values for Total Solar Irradiation

The total solar irradiation $I_{t\theta}$ of a terrestrial surface of any orientation and tilt with an incident angle θ is the sum of the direct component $I_{DN} \cos \theta$ plus the diffuse component $I_{d\theta}$ coming from the sky plus whatever amount of reflected shortwave radiation I_r may reach the surface from the earth or adjacent surfaces:

$$I_{t\theta} = I_{DN} \cos \theta + I_{d\theta} + I_r \quad (12)$$

The diffuse component is difficult to estimate because of its wide variations and nondirectional nature. [Figure 5](#) shows typical values of diffuse irradiation of horizontal and vertical surfaces. For additional information on calculating clear-sky solar radiation, see [Chapter 14 of the 2021 ASHRAE Handbook—Fundamentals](#).

The maximum daily amount of solar irradiation that can be received at any given location is that which falls on a flat plate with its surface kept normal to the sun's rays so it receives both direct and diffuse radiation. For fixed flat-plate collectors, the total amount of clear-day irradiation depends on the orientation and slope. As shown in [Figure 6](#) for 40° north latitude, the total irradiation of horizontal surfaces reaches its maximum in midsummer, whereas vertical south-facing surfaces experience their maximum irradiation during the winter. These curves show the combined effects of the varying length of days and changing solar altitudes.

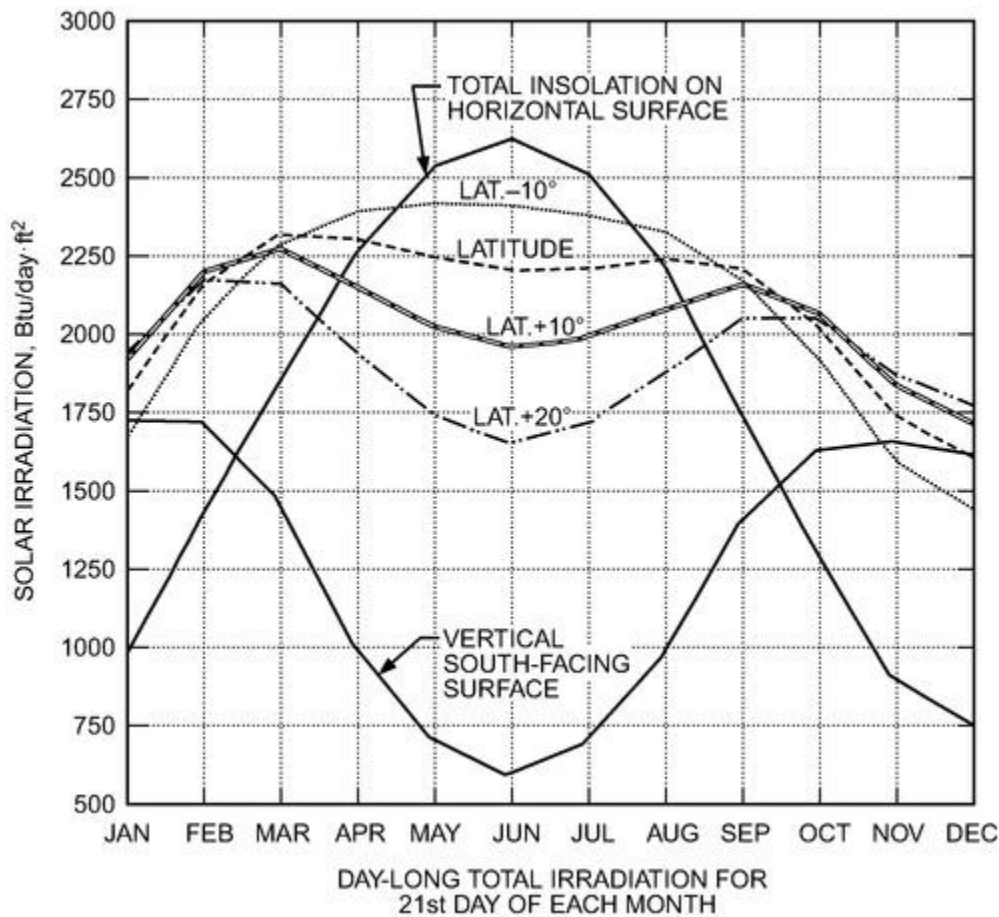


Figure 6. Total Daily Irradiation for Horizontal, Tilted, and Vertical Surfaces at 40° North Latitude

In general, flat-plate collectors are mounted at a fixed tilt angle Σ (above the horizontal) to give the optimum amount of irradiation for each purpose. Collectors intended for winter heating benefit from higher tilt angles than those used to operate cooling systems in summer. Solar water heaters, which should operate satisfactorily throughout the year, require an angle that is a compromise between the optimal values for summer and winter. Figure 6 shows the monthly variation of total day-long irradiation on the 21st day of each month at 40° north latitude for flat surfaces with various tilt angles.

NREL tables (redc.nrel.gov/solar/pubs/redbook/) gives the average solar irradiation of each month, at latitudes 24 to 64° north, on surfaces with the following orientations: normal to the sun's rays (direct normal data do not include diffuse irradiation); horizontal; south-facing, tilted at (LAT-15), LAT, (LAT+15), and 90° from the horizontal. The day-long total irradiation for fixed surfaces is highest for those facing south, but a deviation in azimuth of 15 to 20° causes only a small reduction.

The preceding data apply to clear days. Irradiation for average days may be estimated for any specific location by referring to publications of the U.S. Weather Service. The *Climatic Atlas of the United States* website (NOA 2010; www.ncdc.noaa.gov/climateatlas/) gives maps of monthly and annual values of percentage of possible sunshine, total hours of sunshine, mean solar radiation, mean sky cover, wind speed, and wind direction. The European Solar Radiation Atlas (Scharmer and Grief 2000) is a database that provides spatial and temporal climatic information for different time scales, including irradiation (global and its components), sunshine duration, air temperature, precipitation, water vapor pressure, and air pressure for a number of stations.

Chapter 14 in the 2021 ASHRAE Handbook—Fundamentals also provides several sources for obtaining solar data.

The total daily horizontal irradiation data reported by the U.S. Weather Bureau for approximately 100 stations before 1964 show that the percentage of total clear-day irradiation is approximately a linear function of the percentage of possible sunshine. The irradiation is not zero for days when the percentage of possible sunshine is reported as zero, because substantial amounts of energy reach the earth through diffuse radiation. Instead, the following relationship exists for the percentage of possible sunshine (ratio of day-long horizon irradiation to clear-day total horizon irradiation):

$$\frac{\text{Day-long actual } I_{tH}}{\text{Clear day } I_{tH}} 100 = a + b \quad (13)$$

where a and b are empirical constants for any specified month at any given location. See Duffie and Beckman (2006) and Jordan and Liu (1977).

Longwave Atmospheric Radiation

In addition to the shortwave (0.3 to 2.0 μm) radiation it receives from the sun, the earth receives longwave radiation (4 to 100 μm , with maximum intensity near 10 μm) from the atmosphere. In turn, a surface on the earth emits longwave radiation q_{Rs} that can be expressed in terms of the Stefan-Boltzmann law:

$$q_{Rs} = e_s \sigma T_s^4 \quad (14)$$

where

e_s = surface emittance

σ = Stefan-Boltzmann constant, $0.1712 \times 10^{-8} \text{ Btu/h} \cdot \text{ft}^2 \cdot ^\circ\text{R}^4$

T_s = absolute temperature of surface, $^\circ\text{R}$

For most nonmetallic surfaces, the longwave hemispheric emittance is high, ranging from 0.84 for glass and dry sand to 0.95 for black built-up roofing. For highly polished metals and certain selective surfaces, e_s may be as low as 0.05 to 0.20.

Atmospheric radiation comes primarily from water vapor, carbon dioxide, and ozone (Bliss 1961); very little comes from oxygen and nitrogen, although they make up 99% of the air.

Approximately 90% of the incoming atmospheric radiation comes from the lowest 300 ft. Thus, air conditions at ground level T_{at} largely determine the magnitude of the incoming radiation. Downward radiation from the atmosphere q_{Rat} may be expressed as

$$q_{Rat} = e_{at} \sigma T_{at}^4 \quad (15)$$

The emittance of the sky e_{at} is a complex function of air temperature and moisture content. The dew point of the atmosphere near the ground determines the total amount of moisture in the atmosphere above the place where the dry-bulb (db) and dew-point (dp) temperatures of the atmosphere are determined (Reitan 1963). Bliss (1961) found that the sky emittance is related to the dew-point temperature, as shown by [Table 1](#).

Table 1 Sky Emittance and Amount of Precipitable Moisture Versus Dew-Point Temperature

Dew Point, $^\circ\text{F}$	Sky Emittance, e_{at}	Precipitable Water, in.
-20	0.68	0.12
-10	0.71	0.16
0	0.73	0.18
10	0.76	0.22
20	0.77	0.29
30	0.79	0.41
40	0.82	0.57
50	0.84	0.81
60	0.86	1.14
70	0.88	1.61

The apparent sky temperature T_{sky} is defined as the temperature at which the sky (as a blackbody) emits radiation at the rate being physically emitted by the atmosphere at the ground level temperature with its actual emittance e_{at} . Then,

$$\sigma T_{sky}^4 = e_{at} \sigma T_{at}^4 \quad (16)$$

or

$$T_{sky}^4 = e_{at} T_{at}^4 \quad (17)$$

Example 3. Consider a summer night condition when ground-level temperatures are 65°F dew point and 85°F dry bulb. From [Table 1](#), e_{at} at 65°F dew point is 0.87, and the apparent sky temperature is

$$T_{sky} = 0.87^{0.25}(85 + 459.6) = 526.0^\circ\text{R}$$

Thus, $T_{sky} = 526.0 - 459.6 = 66.4^\circ\text{F}$, which is 18.6°F below the ground-level dry-bulb temperature.

For a winter night in Arizona, when temperatures at ground level are 60°F db and 25°F dp, from [Table 1](#), the sky emittance is 0.78, and the apparent sky temperature is 488.3°R or 28.7°F.

A simple relationship, which ignores vapor pressure of the atmosphere, may also be used to estimate the apparent sky temperature:

$$T_{sky} = 0.0411 T_{at}^{1.5} \quad (18)$$

where T is in degrees Rankine.

If the temperature of the radiating surface is assumed to equal the atmospheric temperature, the heat loss from a black surface ($e_s = 1.0$) may be found from [Figure 7](#).

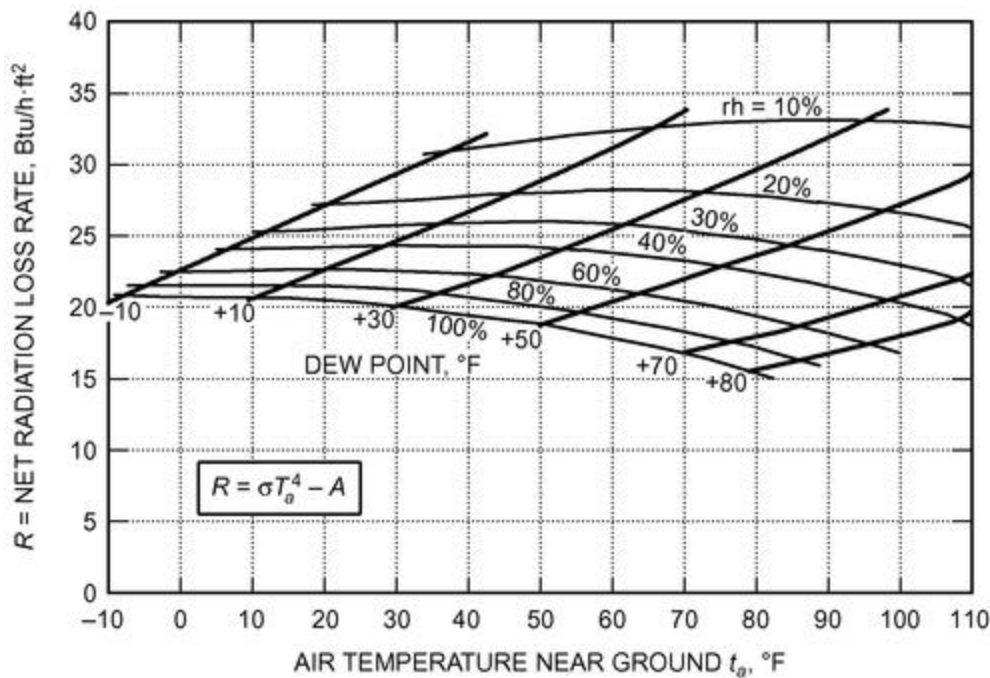


Figure 7. Radiation Heat Loss to Sky from Horizontal Blackbody

Example 4. For the conditions in the previous example for summer, 85°F db and 65°F dp, the rate of radiative heat loss is about 23 Btu/h · ft². For winter, 60°F db and 25°F dp, the heat loss is about 27 Btu/h · ft².

Where a rough, unpainted roof is used as a heat dissipater, the rate of heat loss rises rapidly as the surface temperature goes up. For the summer example, a painted metallic roof, $e_s = 0.96$, at 100°F (559.6°R) will have a heat loss rate of

$$\begin{aligned} q_{Rs} &= 0.96 \times 0.1712 \times 10^{-8} [559.6^4 - 526.0^4] \\ &= 35.4 \text{ Btu/h} \cdot \text{ft}^2 \end{aligned}$$

This analysis shows that radiation alone is not an effective means of dissipating heat under summer conditions of high dew-point and ambient temperatures. In spring and fall, when both the dew-point and dry-bulb temperatures are relatively low, radiation becomes much more effective.

On overcast nights, when cloud cover is low, the clouds act much like blackbodies at ground-level temperature, and virtually no heat can be lost by radiation. Exchange of longwave radiation between the sky and terrestrial surfaces occurs in the daytime and at night, but the much greater magnitude of the solar irradiation masks the longwave effects.

2. SOLAR ENERGY HARNESSING

Solar energy can be converted by (1) chemical, (2) electrical, and (3) thermal processes. Photosynthesis is a chemical process through which plants and other organisms convert CO₂ to O₂ and carbohydrates. Photovoltaic cells convert solar energy to electricity. The section on Photovoltaic Applications discusses some applications for these devices. The thermal conversion process provides thermal energy for space heating and cooling, domestic water heating, power generation, distillation, and process heating.

Solar Thermal Collection By Flat-Plate Solar Collectors (FPC)

The solar irradiation calculation methods presented in the previous sections may be used to estimate how much energy is likely to be available at any specific location, date, and time of day for collection by either a concentrating

device, which uses only the direct rays of the sun, or by a flat-plate solar thermal collector (from now on called a **flat-plate collector**), which can use both direct and diffuse irradiation. Temperatures needed for space heating and cooling do not exceed 200°F, even for absorption refrigeration, and they can be attained with carefully designed flat-plate collectors.

A flat-plate collector generally consists of the following components (see [Figure 8](#)):

- **Glazing.** One or more sheets of glass or other radiation-transmitting material.
- **Tubes, fins, or passages.** To conduct or direct the heat transfer fluid from the inlet to the outlet.
- **Absorber plates.** Flat, corrugated, or grooved plates, to which the tubes, fins, or passages are attached. The plate may be integral to the tubes.
- **Headers or manifolds.** To admit and discharge the heat transfer fluid.
- **Insulation.** To minimize heat loss from the back and sides of the collector frame.
- **Container or casing.** To surround the other components and protect them from dust, moisture, etc.

Collectors have been built in various designs from many different materials ([Figure 9](#)). They have been used to heat fluids such as water, water plus an antifreeze additive, or air. Their major purpose is to collect as much solar energy as possible at the lowest possible total cost. The collector should also have a long effective life, despite the adverse effects of the sun's ultraviolet radiation; corrosion or clogging because of acidity, alkalinity, or hardness of the heat transfer fluid; freezing or air binding in the case of water, or deposition of dust or moisture in the case of air; and broken glazing because of thermal expansion, hail, vandalism, or other causes. These problems can be minimized by using tempered glass.

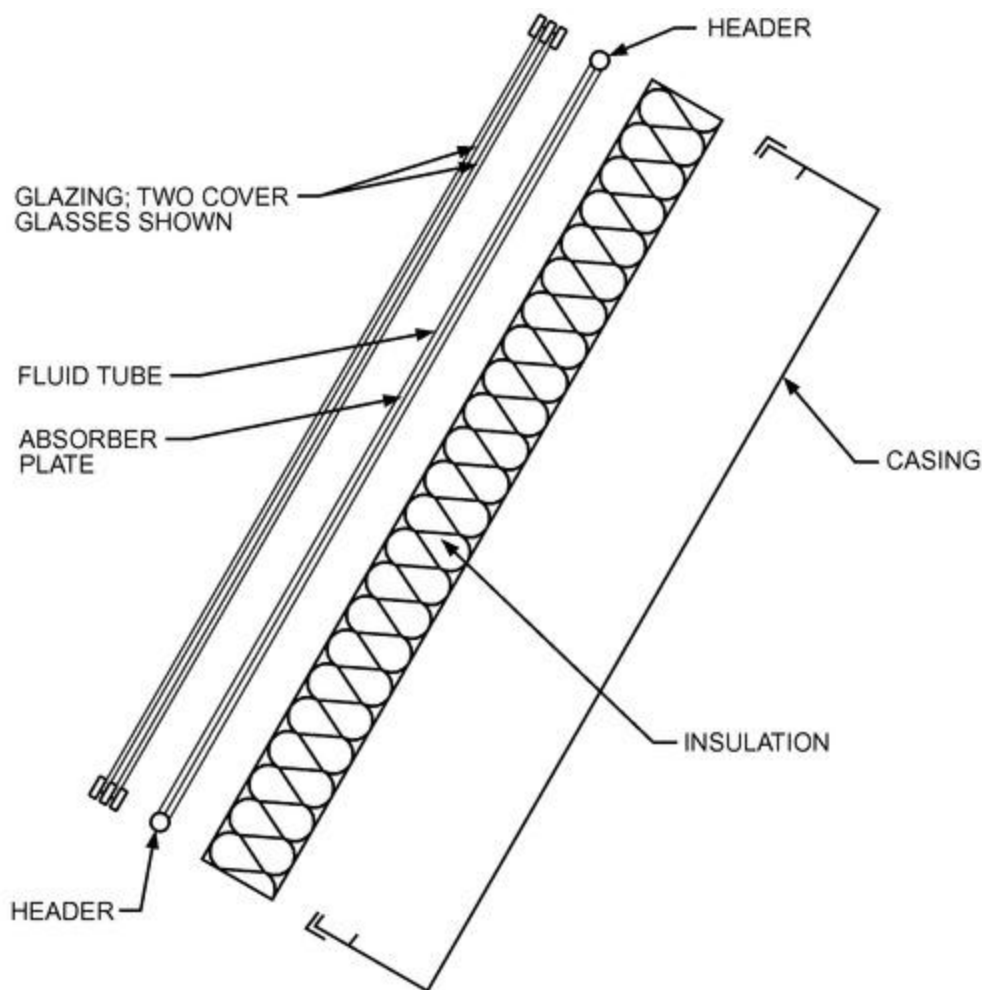


Figure 8. Exploded Cross Section Through Double-Glazed Solar Water Heater

Recently, water circulation within collectors has largely been eliminated by using heat pipes. This increases the rate of use of the solar exergy because pumps demand electrical unit exergy, which is much higher than solar thermal exergy harnessed from the collectors.

Glazing Materials

Glass has been widely used to cover flat-plate solar collectors because it can transmit as much as 90% of the incoming shortwave solar irradiation while transmitting very little of the longwave radiation emitted outward from the absorber plate. Glass with low iron content has a relatively high transmittance for solar radiation (approximately 0.85 to 0.90 at normal incidence). However, its transmittance is essentially zero for the longwave thermal radiation (5.0 to 50 μm) emitted by sun-heated surfaces. Note that commercially available grades of window and greenhouse glass have normal incidence transmittances of about 0.87 and 0.85, respectively. For direct radiation, the transmittance varies markedly with the angle of incidence, as shown in [Table 2](#), which gives transmittances for single and double glazing using double-strength clear window glass.

Plastic films and sheets also have high shortwave transmittance, but because most usable varieties also have transmission bands in the middle of the thermal radiation spectrum, their longwave transmittances may be as high as 0.40.

Plastics are also generally limited in the temperatures they can sustain without deteriorating or undergoing dimensional changes. Only a few kinds of plastics can withstand the sun's ultraviolet radiation for long periods. However, they are not broken by hail and other stones and, in the form of thin films, they are completely flexible and have low mass.

The glass generally used in solar collectors may be either single-strength (0.085 to 0.100 in. thick) or double-strength (0.115 to 0.133 in. thick).

Table 2 Variation with Incident Angle of Transmittance for Single and Double Glazing and Absorptance for Flat-Black Paint

Incident Angle, Deg	Transmittance		Absorptance of Flat-Black Paint
	Single Glazing	Double Glazing	
0	0.87	0.77	0.96
10	0.87	0.77	0.96
20	0.87	0.77	0.96
30	0.87	0.76	0.95
40	0.86	0.75	0.94
50	0.84	0.73	0.92
60	0.79	0.67	0.88
70	0.68	0.53	0.82
80	0.42	0.25	0.67
90	0.00	0.00	0.00

The 4% reflectance from each glass/air interface is the most important factor in reducing transmission, although a gain of about 3% in transmittance can be obtained by using water-white glass. Antireflective coatings and surface texture can also improve transmission significantly. The effect of dirt and dust on collector glazing may be quite small, and the cleansing effect of an occasional rainfall is usually adequate to maintain the transmittance within 2 to 4% of its maximum.

The glazing should admit as much solar irradiation as possible and reduce upward heat loss as much as possible. Although glass is virtually opaque to the longwave radiation emitted by absorber plates, absorption of this radiation causes an increase in the glass temperature and a loss of heat to the surrounding atmosphere by radiation and convection takes place. This heat loss can be reduced by applying an infrared-reflective coating on the underside of the glass; however, such coatings are expensive and reduce the effective solar transmittance of the glass by as much as 10%.

In addition to serving as a heat trap by admitting shortwave solar radiation and retaining longwave thermal radiation, the glazing also reduces heat loss by convection. The insulating effect of the glazing is enhanced by using several sheets of glass or glass plus plastic. Loss from the back of the plate rarely exceeds 10% of the upward loss.

Absorber Plates

The absorber plate absorbs as much of the irradiation as possible through the glazing, while losing as little heat as possible up to the atmosphere and down through the back of the casing. The absorber plates transfer retained heat to the transport fluid. The absorptance of the collector surface for shortwave solar radiation depends on the nature and color of the coating and on the incident angle, as shown in [Table 2](#) for a typical flat-black paint.

By suitable electrolytic or chemical treatments, selective surfaces can be produced with high values of solar radiation absorptance α and low values of longwave emittance e . Essentially, typical selective surfaces consist of a thin upper layer, which is highly absorbent to shortwave solar radiation but relatively transparent to longwave thermal radiation,

deposited on a substrate with a high reflectance and a low emittance for longwave radiation. Selective surfaces are particularly important when the collector surface temperature is much higher than the ambient air temperature.

For fluid-heating collectors, passages must be integral with, or firmly bonded to, the absorber plate. A major problem is obtaining a good thermal bond between tubes and absorber plates without incurring high costs for labor or materials. Materials most frequently used for absorber plates are copper, aluminum, and steel. UV-resistant plastic extrusions are used for low-temperature application. If the entire absorber area is in contact with the heat transfer fluid, the material's thermal conductance is not important.

Whillier (1964) concluded that steel tubes are as effective as copper if the bond conductance between tube and plate is good. Potential corrosion problems should be considered with the use of any metal. Bond conductance can range from 1000 Btu/h · ft² · °F for a securely soldered or brazed tube, to 3 Btu/h · ft² · °F for a poorly clamped or badly soldered tube. Plates of copper, aluminum, or stainless steel with integral tubes are among the most effective types available. [Figure 9](#) shows a few of the solar water and air heaters that have been used with varying degrees of success.

Flat-Plate Collector (FPC) Performance

The performance of collectors may be analyzed using a procedure originated by Hottel and Woertz (1942), according to the quantity of energy (First Law of Thermodynamics) and extended by Whillier (in Jordan and Liu 1977). The basic equation is

$$q_u = I_{t\theta}(\tau\alpha)_\theta - U_L(t_p - t_a) = \dot{m} c_p(t_{fe} - t_{fi})/A_{ap} \quad (19)$$

[Equation \(19\)](#) also may be adapted for use with concentrating collectors:

$$q_u = I_{DN}(\tau\alpha)_\theta(\rho\Gamma) - U_L(A_{abs}/A_{ap})(t_{abs} - t_a) \quad (20)$$

where

q_u	=	useful heat gained by collector per unit of aperture area, Btu/h · ft ²
$I_{t\theta}$	=	total irradiation of collector, Btu/h · ft ²
I_{DN}	=	direct normal irradiation, Btu/h · ft ²
$(\tau\alpha)_\theta$	=	transmittance τ of cover times absorptance α of plate at prevailing incident angle θ
U_L	=	overall heat loss coefficient, Btu/h · ft ² · °F
t_p	=	temperature of absorber plate, °F
t_a	=	temperature of atmosphere, °F
t_{abs}	=	temperature of absorber, °F
\dot{m}	=	fluid flow rate, lb/h
c_p	=	specific heat of fluid, Btu/lb · °F
t_{fe}, t_{fi}	=	temperatures of fluid leaving and entering collector, °F
$\rho\Gamma$	=	reflectance of concentrator surface times fraction of reflected or refracted radiation that reaches absorber
A_{abs}, A_{ap}	=	areas of absorber surface and of aperture that admit or receive radiation, ft ²

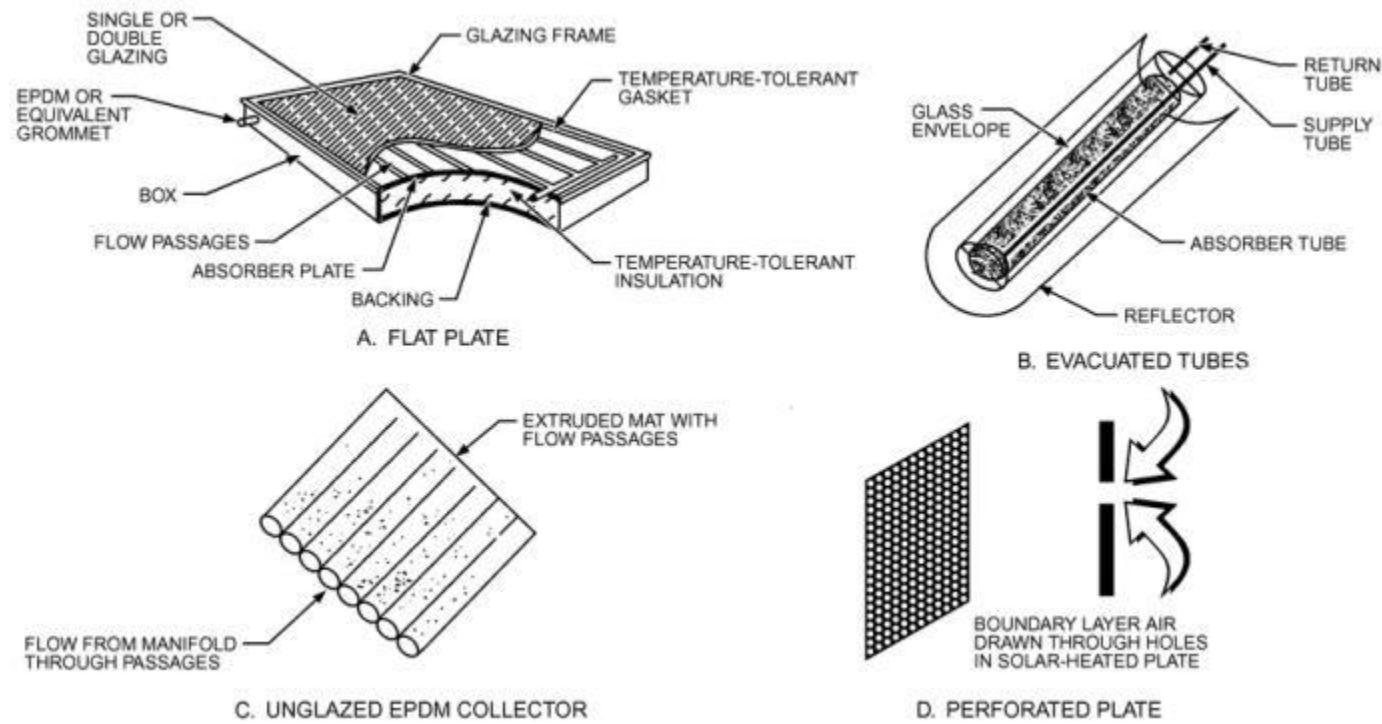


Figure 9. Various Types of Non-Concentrating Solar Collectors

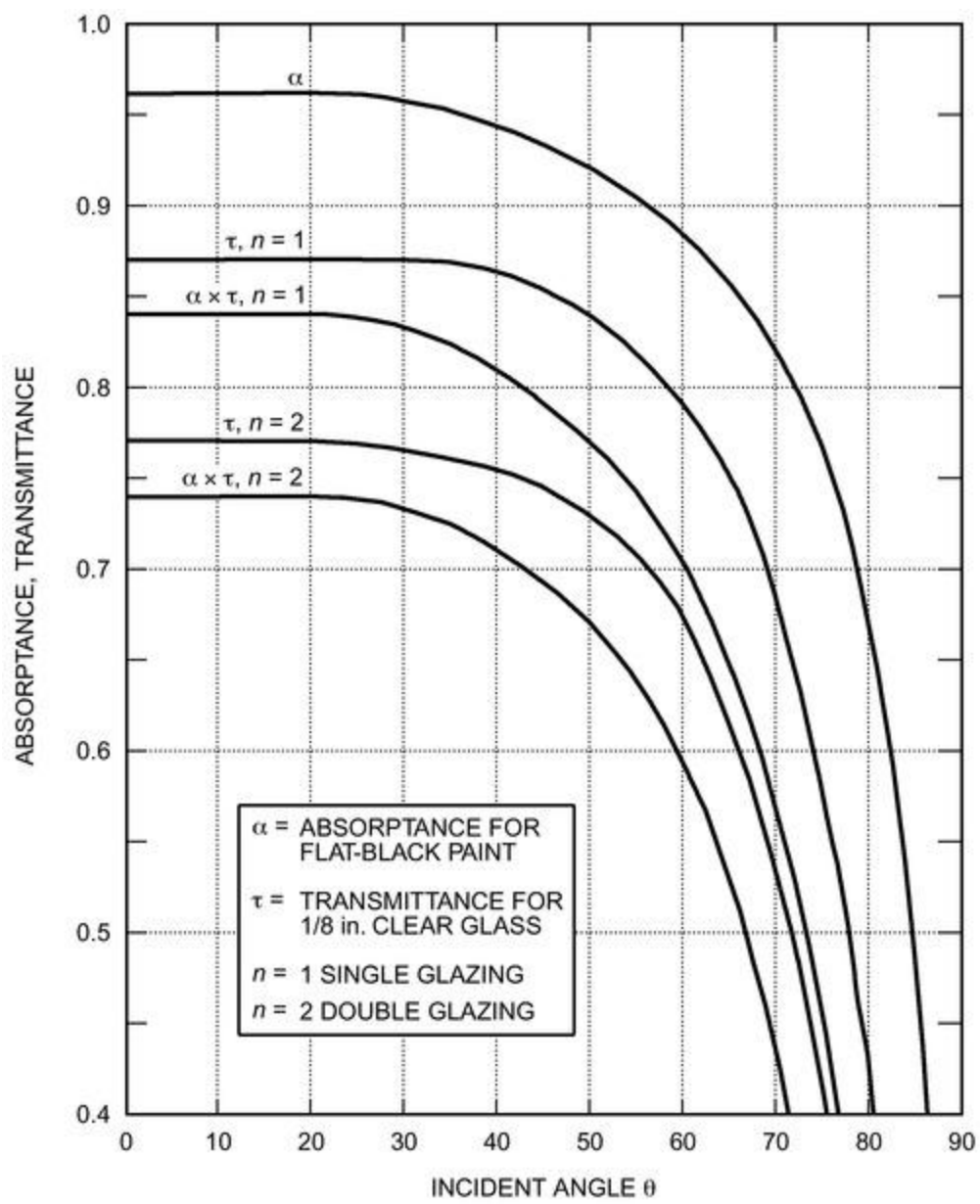
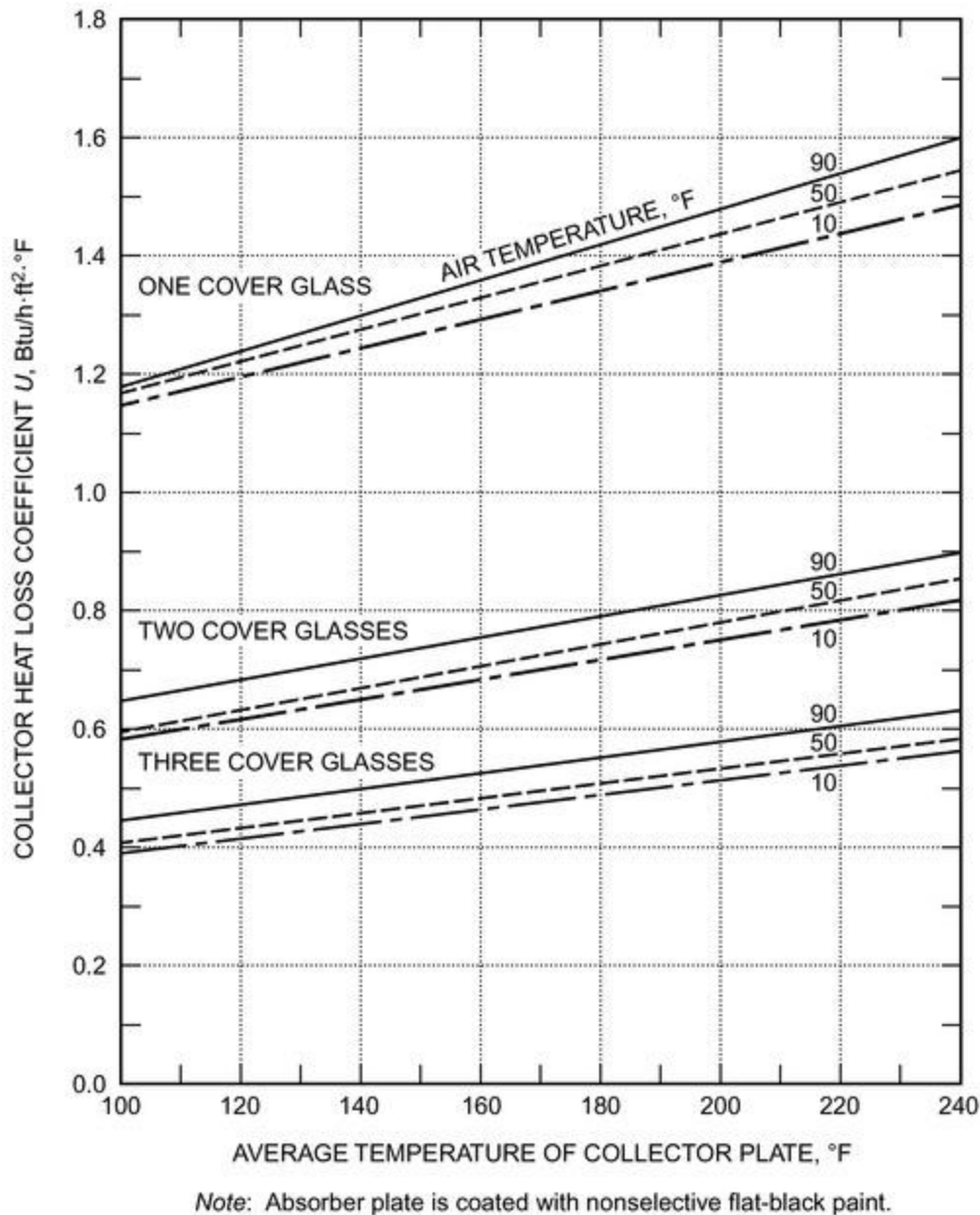


Figure 10. Variation of Absorptance and Transmittance with Incident Angle

The transmittance for single and double glazing and the absorptance for flat-black paint may be found in [Table 2](#) for incident angles from 0 to 90°. These values, and the products of τ and α , are also shown in [Figure 10](#). The solar-optical properties of the glazing and absorber plate change little for θ between 0° and 30°, but, because all values reach zero when $\theta = 90^\circ$, they drop off rapidly for values of θ beyond 40°.

For nonselective absorber plates, U_L varies with the temperature of the plate and the ambient air, as shown in [Figure 11](#). For selective surfaces, which strongly reduce the emittance of the absorber plate, U_L is much lower than the values shown in [Figure 11](#). Ask manufacturers of such surfaces for values applicable to their products, or consult test results that give the necessary information.

**Figure 11. Variation of Overall Heat Loss Coefficient U_L with Absorber Plate Temperature and Ambient Air Temperatures for Single-, Double-, and Triple-Glazed Collectors**

Example 5. A flat-plate collector is operating in Denver, latitude: 40° north, on July 21 at noon solar time, and the total solar irradiation incident on the plane of the collector $I_{t\theta}$ is 306 Btu/h · ft². The atmospheric temperature is 85°F, and the average temperature of the absorber plate is 140°F. The collector is single-glazed with flat-black paint on the absorber. The collector faces south, and the tilt angle is 30° from the horizontal. Find the rate of heat collection and collector efficiency. Neglect losses from the back and sides of the collector.

Solution: From [Equation \(1\)](#) for July 21 ($N = 202$), $\delta = 20.4^\circ$.

From [Equation \(2\)](#),

$$\beta_N = 90^\circ - 40^\circ + 20.4^\circ = 70.4^\circ$$

From [Equation \(3\)](#), $H = 0$; therefore from [Equation \(7\)](#), $\sin \phi = 0$ and thus, $\phi = 0^\circ$. Because the collector faces south, $\psi = 0^\circ$, and $\gamma = \phi$. Thus $\gamma = 0^\circ$. Then [Equation \(9\)](#) gives

$$\begin{aligned}\cos \theta &= \cos 70.4^\circ \cos 0^\circ \sin 30^\circ + \sin 70.4^\circ \cos 30^\circ \\ &= (0.335)(1)(0.5) + (0.942)(0.866) \\ &= 0.983 \\ \theta &= 10.6^\circ\end{aligned}$$

From [Figure 11](#), for $n = 1$, $\tau = 0.87$ and $\alpha = 0.96$.

From [Figure 12](#), for an absorber plate temperature of 140°F and an air temperature of 85°F , $U_L = 1.3 \text{ Btu/h} \cdot \text{ft}^2 \cdot ^\circ\text{F}$.

Then from [Equation \(19\)](#),

$$q_u = 306(0.87 \times 0.96) - 1.3(140 - 85) = 184 \text{ Btu/h} \cdot \text{ft}^2$$

Collector efficiency η is

$$184/306 = 0.60$$

The general expression for collector efficiency is

$$\eta = (\tau\alpha)_\theta - U_L(t_p - t_a)/I_{t\theta} \quad (21)$$

For incident angles below about 35° , the product $\tau\alpha$ is essentially constant, and [Equation \(28\)](#) is linear with respect to the parameter $(t_p - t_a)/I_{t\theta}$, as long as U_L remains constant.

ASHRAE (in Jordan and Liu 1977) suggested introducing an additional term, the **collector heat removal factor** F_R , to allow the use of the fluid inlet temperature in [Equations \(19\)](#) and [\(21\)](#):

$$q_u = F_R [I_{t\theta}(\tau\alpha)_\theta - U_L(t_{fi} - t_a)] \quad (22)$$

$$\eta = F_R (\tau\alpha)_\theta - F_R U_L(t_{fi} - t_a)/I_{t\theta} \quad (23)$$

where F_R equals the ratio of the heat actually delivered by the collector to the heat that would be delivered if the absorber were at t_{fi} . F_R is found from the results of a test performed in accordance with ISO *Standard* 9806-2017. The Solar Rating and Certification Corporation (SRCC) conducts this test in the United States and publishes the results, along with day-long performance outputs. Similar organizations around the world (e.g., the International Organization for Standardization [ISO], the European Committee for Standardization [CEN], Commonwealth Scientific and Industrial Research Organization [CISRO]) provide similar test results. For additional information on SRCC ratings, see [Chapter 37 of the 2020 ASHRAE Handbook—HVAC Systems and Equipment](#).

The results of such a test are plotted in [Figure 12](#). When the parameter is zero, because there is no temperature difference between fluid entering the collector and the atmosphere, the value of the y -intercept equals $F_R(\tau\alpha)$. The slope of the efficiency line equals the overall heat loss factor U_L multiplied by F_R . For the single-glazed, nonselective collector with the test results shown in [Figure 12](#), the y -intercept is 0.82, and the x -intercept is $0.69 \text{ ft}^2 \cdot \text{h} \cdot ^\circ\text{F/Btu}$. This collector used high-transmittance single glazing, $\tau = 0.91$, and black paint with an absorptance of 0.97, thus $F_R = 0.82/(0.91 \times 0.97) = 0.93$.

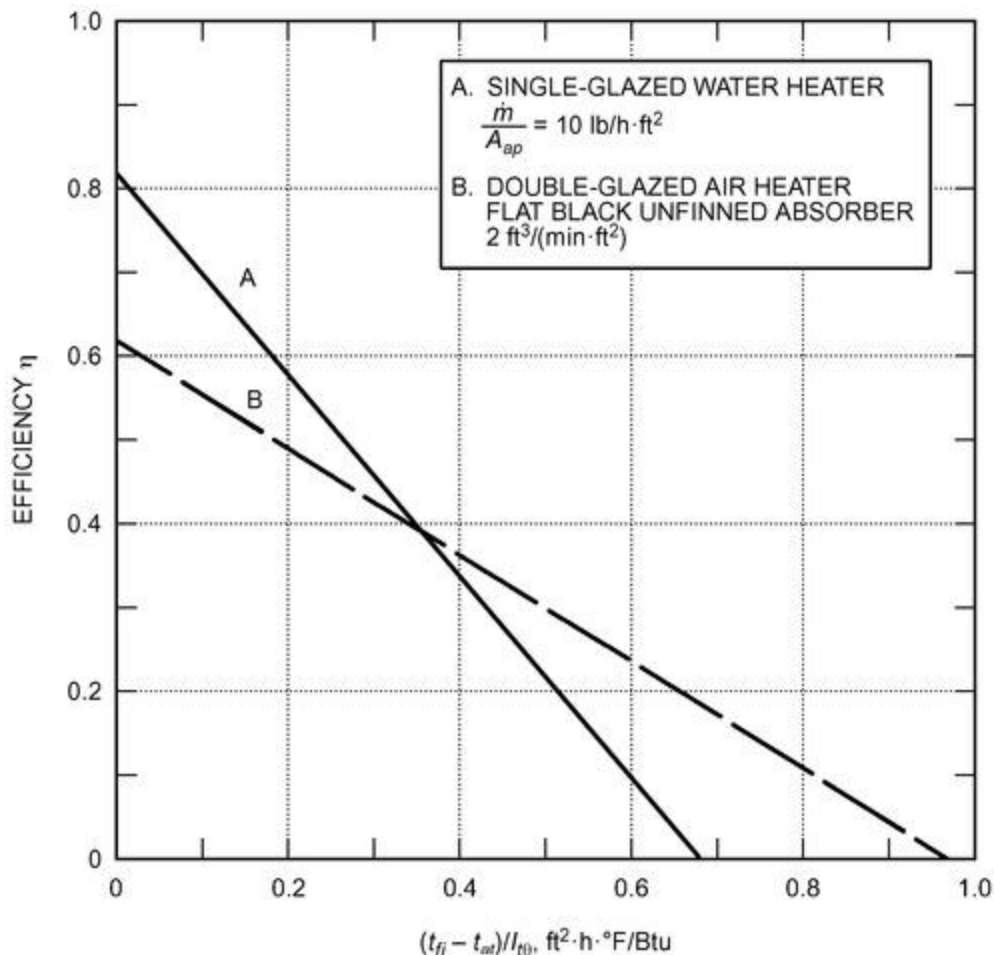


Figure 12. Efficiency Versus $(t_{fi} - t_{at})/I_{t0}$ for Single-Glazed Solar Water Heater and Double-Glazed Solar Air Heater

Assuming that the relationship between η and the parameter is actually linear, as shown, then the slope is $-0.82/0.69 = -1.19$; thus $U_L = 1.19/F_R = 1.19/0.93 = 1.28 \text{ Btu/h} \cdot \text{ft}^2 \cdot ^\circ\text{F}$. The tests on which [Figure 13](#) is based were run indoors. Wind speed and fluid velocity can affect measured efficiency.

[Figure 12](#) also shows the efficiency of a double-glazed air heater with an unfinned absorber coated with flat-black paint. The y-intercept for the air heater B is considerably less than it is for water heater A because (1) transmittance of the double glazing used in B is lower than the transmittance of the single glazing used in A and (2) F_R is lower for B than for A because of the lower heat transfer coefficient between air and the unfinned metal absorber.

The x-intercept for air heater B is greater than for water heater A because the upward loss coefficient U_L is much lower for the double-glazed air heater than for the single-glazed water heater. The data for both A and B were taken at near-normal incidence with high values of I_{t0} . For Example 5, using a single-glazed water heater, the value of the parameter would be close to $(140 - 85)/306 = 0.18 \text{ ft}^2 \cdot \text{h} \cdot ^\circ\text{F/Btu}$, and the estimated efficiency, 0.60, agrees closely with the test results.

When irradiation is below about $100 \text{ Btu/h} \cdot \text{ft}^2$, losses from the collector may exceed the heat that can be absorbed. This situation varies with the temperature difference between the collector inlet temperature and the ambient air, as suggested by [Equation \(22\)](#).

When the incident angle rises above 30° , the product of the glazing's transmittance and the absorber plate's absorptance $\tau\alpha$ begins to diminish; thus, heat absorbed also drops. Losses from the collector are generally higher as time moves farther from solar noon, and consequently efficiency also drops. Thus, day-long efficiency is lower than near-noon performance. During early afternoon, efficiency is slightly higher than at the comparable morning time, because the ambient air temperature is lower in the morning than in the afternoon.

ISO Standard 9806-2017 describes the **incident angle modifier**, which may be found by tests run when the incident angle is set at 30° , 45° , and 60° . The incident angle modifier is the ratio of the actual $(\tau\alpha)_\theta$ factor at some incidence angle θ to the normal $(\tau\alpha)_n$ factor at normal incident radiation; for normal angles of incidence, the modifier is unity. Simon (1976) showed that for many flat-plate collectors, the incident angle modifier is a linear function of the quantity $(1/\cos \theta - 1)$. For evacuated tubular collectors, the incident angle modifier may grow with θ . For additional information on the incident angle modifier, see ISO Standard 9806-2017 and [Chapter 37 of the 2020 ASHRAE Handbook—HVAC Systems and Equipment](#).

The efficiency should be reported in terms of the gross collector area A_g rather than the aperture area A_{ap} . The reported efficiency is lower than that given by [Equation \(23\)](#), but the total energy collected is not changed by this simplification:

$$\eta_g = \frac{\eta_{ap} A_{ap}}{A_g} \quad (24)$$

Solar Concentrating Collectors

Temperatures far above those attainable by flat-plate collectors can be reached if a large amount of solar radiation is concentrated on a relatively small collection area. Simple **reflectors** can markedly increase the amount of direct radiation reaching a collector, as shown in [Figure 13A](#).

Because of the apparent movement of the sun across the sky, conventional concentrating collectors must follow the sun's daily motion. There are two methods by which the sun's motion can be readily tracked. The altazimuth method requires the tracking device to turn in both altitude and azimuth; when performed properly, this method enables the concentrator to track the sun exactly. **Paraboloidal solar furnaces** ([Figure 13B](#)) generally use this system. The polar, or equatorial, mounting points the axis of rotation at the North Star, tilted upward at the local latitude angle. By rotating the collector 15° per hour, it tracks the sun almost perfectly (perfectly on March 21 and September 21). If the collector surface or aperture must be kept normal to the solar rays, a second motion is needed to correct for the change in the solar declination. This motion is not essential for most solar collectors.

The maximum variation in the angle of incidence for a collector on a polar mount is $\pm 23.5^\circ$ on June 21 and December 21; the incident angle correction then is $\cos 23.5^\circ = 0.917$.

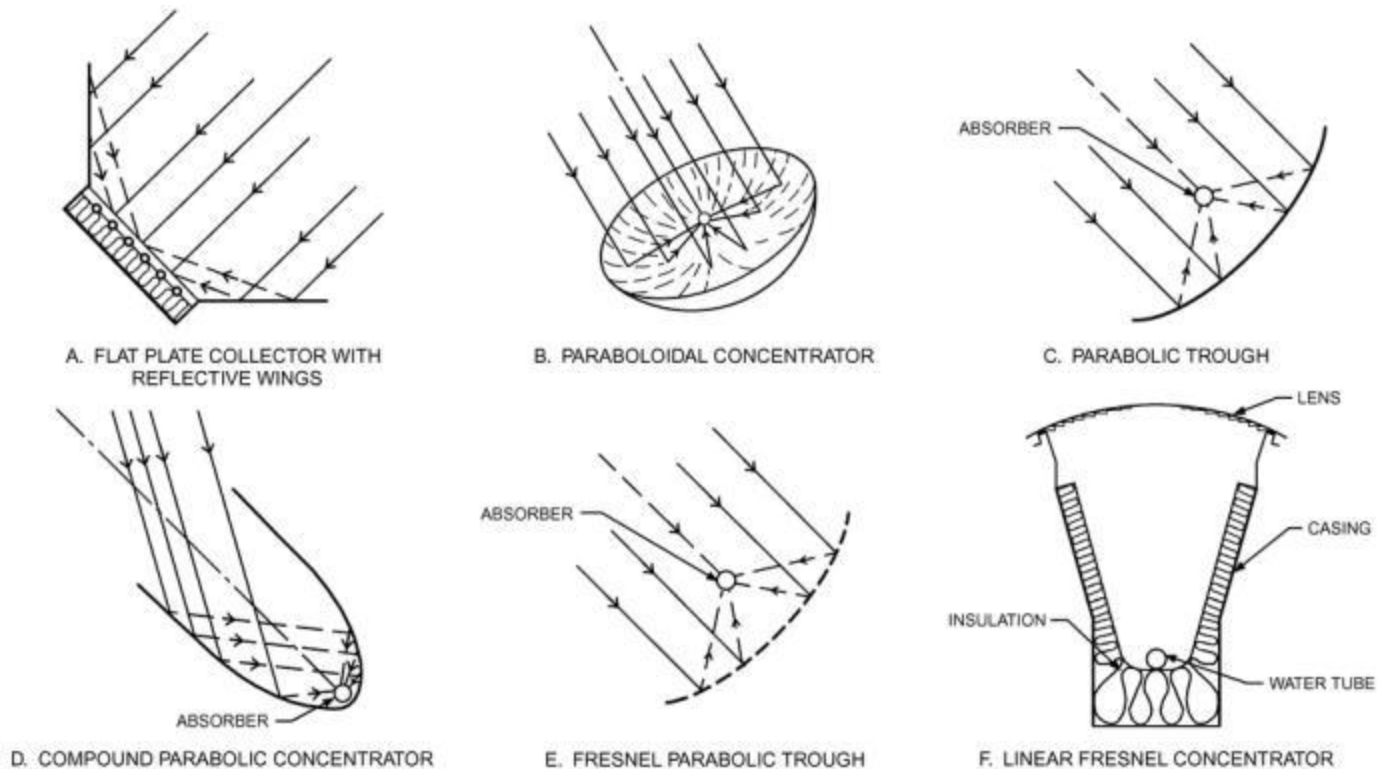


Figure 13. Types of Concentrating Collectors

Horizontal reflective parabolic troughs, oriented east and west ([Figure 13C](#)), require continuous adjustment to compensate for changes in the sun's declination. There is inevitably some morning and afternoon shading of the reflecting surface if the concentrator has opaque end panels. The necessity of moving the concentrator to accommodate the changing solar declination can be reduced by moving the absorber or by using a trough with two sections of a parabola facing each other, as shown in [Figure 13D](#). Known as a **compound parabolic concentrator (CPC)**, this design can accept incoming radiation over a relatively wide range of angles. By using multiple internal reflections, any accepted radiation that is accepted finds its way to the absorber surface located at the bottom of the apparatus. By filling the collector shape with a highly transparent material having an index of refraction greater than 1.4, the acceptance angle can be increased. By shaping the surfaces of the array properly, total internal reflection occurs at the medium/air interfaces, which results in a high concentration efficiency. Known as a **dielectric compound parabolic concentrator (DCPC)**, this device has been applied to the photovoltaic generation of electricity (Cole et al. 1977).

The parabolic trough of [Figure 13E](#) can be simulated by many flat strips, each adjusted at the proper angle so that all reflect onto a common target. By supporting the strips on ribs with parabolic contours, a relatively efficient

concentrator can be produced with less tooling than the complete reflective trough.

Another concept applies this segmental idea to flat and cylindrical lenses. A modification is shown in [Figure 13F](#), in which a linear **Fresnel lens**, curved to shorten its focal distance, can concentrate a relatively large area of radiation onto an elongated receiver. Using the equatorial sun-tracking mounting, this type of concentrator has been used to attain temperatures well above those that can be reached with flat-plate collectors.

One disadvantage of concentrating collectors is that, except at low concentration ratios, they can use only the direct component of solar radiation, because most types cannot concentrate the diffuse component. However, an advantage of concentrating collectors is that, in summer, when the sun rises and sets well to the north of the east-west line, the sun tracker, with its axis oriented north-south, can begin to accept radiation directly from the sun long before a fixed, south-facing flat plate can receive anything other than diffuse radiation from the portion of the sky that it faces. At 40° north latitude, for example, the cumulative direct radiation available to a sun tracker (on a clear day) is 3180 Btu/ft², whereas the total radiation falling on the flat plate tilted upward at an angle equal to the latitude is only 2220 Btu/ft² each day. Thus, in relatively sunny areas, the concentrating collector may capture more radiation per unit of aperture area than a flat-plate collector.

For extremely high inputs of radiant energy, many flat mirrors or heliostats using altazimuth mounts can be used to reflect their incident direct solar radiation onto a common target. Using slightly concave mirror segments on the heliostats, large amounts of thermal energy can be directed into the cavity of a steam generator to produce steam at high temperature and pressure.

3. WATER HEATING SYSTEMS

A solar water heater includes a solar collector that absorbs solar radiation and converts it to heat, which is then absorbed by a heat transfer fluid (water, a nonfreezing liquid, or air) that passes through the collector. The heat transfer fluid's absorbed thermal energy can be either stored or used directly.

Portions of the solar energy system are exposed to the weather, so they must be protected from freezing. The system must also be protected from overheating caused by high insolation levels during periods of low energy demand.

In solar water heating systems, water is heated directly in the collector or indirectly by a heat transfer fluid heated in the collector, passes through a heat exchanger, and transfers its heat to domestic or service water. The heat transfer fluid is transported by either natural or forced circulation. Natural circulation occurs by natural convection (thermosiphon), whereas forced circulation uses pumps or fans. Except for thermosiphon systems, which need no control, solar domestic and service water heaters are controlled by differential thermostats.

Five types of solar energy systems are used to heat domestic and service hot water: thermosiphon, direct circulation, indirect, integral collector storage, and site built. Recirculation and draindown are used to protect direct solar water heaters from freezing.

1.1 HOT-WATER SYSTEM COMPONENTS

This section describes the major components involved collecting, storing, transferring, controlling, and distributing of solar heat for a domestic hot-water (DHW) system.

Collectors. Flat-plate collectors are most commonly used for water heating because of the year-round load requiring temperatures of 80 to 180°F. For discussions of other collectors and applications, see [Chapter 37 of the 2020 ASHRAE Handbook—HVAC Systems and Equipment](#), and previous chapter sections. Collectors must withstand extreme weather (e.g., freezing, stagnation, high winds), as well as system pressures.

Heat Transfer Fluids. Heat transfer fluids transport heat from the solar collectors to the domestic water. There are potential chemical and mechanical problems with this transfer, primarily in systems where a heat exchanger interface exists with the potable water supply. The chemical compositions of the heat transfer fluids (pH, toxicity, and chemical durability) and their mechanical properties (specific heat and viscosity) must be considered.

Except for unusual cases, or when potable water is circulated, the energy transfer fluid is nonpotable and could contaminate the potable water. Even potable or nontoxic fluids in closed circuits are likely to become nonpotable because of contamination from metal piping, solder joints, and packing, or by the inadvertent installation of a toxic fluid at a later date.

Thermal Energy Storage. Heat collected by solar heating and service water heaters is virtually always stored in liquid tanks. Storage tanks and bins should be well insulated. In domestic hot-water systems, heat is usually stored in one or two tanks. The hot-water outlet is at the top of the tank, and cold (makeup) water enters the tank through a dip tube that extends down to within 4 to 6 in. of the tank bottom. The outlet on the tank to the collector loop should be approximately 4 in. above the tank bottom to prevent scale deposits from being drawn into the collectors. Water from the collector array returns to the top of the storage tank. A plumbing arrangement connecting the collector array to the middle to lower portion of the tank may take advantage of thermal stratification, depending on the delivery temperature from the collectors and the flow rate through the storage tank.

Single-tank electric auxiliary systems often incorporate storage and auxiliary heating in the same vessel. Conventional electric water heaters commonly have two heating elements: one near the top and one near the bottom. If a dual-element tank is used in a solar energy system, the bottom element should be disconnected and the top left functional

to take advantage of fluid stratification. Standard gas- and oil-fired water heaters should not be used in single-tank arrangements. In gas and oil water heaters, heat is added to the bottom of the tanks, reducing both stratification and collection efficiency in single-tank systems.

Dual-tank systems often use the solar domestic hot-water storage tank as a preheat tank. The second tank is normally a conventional domestic hot-water tank containing the auxiliary heat source. Multiple tanks are sometimes used in large institutions, where they operate similarly to dual-tank heaters. Although using two tanks may increase collector efficiency and the solar fraction, it increases tank heat losses. The makeup water inlet is usually a dip tube that extends near the bottom of the tank.

Estimates for sizing storage tanks usually range from 1 to 2.5 gal per square foot of solar collector area. The estimate used most often is 1.8 gal per square foot of collector area, which usually provides enough heat for a sunless period of about a day. The storage volume, however, also depends on the average storage temperature, and the storage volume should be analyzed and sized according to the project water requirements and draw schedule; however, solar applications typically require larger-than-normal tanks, usually the equivalent of the average daily load.

For details on thermal energy storage, see [Chapter 37 of the 2020 ASHRAE Handbook—HVAC Systems and Equipment](#).

Heat Exchangers. Indirect solar water heaters require one or more heat exchangers. Heat transfer from solar collectors to potable hot water has the potential to contaminate the water. Heat exchangers influence the effectiveness of energy collected to heat domestic water. They also separate and protect the potable water supply from contamination when nonpotable heat transfer fluids are used in the collector loop. For this reason, various codes regulate the need for and design of heat exchangers.

Heat exchanger selection should consider the following:

- Heat exchange effectiveness
- Pressure drop, operating power, and flow rate
- Design pressure, configuration, size, materials, and location
- Cost and availability
- Reliable protection of potable water supply from contamination by heat transfer fluid
- Leak detection, inspection, and maintainability
- Material compatibility with other elements (e.g., metals and fluids)
- Thermal compatibility with design parameters such as operating temperature, and fluid thermal properties

Heat exchanger selection depends on the characteristics of fluids that pass through the heat exchanger and the properties of the exchanger itself. Fluid characteristics to consider are fluid type, specific heat, mass flow rate, and hot- and cold-fluid inlet and outlet temperatures. Physical properties of the heat exchanger to consider are the overall heat transfer coefficient of the heat exchanger and the heat transfer surface area.

For most solar domestic hot-water designs, only the hot and cold inlet temperatures are known; the other temperatures must be calculated using the heat exchanger's physical properties. Two quantities that are useful in determining a heat exchanger's heat transfer and a collector's performance characteristics when it is combined with a given heat exchanger are the (1) fluid capacitance rate, which is the product of the mass flow rate and specific heat of fluid passing through the heat exchanger, and (2) heat exchanger effectiveness, which relates the capacitance rate of the two fluids to the fluid inlet and outlet temperatures. Effectiveness is equal to the ratio of the actual heat transfer rate to the maximum heat transfer rate theoretically possible. Generally, a heat exchanger effectiveness of 0.4 or greater is desired.

Expansion Tanks. An indirect solar water heater operating in a closed collector loop requires an expansion tank to prevent excessive pressure. Fluid in solar collectors under stagnation conditions can boil, causing excessive pressure to develop in the collector loop, and expansion tanks must be sized for this condition. Expansion tank sizing formulas for closed-loop hydronic systems, found in [Chapter 13 of the 2020 ASHRAE Handbook—HVAC Systems and Equipment](#), may be used for solar heater expansion tank sizing, with the volume of water in the system defined as the total volume of fluid in the solar collectors and of any piping located above the collectors, if significant. This sizing method provides a passive means for eliminating fluid loss through overtemperature or stagnation, common problems in closed-loop solar systems. It results in a larger expansion tank than typically found in hydronic systems, but the increase in cost is small compared to the savings in fluid replacement and maintenance costs (Lister and Newell 1989).

Pumps. Pumps circulate heat transfer liquid through collectors and heat exchangers. In solar domestic hot-water heaters, the pump is usually a centrifugal circulator driven by a motor of less than 300 W. The flow rate for collectors generally ranges from 0.015 to 0.04 gpm/ft². Pumps used in drainback systems must provide pressure to overcome friction and to lift the fluid to the collectors. The size of the pumps and piping must be carefully optimized, considering that pumps consume electrical energy.

Piping. Piping can be plastic, copper, galvanized steel, or stainless steel. The most widely used is nonlead, sweat-soldered L-type copper tubing. M-type copper is also acceptable if allowed by local building codes. If water/glycol is the heat transfer fluid, galvanized pipes or tanks must not be used because unfavorable chemical reactions will occur; copper piping is recommended instead. Also, if glycol solutions or silicone fluids are used, they may leak through joints where water would not. Piping should be compatible with the collector fluid passage material; for example, copper or plastic piping should be used with collectors having copper fluid passages.

Piping that carries potable water can be plastic, copper, galvanized steel, or stainless steel. In indirect systems, corrosion inhibitors must be checked and adjusted no less than annually, preferably every three months. Inhibitors should also be checked if the system overheats during stagnation. If dissimilar metals are joined, dielectric or nonmetallic couplings should be used. The best protection is sacrificial anodes or getters in the fluid stream. Their location depends on the material to be protected, anode material, and electrical conductivity of the heat transfer fluid. Sacrificial anodes of magnesium, zinc, or aluminum are often used to reduce corrosion in storage tanks. Because many possibilities exist, each combination must be evaluated. A copper-aluminum or copper-galvanized steel joint is unacceptable because of severe galvanic corrosion. Aluminum, copper, and iron have a greater potential for corrosion.

Elimination of air, accommodating thermal pipe expansion/contraction, and proper piping slope must be considered to avoid possible failures. Collector pipes (particularly manifolds) should be designed to allow expansion from stagnation temperature to extreme cold weather temperature. Expansion can be controlled with offset elbows in piping, hoses, or expansion couplings. Expansion loops should be avoided unless installed horizontally, particularly in systems that must drain for freeze protection. The collector array piping should slope 0.06 in. per foot for drainage (DOE 1978a).

Air can be eliminated by placing air vents at all piping high points and by air purging during filling. Flow control, isolation, and other valves in the collector piping must be chosen carefully so that these components do not restrict drainage significantly or back up water behind them. In systems without antifreeze, the collectors must drain completely.

Valves and Gages. Valves in solar domestic hot-water systems must be located to ensure system efficiency, satisfactory performance, and safety of equipment and personnel. Drain valves must be ball type; gate valves may be used if the stem is installed horizontally. Check valves or other valves used for freeze protection or reverse thermosiphoning must be reliable to avoid significant damage.

Auxiliary Heat Sources. On sunny days, a typical solar energy system should supply water at a predetermined temperature, and the solar storage tank should be large enough to hold sufficient water for a day or two. Because of the intermittent nature of solar radiation, an auxiliary heater must be installed to handle hot-water requirements. If a utility is the auxiliary energy source, auxiliary heater operation can be timed to take advantage of off-peak utility rates. The auxiliary heater should be carefully integrated with the solar energy heater to obtain maximum solar energy use. For example, the auxiliary heater should not destroy any stratification in the solar-heated storage tank, which would reduce collector efficiency.

Ductwork, particularly in systems with air-type collectors, must be sealed carefully to avoid leakage in duct seams, damper shafts, collectors, and heat exchangers. Ducts should be sized using conventional air duct design methods.

Controls. Controls regulate solar energy collection by controlling fluid circulation, activate system protection against freezing and overheating, and initiate auxiliary heating when it is required. The three major control components are sensors, controllers, and actuators. Sensors detect conditions or measure quantities, such as temperature. Controllers receive output from the sensors, select a course of action, and signal a component to adjust the condition. Actuators, such as pumps, valves, dampers, and fans, execute controller commands and regulate the system. The trend is to maintain a near-constant temperature difference between the collector outlet and inlet, to maximize daily heat collection. Currently, controls operate in a user-adjustable temperature difference range.

Temperature sensors measure the temperature of the absorber plate near the collector outlet and the bottom of the storage tank. The sensors send signals to a controller, such as a differential temperature thermostat, for interpretation.

The differential thermostat compares signals from the sensors with adjustable set points for high and low-temperature differentials. The controller performs different functions, depending on which set points are met. In liquid systems, when the temperature difference between the collector and storage reaches a high set point, usually 12 to 15°F, the pump starts, automatic valves are activated, and circulation begins. When the temperature difference reaches a low set point, usually 4°F, the pump is shut off and the valves are de-energized and returned to their normal positions. To restart the system, the differential temperature set point must again be met. If the system has either freeze or overheat protection, the controller opens or closes valves or dampers and starts or stops pumps or fans to protect the system when its sensors detect conditions indicating that either freezing or overheating is about to occur.

Sensors must be selected to withstand high temperatures, such as may occur during collector stagnation. Collector loop sensors should be located as close as possible to the outlet of the collectors, either in or on a pipe above or near the collector or in the collector outlet passage.

The storage temperature sensor should be near the bottom of the storage tank to detect fluid temperature before it is pumped to the collector or heat exchanger. Storage fluid is usually coldest at that location because of thermal stratification and the location of the makeup water supply. The sensor should be either securely attached to the tank and well insulated, or immersed inside the tank near the collector supply.

The freeze protection sensor, if required, should be located so that it detects the coldest liquid temperature when the collector is shut down. Common locations are the back of the absorber plate at the bottom of the collector, the collector intake or return manifolds, or the center of the absorber plate. The center of the absorber plate is recommended

because reradiation to the night sky freezes the collector heat transfer fluid, even though the ambient temperature is above freezing. Some system types, such as the recirculation system, have two sensors for freeze protection; others, such as the draindown, use only one.

Control of on/off temperature differentials affects system efficiency. If the differential is too high, the collector starts later than it should; if it is too low, the collector starts too soon. The turn-on differential for liquid systems usually ranges from 10 to 30°F and is commonly lower in warmer climates and higher in cold climates. For air systems, the range is usually 25 to 45°F.

The turn-off temperature differential is more difficult to estimate. Selection depends on a comparison between the value of the energy collected and the cost of collecting it. It varies with individual systems, but a value of 4°F is typical and generally the fixed default value in the control system.

Water temperature in the collector loop depends on ambient temperature, solar radiation, radiation from the collector to the night sky, and collector loop insulation. Freeze protection sensors should be set to detect 40°F.

Sensors are important but often overlooked control components. They must be selected and installed properly because no control can produce accurate outputs from unreliable sensor inputs. Sensors are used in conjunction with a differential temperature controller and are usually supplied by the controller manufacturer. Sensors must survive the anticipated operating conditions without physical damage or loss of accuracy. Low-voltage sensor circuits must be located away from high-voltage lines to avoid electromagnetic interference. Sensors attached to collectors should be able to withstand the stagnation temperature.

Sensor calibration, which is often overlooked by installers and maintenance personnel, is critical to system performance; a routine calibration maintenance schedule is essential.

Another control option is to use a photovoltaic (PV) panel that powers a DC pump. A properly sized and oriented PV panel converts sunlight into electricity to run a small circulating pump. No additional sensing is required because the PV panel and pump output increase with sunlight intensity and stop when no sunlight (collector energy) is available. However, to prevent operation when the collector outlet temperature is lower than the storage tank, a DC-powered differential controller may be used. Cromer (1984) showed that, with proper matching of pump and PV electrical characteristics, PV panel sizes as low as 5 W per 40 ft² panel may be sufficient. Difficulty with late starting and running too long in the afternoon can be alleviated by tilting the PV panel slightly to the east during commissioning of the installed system. Electronic devices such as a maximum power point tracker and linear current booster can also improve pump performance at start-up (Bai et al. 2011).

Thermosiphon Systems

Thermosiphon systems ([Figure 14](#)) heat potable water or a heat transfer fluid and rely on natural convection to transport it from the collector to storage. For direct systems, pressure-reducing valves are required when the city water pressure is greater than the working pressure of the collectors. In a thermosiphon system, the storage tank must be elevated above the collectors, which sometimes requires designing the upper-level floor and ceiling joists to bear this additional load. Extremely hard or acidic water can cause scale deposits that clog or corrode the absorber fluid passages. Thermosiphon flow is induced whenever there is sufficient sunshine, so these systems do not need pumps.

Direct-Circulation Systems

A direct-circulation system ([Figure 15](#)) pumps potable water from storage to the collectors when there is enough solar energy available to warm it. It then returns the heated water to the storage tank until needed. Collectors can be mounted either above or below the storage tank. Direct-circulation systems are only feasible in areas where freezing is infrequent. Freeze protection is provided either by recirculating warm water from the storage tank or by flushing the collectors with cold water. Direct water-heating systems should not be used in areas where the water is extremely hard or acidic because scale deposits may clog or corrode the absorber fluid passages, rendering the system inoperable.

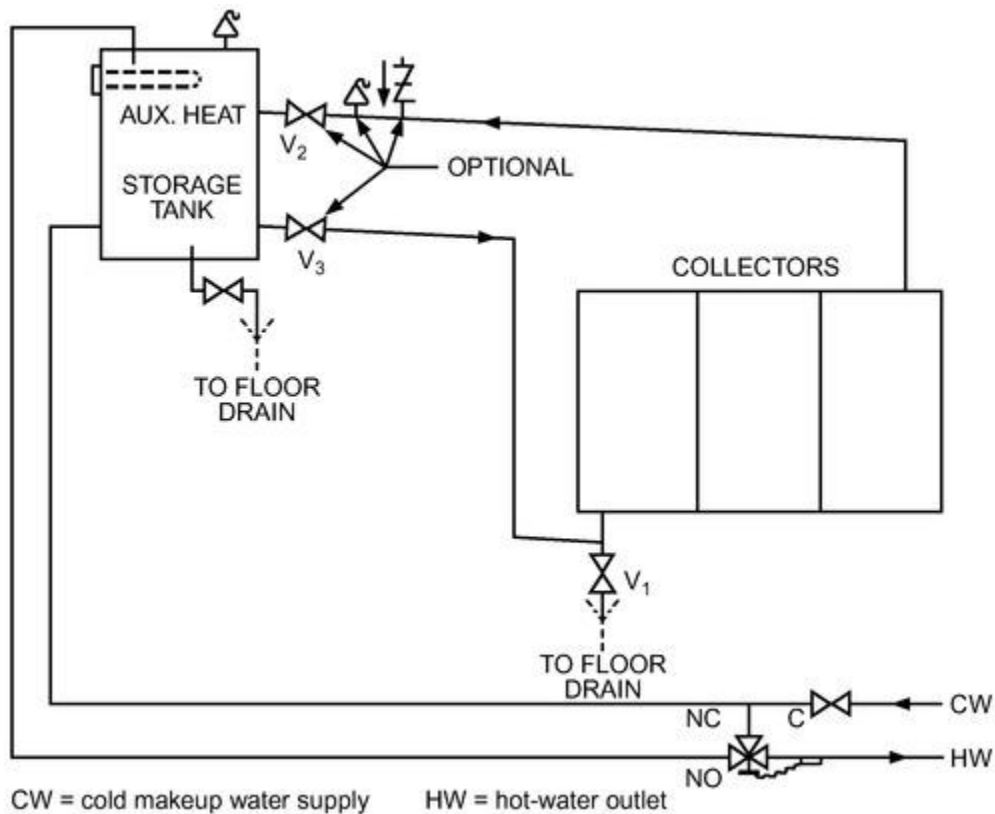


Figure 14. Thermosiphon System

Direct-circulation systems are exposed to city water line pressures and must withstand pressures as required by local codes. Pressure-reducing valves and pressure-relief valves are required when city water pressure is greater than the working pressure of the collectors. Direct-circulation systems often use a single storage tank for both solar energy storage and the auxiliary water heater, but two-tank storage systems can be used.

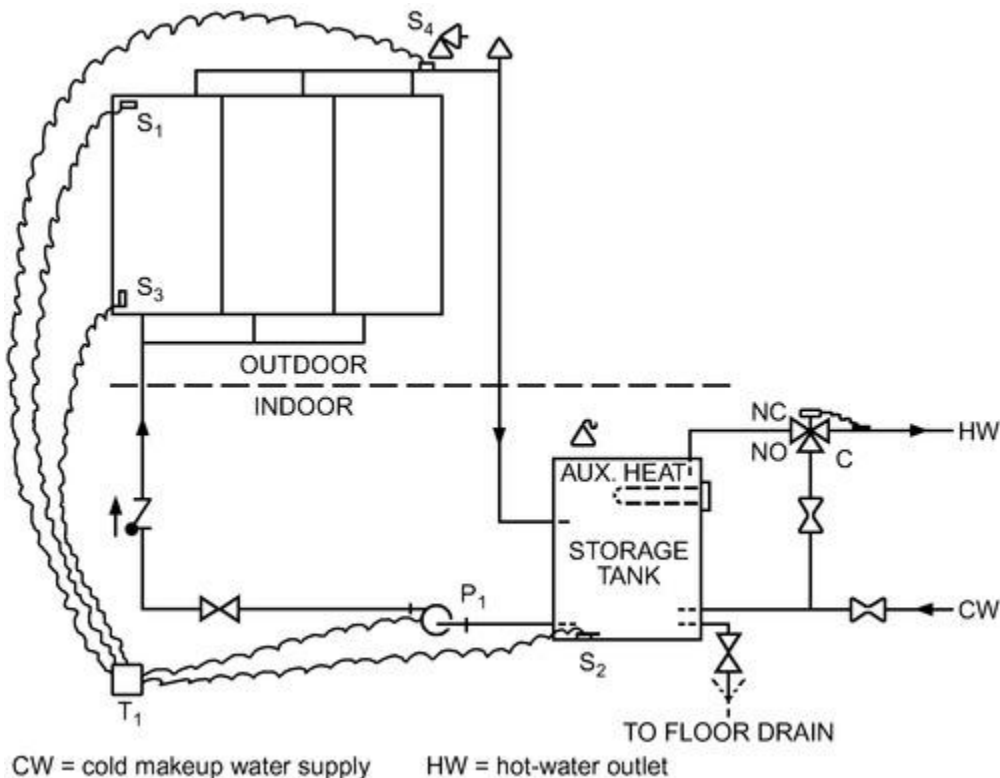


Figure 15. Direct Circulation System

Draindown Systems. Draindown systems (Figure 16) are direct-circulation water-heating systems in which potable water is pumped from storage to the collector array, where it is heated. Circulation continues until usable solar heat is no longer available. When a freezing condition is anticipated or a power outage occurs, the system drains automatically

by isolating the collector array and exterior piping from the city water pressure and using one or more valves for draining. Solar collectors and associated piping must be carefully sloped to drain the collector's exterior piping.

Indirect Water-Heating Systems

Indirect water-heating systems (Figure 17) circulate a freeze-protected heat transfer fluid through the closed collector loop to a heat exchanger, where its heat is transferred to the potable water. The most commonly used heat transfer fluids are water/ethylene glycol and water/propylene glycol solutions, although other heat transfer fluids such as silicone oils, hydrocarbons, and refrigerants can also be used (ASHRAE 1983). These fluids are nonpotable, sometimes toxic, and normally require double-wall heat exchangers. The double-wall heat exchanger can be located inside the storage tank, or an external heat exchanger can be used. The collector loop is closed and therefore requires an expansion tank and a pressure-relief valve. A one- or two-tank storage can be used. Additional overtemperature protection may be needed to prevent the collector fluid from decomposing or becoming corrosive.

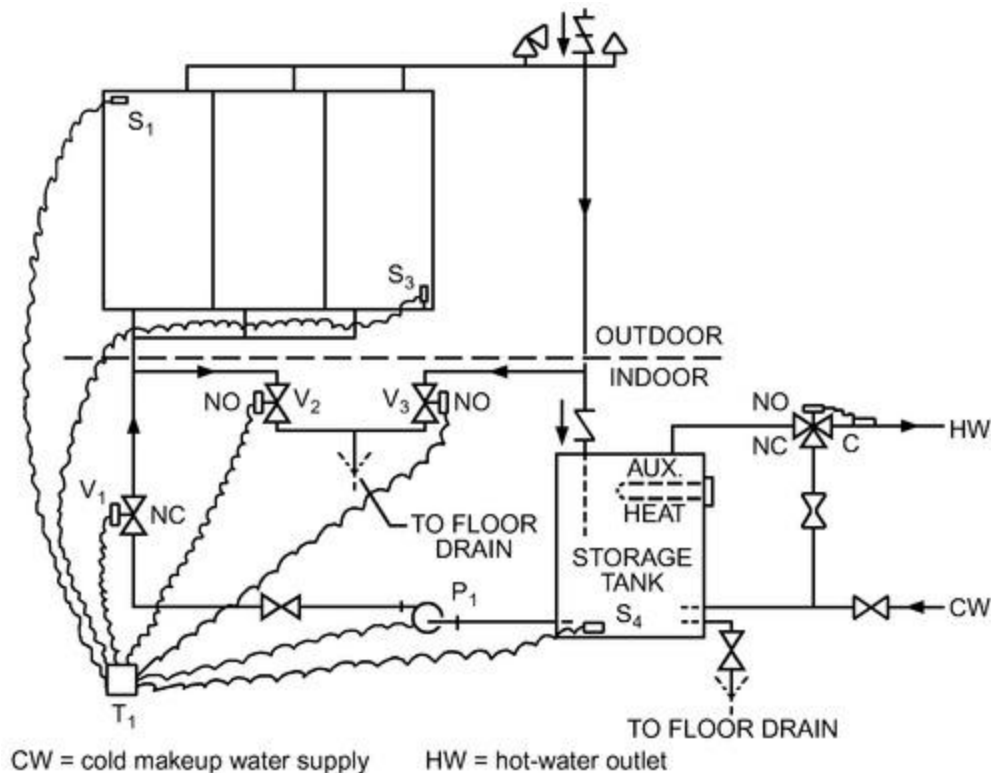


Figure 16. Draindown System

Designers should avoid automatic water makeup in systems using water/antifreeze solutions because a significant leak may raise the freezing temperature of the solution above the ambient temperature, causing the collector array and exterior piping to freeze. Also, antifreeze systems with large collector arrays and long pipe runs may need a time-delayed bypass loop around the heat exchanger to avoid freezing the heat exchanger on start-up.

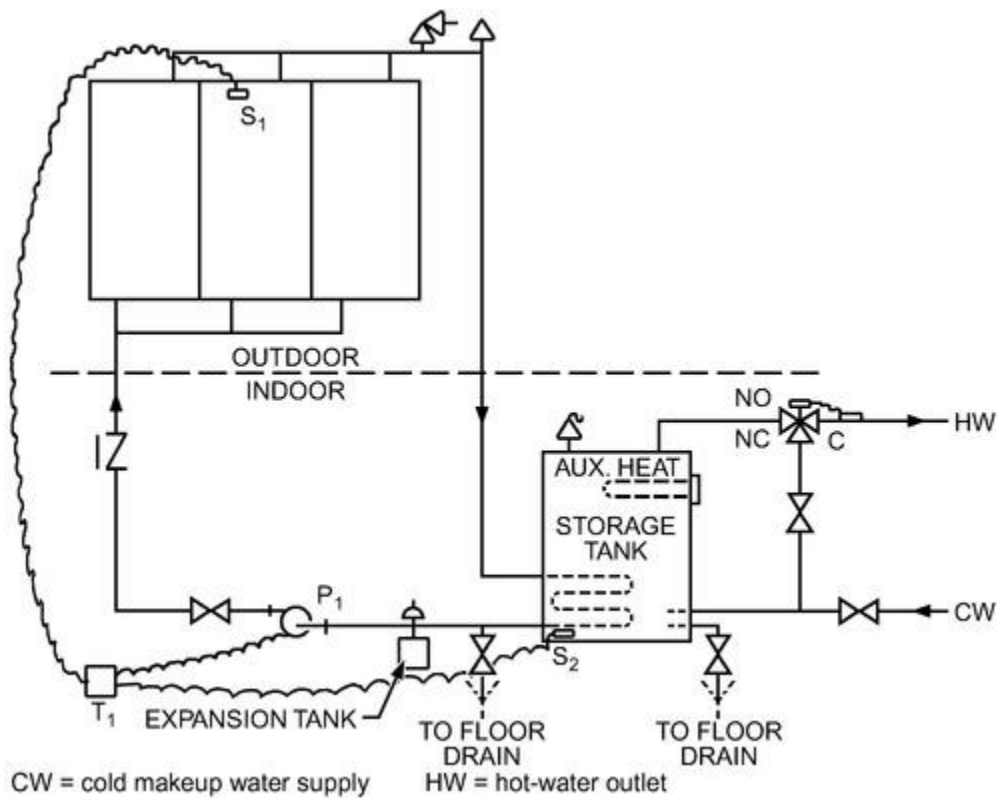


Figure 17. Indirect Water Heating

Drainback Systems. Drainback systems are generally indirect water-heating systems that circulate treated (typically demineralized water or 50% glycol/water) or untreated water through the closed collector loop to a heat exchanger, where its heat is transferred to the potable water. Circulation continues until usable energy is no longer available. When the pump stops, the collector fluid drains by gravity to the storage unit or tank. In a pressurized system, the tank also serves as an expansion tank, so it must have a temperature- and pressure-relief valve to protect against excessive pressure. In an unpressurized system ([Figure 18](#)), the tank is open and vented to the atmosphere.

The collector loop is isolated from the potable water, so valves are not needed to actuate draining, and scaling is not a problem. The collector array and exterior piping must be sloped to drain completely, and the pumping pressure must be sufficient to lift water to the top of the collector array.

Integral Collector Storage Systems

Integral collector storage (ICS) systems use hot-water storage as part of the collector. Some types use the surface of a single tank as the absorber, and others use multiple long, thin tanks placed side by side horizontally to form the absorber surface. In this latter type of ICS, hot water is drawn from the top tank, and cold replacement water enters the bottom tank. Because of the greater nighttime heat loss from ICS systems, they are typically less efficient than pumped systems, and using selective surfaces (see [Chapter 37 of the 2020 ASHRAE Handbook—Systems and Equipment](#)) is strongly recommended. ICS systems are normally installed as solar preheaters without pumps or controllers. Flow through the ICS system occurs on demand, as hot water flows from the collector to a hot-water auxiliary tank in the structure.

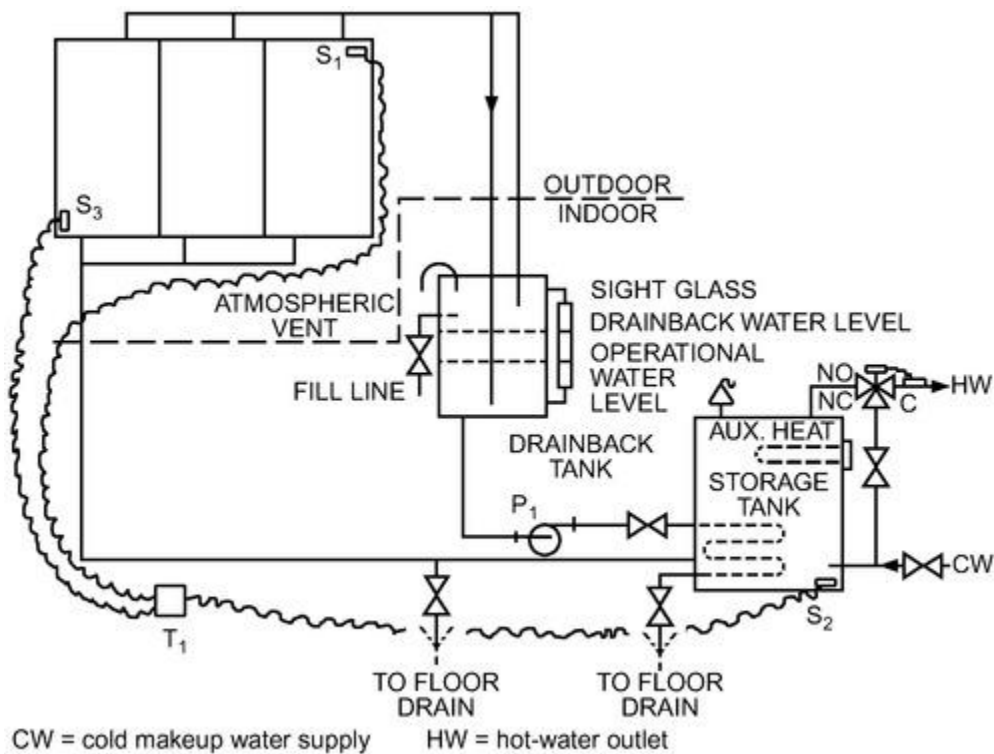


Figure 18. Drainback System

SRCC provides annual performance results for these various types of systems at www.solar-rating.org.

Site-Built Systems

Site-built, large-volume solar air- or water-heating equipment is used in commercial and industrial applications. These site-built systems are based on a transpired solar collector for air heating and shallow solar pond technologies.

Transpired Solar Collector. This collector preheats outdoor air by drawing it through small holes in a metal panel. It is typically installed on south-facing walls and is designed to heat outdoor air for building ventilation or process applications (Kutscher 1996). The prefabricated panel, made of dark metal with thousands of small holes, efficiently heats and captures fresh air by drawing it through a perforated absorber, eliminating the cost and reflection losses associated with a glazing. The sun heats the metal panel, which in turn heats a boundary layer of air on its surface. Air is heated as it is drawn through the small holes into a ventilation system for delivery as ventilation air, for crop drying, or other process applications (Shukla et al. 2012).

Shallow Solar Pond. The shallow solar pond (SSP) is a large-scale ICS solar water heater (Figure 19) capable of providing more than 5000 gal of hot water per day for commercial and industrial use. These ponds are built-in standard modules tied together to supply the required load. The SSP module can be ground mounted or installed on a roof. It is typically 16 ft wide and up to 200 ft long. The module contains one or two flat water bags similar to a water bed. The bags rest on a layer of insulation inside concrete or fiberglass curbs. The bag is protected against damage and heat loss by greenhouse glazing. A typical pond filled to a 4 in. depth holds approximately 6000 gal of water.

Pool Heaters

Solar pool heaters do not require a separate storage tank, because the pool itself serves as storage. In most cases, the pool's filtration pump forces the water through the solar panels or plastic pipes. In some retrofit applications, a larger pump may be required to handle the solar heater's needs, or a small pump may be added to boost pool water to the solar collectors.

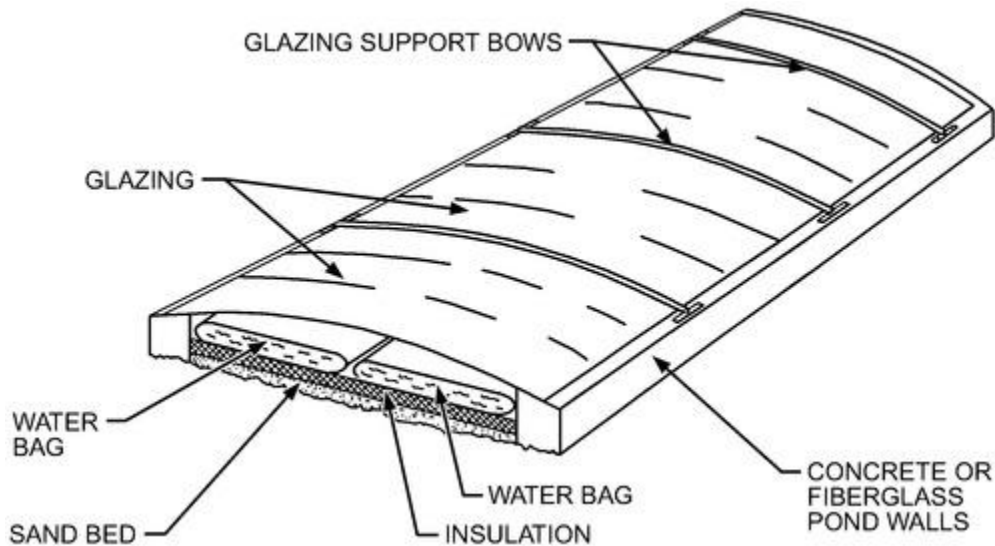


Figure 19. Shallow Solar Pond

Automatic control may be used to direct the flow of filtered water to the collectors when solar heat is available; this may also be accomplished manually. Normally, solar heaters are designed to drain down into the pool when the pump is turned off; this provides the collectors with freeze protection.

Four primary types of collector designs are used for swimming pool heat: (1) rigid black plastic panels (polypropylene), usually 4 by 10 ft or 4 by 8 ft; (2) tube-on-sheet panels, which typically have a metal deck (copper or aluminum) with copper water tubes; (3) an ethylene propylene-diene monomer (or ethylene-propylene terpolymer) (EPDM) rubber mat, extruded with water passages running its length; and (4) arrays of black plastic pipe, usually 1.5 in. diameter acrylonitrile butadiene styrene (ABS) plastic (Root et al. 1985).

Hot-Water Recirculation

Domestic hot-water (DHW) recirculation systems (Figures 20 and 21), which continuously circulate domestic hot water throughout a building, are found in motels, hotels, hospitals, dormitories, office buildings, and other commercial buildings. Recirculation heat losses in these systems are usually a significant part of the total water-heating load. In Figures 20 and 21, the three-way valve prevents heated water from returning to the solar storage tank when the return temperature is greater than the solar tank temperature. This ensures that heated water is used only when it is hot enough and prevents heating of the solar tank by the conventional heater. Using a cycle timer to control the DHW circulating pump that is synchronized with the building hot-water consumption profile can also help reduce circulation losses. The return line on the makeup preheat system can go directly to the conventional water heater to eliminate the three-way valve and prevent the solar tank from being heated by auxiliary energy.

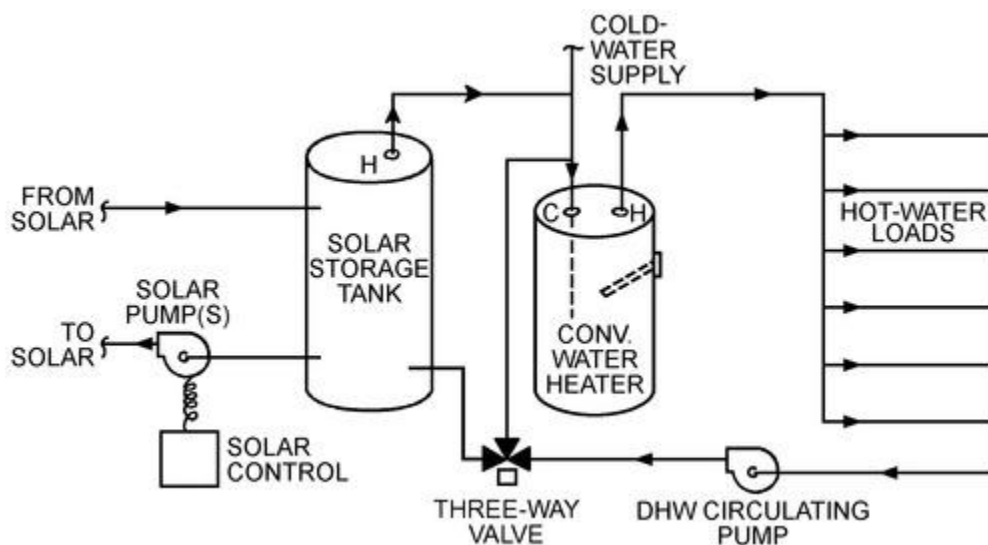


Figure 20. DHW Recirculation System

4. ACTIVE AND PASSIVE SYSTEMS FOR SOLAR HEATING AND COOLING SYSTEMS

The components and subsystems discussed previously may be combined to create a wide variety of solar heating and cooling systems. These systems fall into two principal categories: passive and active.

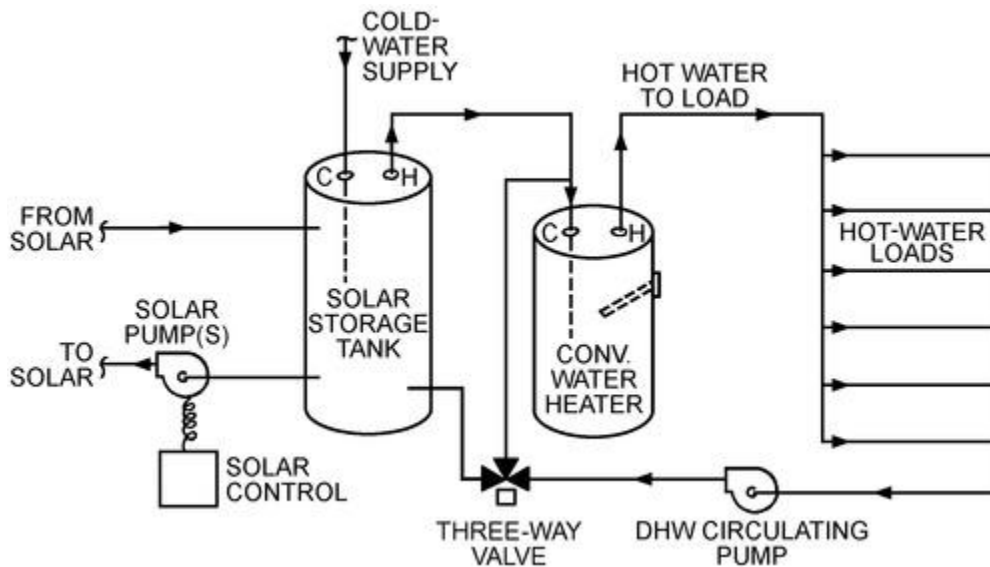


Figure 21. DHW Recirculation System with Makeup Preheat

Passive solar systems require little, if any, nonrenewable energy to make them function (Yellott 1977; Yellott et al. 1976). Every building is passive because the sun tends to warm it by day, and it loses heat at night. Passive systems incorporate solar collection, storage, and distribution into the architectural design of the building and make minimal or no use of fans to deliver the collected energy to the conditioned spaces. Passive solar heating, cooling, and lighting design must consider the building envelope and its orientation, the thermal storage mass, and window configuration and design. Athienitis and Santamouris (2002), Balcomb et al. (1984), DOE (1980/1982), LBL (1981), and Mazria (1979) give estimates of energy savings resulting from the application of passive solar design concepts.

One passive solar system is the **trombe wall**, which is a solar FPC usually on a vertical or inclined position as BIPV. It absorbs and stores solar heat on the thick trombe wall; this heat is used in heating indoor air by either natural or forced convection. Efficiency is around 13% (Torcellini and Pless 2004).

Active solar systems use either liquid or air as the collector fluid. Active systems must have a continuous availability of electricity to operate pumps and fans. A complete system includes solar collectors, energy storage devices, and pumps or fans for transferring energy to storage or to the load. The load can be space cooling, heating, or hot water. Although it is technically possible to construct a solar heating and cooling system to supply 100% of the design load, such a system would be uneconomical and oversized. The size of the solar system, and thus its ability to meet the load, is determined by life-cycle cost analysis that weighs the cost of energy saved against the amortized solar cost.

Active solar energy systems have been combined with heat pumps for water and/or space heating. The most economical arrangement in residential heating is a solar system in parallel with a heat pump, which supplies auxiliary energy when the solar source is unavailable. For domestic water systems requiring high water temperatures, a heat pump placed in series with the solar storage tank may be advantageous. Freeman et al. (1979) and Morehouse and Hughes (1979) present information on performance and estimated energy savings for solar-heat pumps.

Hybrid systems combine elements of both active and passive systems. They require some nonrenewable energy, but the amount is so small that they can maintain a coefficient of performance (COP) of about 50. An example is a floor slab thermal storage system that reradiates heat to a load (e.g., a building conditioned space) from a thermal mass surface after having been charged using an air collection system where insulated ducts feed warm air into cavities created within the heat storage slab (Howard 1986). Combining passive with active solar systems and other renewable energy sources is often the most satisfactory way to achieve very high annual solar savings (Swift and Lawrence 2010).

Passive Systems

A well-designed passive solar building needs (1) an appropriate thermal load (i.e., minimize heating loads first); (2) aperture, such as clear, glazed windows; (3) thermal storage (e.g., massive floors or walls, containers of water) to minimize overheating and to allow the use of heat at night; (4) control, either manual or automatic, to address overheating; and (5) night insulation of the aperture so that there is not a net heat loss (Swift and Lawrence 2010). Passive systems may be divided into several categories. The first residence to which the name **solar house** was applied used a large expanse of south-facing glass to admit solar radiation; this is known as a **direct-gain** passive system. The solar collector (windows) and storage (e.g., floors, walls) are part of the occupied space and typically have the highest percentage of heating load met by solar energy. The optimal thermal mass is often around 8 in. thick high-density concrete for direct-gain floors over-conditioned basements. Optimization requires a design concept that captures and stores the highest amount of solar energy without unnecessarily increasing cost or complexity. Direct-gain surfaces should have high absorptivity (dark color) and should not be covered by carpet, tile, much furniture, or other obstacles that prevent absorption of available solar radiation. To reduce heat losses, the building's thermal mass should be well insulated from the outdoor environment or ground.

Indirect-gain passive systems use the south-facing wall surface or the roof to absorb solar radiation, which causes a rise in temperature that, in turn, conveys heat into the building in several ways. Pueblos and cliff dwellings built by indigenous peoples in what is now the southwestern United States used this principle. Glass has led to modern adaptations of the indirect-gain principle (Balcomb et al. 1977; Trombe et al. 1977; Wilson 1979). These systems operate as low-efficiency solar flat-plate air-type collectors. Their efficiency is around 13% (NREL 2004).

By glazing a large south-facing, massive masonry wall, solar energy can be absorbed during the day, and heat conduction to the inner surface provides radiant heating at night. The wall's mass and its relatively low thermal diffusivity delay the heat's arrival at the indoor surface until it is needed. The glazing reduces heat loss from the wall back to the atmosphere and increases the system's collection efficiency.

Openings in the wall near the floor and ceiling allow convection to transfer heat to the room. Air in the space between the glass and the wall warms as soon as the sun heats the outer surface of the wall. The heated air rises and enters the building through the upper openings. Cool air flows through the lower openings, and convective heat gain can be established as long as the sun is shining.

In another indirect-gain passive system, a metal roof/ceiling supports transparent plastic bags filled with water (Hay and Yellott 1969). Movable insulation above these water-filled bags is rolled away during the winter day to allow the sun to warm the stored water. The water then transmits heat indoors by convection and radiation. The insulation remains over the water bags at night or during overcast days. During the summer, the water bags are exposed at night for cooling by (1) convection, (2) radiation, and (3) evaporation of water on the bags. The insulation covers the water bags during the day to protect them from unwanted irradiation. Pittenger et al. (1978) tested a building for which water rather than insulation was moved to provide summer cooling and winter heating.

Attached greenhouses (sunspaces) can be used as solar attachments when the orientation and other local conditions are suitable. The greenhouse can provide a buffer between the exterior wall of the building and the outdoors. During daylight, warm air from the greenhouse can be introduced into the house by natural convection or a small fan.

In most passive systems, control is accomplished by moving a component that regulates the amount of solar radiation admitted into the structure. Manually operated window shades or venetian blinds are the most widely used and simplest controls, but they may also be operated automatically.

Passive heating and cooling systems have been effective in field demonstrations. A well-designed passive-solar-heated building may provide 45 to nearly 100% of daily heat requirements. Architectural design features can dramatically reduce air-conditioning loads through heat gain avoidance techniques and natural cooling, where climatically appropriate (Howard and Pollock 1982; Howard and Saunders 1989).

Passive solar daylighting has been shown to be cost effective, providing dual benefits: it both reduces electric power demand and lowers cooling costs in properly designed interiors and atrium spaces.

5. COOLING BY NOCTURNAL RADIATION AND EVAPORATION

Radiative cooling is a natural heat loss that causes the formation of dew, frost, and ground fog. Because its effects are the most obvious at night, it is sometimes termed **nocturnal radiation**, although the process continues throughout the day. Thermal infrared radiation, which affects the surface temperature of a building wall or roof, may be estimated using the **sol-air temperature** concept. Radiative cooling of window and skylight surfaces can be significant, especially during winter when the dew-point temperature is low.

The most useful parameter for characterizing the radiative heat transfer between horizontal nonspectral emitting surfaces and the sky is the **sky temperature** T_{sky} . If S designates the total downward radiant heat flux emitted by the atmosphere, then T_{sky} is defined as

$$T_{sky}^4 = S/\sigma \quad (25)$$

where $\sigma = 0.1712 \times 10^{-8} \text{ Btu/h} \cdot \text{ft}^2 \cdot ^\circ\text{R}^4$.

The sky radiance is treated as if it originates from a blackbody emitter of temperature T_{sky} . The **net radiative cooling rate** R_{net} of a horizontal surface with absolute temperature T_{rad} and a nonspectral emittance ϵ is then

$$R_{net} = \epsilon\sigma(T_{rad}^4 - T_{sky}^4) \quad (26)$$

Values of ϵ for most nonmetallic construction materials are about 0.9.

Radiative building cooling has not been fully developed. Design methods and performance data compiled by Hay and Yellott (1969) and Marlatt et al. (1984) are available for residential roof ponds that use a sealed volume of water covered by sliding insulation panels as the combined rooftop radiator and thermal storage. Other conceptual radiative cooling designs have been proposed, but more developmental work is required (Erell and Etzion 2000; Givoni 1981; Mitchell and Biggs 1979).

The sky temperature is a function of atmospheric water vapor, amount of cloud cover, and air temperature; the lowest sky temperatures occur under an arid, cloudless sky. The monthly average sky temperature depression, which is the average difference between the ambient air temperature and the sky temperature, typically is between 9 and 43°F throughout the continental United States. Martin and Berdahl (1984) calculated this quantity using hourly weather data from 193 sites, as shown in the contour map for July ([Figure 22](#)).

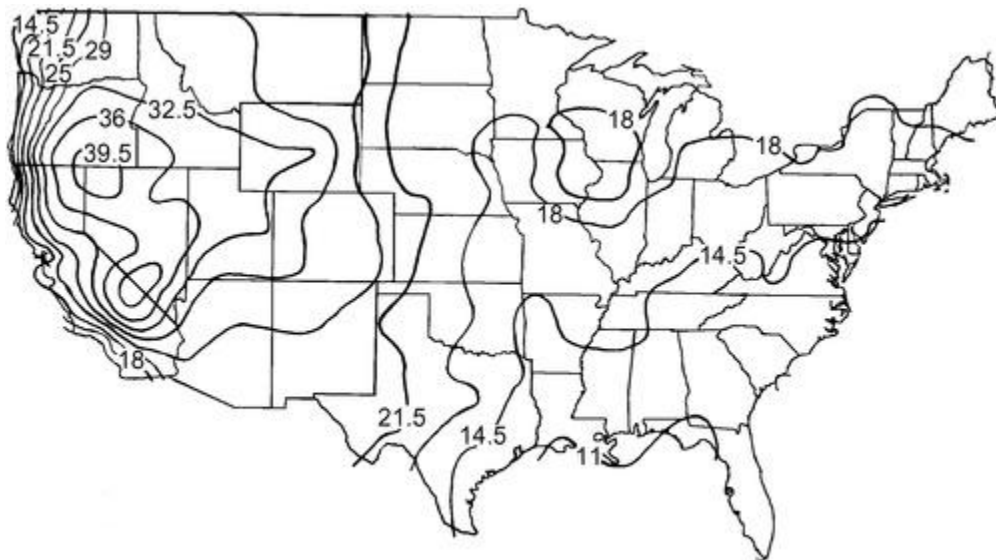


Figure 22. Average Monthly Sky Temperature Depression ($T_{air} - T_{sky}$) for July, °F (Adapted from Martin and Berdahl 1984)

The sky temperature may be too high at night to effectively cool the structure. Martin and Berdahl (1984) suggest that the sky temperature should be less than 61°F to achieve reasonable cooling in July (Figure 23). In regions where sky temperatures fall below 61°F 40% or more of the month, all nighttime hours are effectively available for radiative cooling.

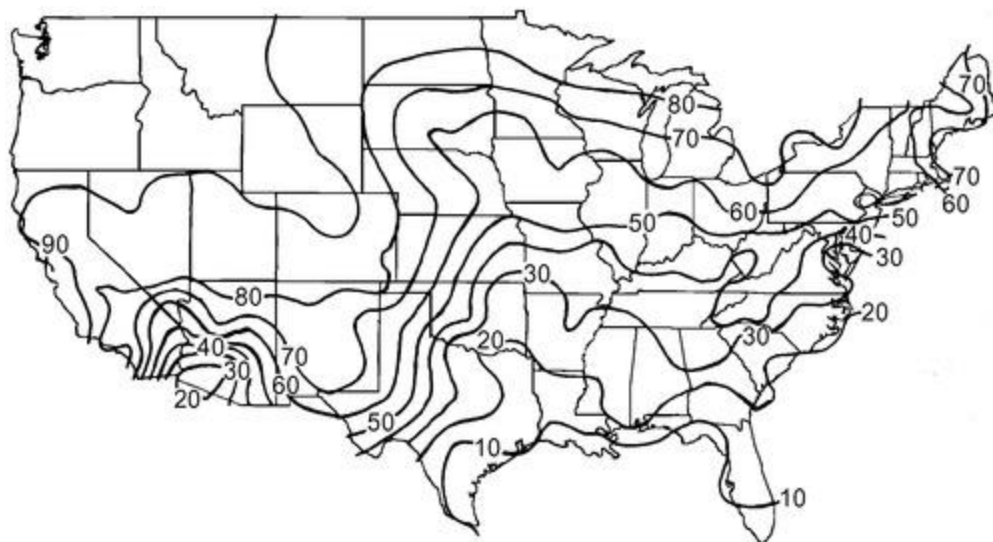


Figure 23. Percentage of Monthly Hours when Sky Temperature Falls below 61°F (Adapted from Martin and Berdahl 1984)

Clark (1981) modeled a horizontal radiator at various surface temperatures in convective contact with outdoor air for 77 U.S. locations. The average monthly cooling rates for a surface temperature of 76°F are plotted in Figure 24. If effective steps are taken to reduce the surface convection coefficient by modifying the radiator geometry or using an infrared-transparent glazing, it may be possible to improve performance beyond these values.

Argiriou et al. (1993) calculated the sky temperature depression and useful cooling energy of a typical flat-plate radiative air cooler for 28 southern European and four southeastern U.S. cities to estimate the effectiveness and feasibility of radiative cooling applications. The mean daily useful cooling energy delivered ranges between 17 and 66 Btu/ft² for average sky conditions and 22 and 70 Btu/ft² for clear-sky conditions. For areas with high humidity levels, such as the southeastern United States, the potential effectiveness is limited to 13 to 43 Btu/ft² for average sky conditions and 22 to 58 Btu/ft² for clear-sky conditions. Using a windscreen can improve performance in locations dominated by high wind speeds.

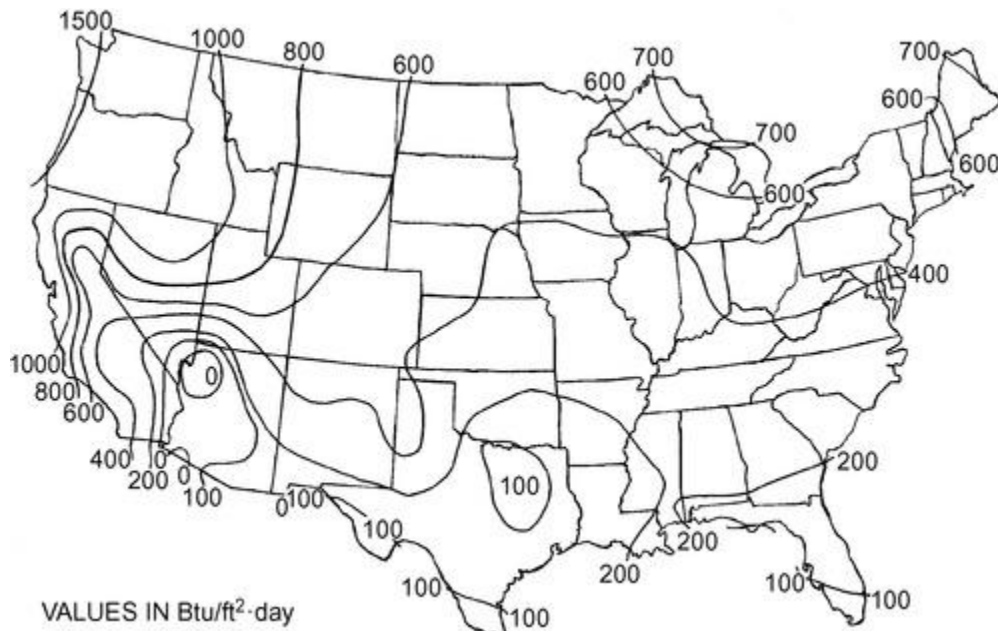


Figure 24. July Nocturnal Net Radiative Cooling Rate from Horizontal Dry Surface at 76°F (Adapted from Clark 1981)

Active Systems

Active systems absorb solar radiation with collectors and convey it to storage using a suitable fluid. As heat is needed, it is obtained from storage via heated air or water. Several types of thermostats exercise control, the first being a differential device that starts the flow of fluid through the collectors when they have been sufficiently warmed by the sun. It also stops fluid flow when the collectors no longer gain heat. In locations where freezing occurs only rarely, a low-temperature sensor on the collector controls a circulating pump when freezing is impending. This process wastes some stored heat, but it prevents costly damage to the collector panels. This system is not suitable for regions where freezing temperatures persist for long periods.

The space-heating thermostat is generally the conventional double-contact type that calls for heat when the temperature in the controlled space falls to a predetermined level. If the temperature in storage is adequate to meet the heating requirement, a pump or fan starts to circulate the warm fluid. If the temperature in the storage subsystem is inadequate, the thermostat calls on the auxiliary or standby heat source.

Space Heating and Service Hot Water

Solar combi systems are solar heating installations providing space heating as well as domestic hot water for the building occupants (IEA Task 26). The primary energy sources are solar and auxiliary sources such as biomass, gas, oil, or electricity, either direct or with a heat pump. The solar contribution (the part of the heating demand met by solar energy) varies from 10% to 100%, depending on the size of the solar collector surface, storage volume, heat load, and climate.

[Figure 25](#) shows one of the many systems for service hot water and space heating. In this case, a large, atmospheric-pressure storage tank is used, from which water is pumped to the collectors by pump P_1 in response to the differential thermostat T_1 . Drainback is used to prevent freezing because the amount of antifreeze required would be prohibitively expensive. Service hot water is obtained by placing a heat exchanger coil in the tank near the top, where, even if stratification occurs, the hottest water will be found.

An auxiliary water heater boosts the temperature of the sun-heated water when required. Thermostat T_2 senses the indoor temperature and starts pump P_2 when heat is needed. If the water in the storage tank becomes too cool to provide enough heat, the second contact on the thermostat calls for heat from the auxiliary heater.

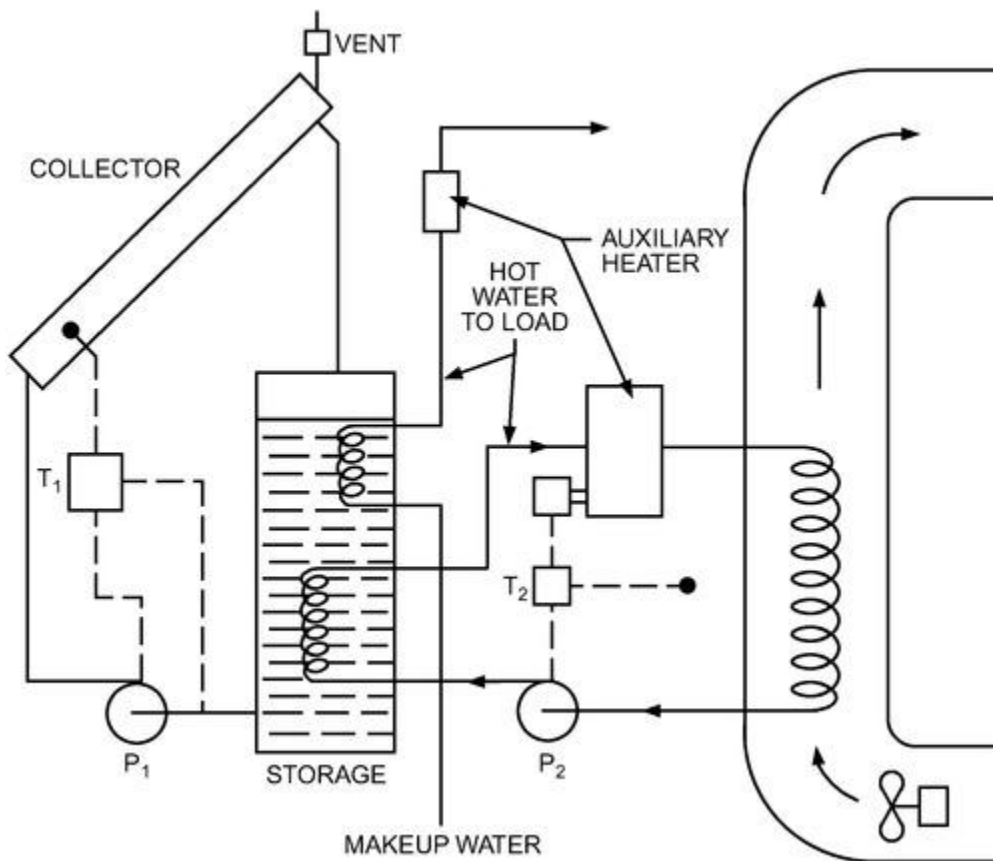


Figure 25. Solar Collection, Storage, and Distribution System for Domestic Hot Water and Space Heating

Standby heat becomes increasingly important as heating requirements increase. The heating load, winter availability of solar radiation, and cost and availability of auxiliary energy must be determined. It is rarely cost effective to provide the entire heating needs for either space or service hot water by using the solar heat collection and storage system alone.

Electric resistance heaters have the lowest first cost, but often have high operating costs. Water-to-air heat pumps, which use sun-heated water from the storage tank as the evaporator thermal energy source, are an alternative auxiliary heat source. The heat pump's COP is 10 to 14. When both summer cooling and winter heating are needed, the heat pump is a logical solution, particularly in large systems where a cooling tower is used to dissipate the heat withdrawn from the system.

The system shown in [Figure 25](#) may be retrofitted into a warm-air furnace. In such systems, the primary heater is deleted from the space heating circuit, and the coil is located in the return duct of the existing furnace. Full back-up is thus obtained, and the auxiliary heater provides only the heat not available at the storage temperature.

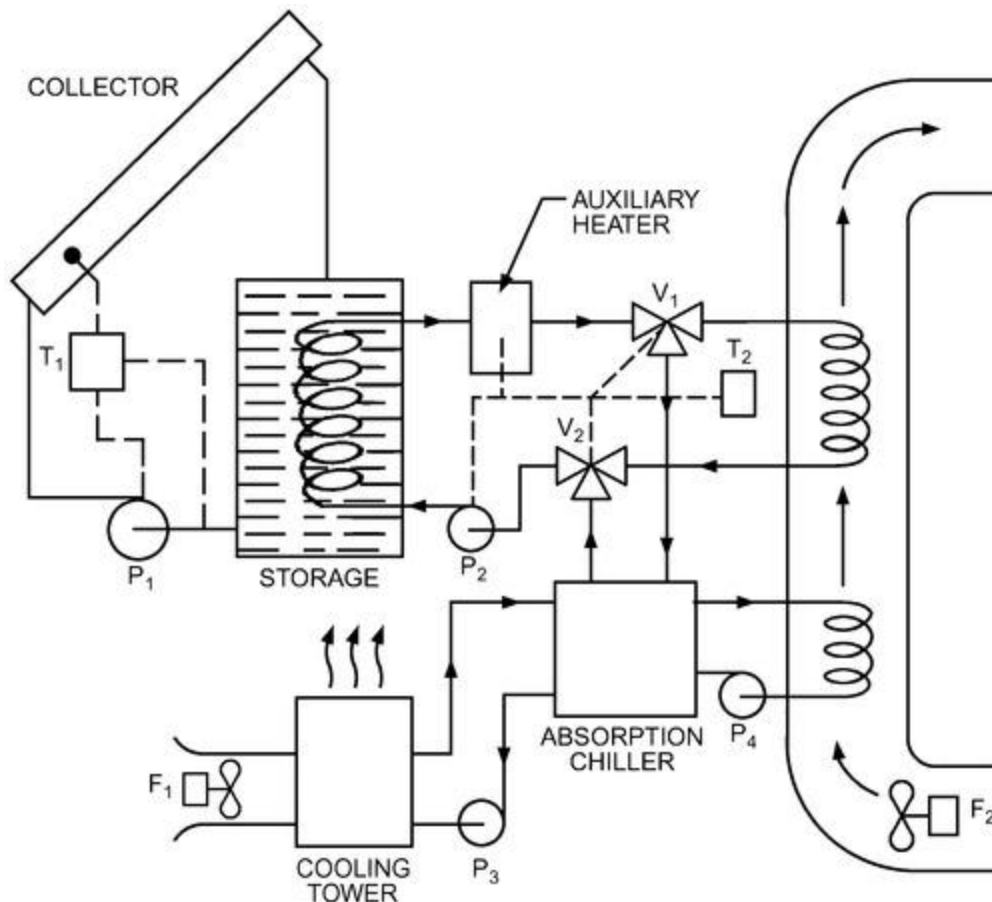
6. COOLING BY SOLAR ENERGY

Peak cooling demand in summer coincides with high solar radiation availability; this creates an excellent opportunity to exploit solar energy with heat-driven cooling machines. The main obstacle for large-scale applications, besides the currently high first cost, is the lack of practical experience with the design, control, operation, installation, and maintenance of these systems. For low-power cooling systems, there are limited commercially available technologies but strong ongoing research. Photovoltaic-operated refrigeration cycles and solar mechanical refrigeration also have applications of practical interest (Klein and Reindl 2005).

Swartman et al. (1974) emphasize various absorption systems. Newton (in Jordan and Liu 1977) discusses commercially available water vapor/lithium bromide absorption refrigeration systems. Standard absorption chillers are generally designed to give rated capacity for activating fluid temperatures well above 200°F at full load and design condenser water temperature. Few flat-plate solar collectors can operate efficiently in this range; therefore, a lower hot-fluid temperature is used when solar energy provides the heat. Both condenser water temperature and percentage of design load are determinants of the optimum energizing temperature, which can be quite low, sometimes below 120°F. Proper control can raise the COP under these part-load conditions. Adsorption cooling machines that operate at lower energizing temperatures but with lower COP may be another option for solar energy systems.

Many large commercial or institutional cooling installations must operate year round, and Newton (in Jordan and Liu 1977) showed that the low-temperature cooling water available in winter enables the LiBr/H₂O to function well with a hot-fluid inlet temperature below 190°F. Residential chillers in sizes as low as 1.5 tons, with an inlet temperature in the

When solar energy is used for cooling as well as for heating, the absorption system shown in [Figure 26](#) or one of its many modifications may be used. The collector and storage must operate at a temperature approaching 200°F on hot summer days when the water from the cooling tower exceeds 80°F, but considerably lower operating water temperatures may be used when cooler water is available from the tower. Controls for collection, cooling, and distribution are generally separated, with the circulating pump P_1 operating in response to the collector thermostat T_1 . Thermostat T_2 senses the indoor air-conditioned space temperature. When T_2 calls for heating, valves V_1 and V_2 direct water flow from the storage tank through the unactivated auxiliary heater to the fan-coil in the air distribution system. The fan F_2 in this unit may respond to the thermostat also, or it may have its own control circuit so that it can bring in outdoor air when the temperature is suitable.



When thermostat T_2 calls for cooling, the valves direct hot water into the absorption unit's generator, and pumps P_3 are activated to pump cooling tower water through the absorber and condenser circuits and chilled water through the cooling coil in the air distribution system. A relatively large hot-water storage tank allows the unit to operate when no sunshine is available. A chilled-water storage tank (not shown) may be added so that the absorption unit can operate during the day whenever water is available at a sufficiently high temperature to make the unit function efficiently. The COP of a typical lithium bromide/water absorption unit may be as high as 0.75 under favorable conditions, but frequent on/off cycling of the unit to meet a high variable cooling load may cause significant loss in performance because the unit must be heated to operating temperature after each shutdown. Modulating systems are analyzed differently than on/off systems.

Smaller domestic units may operate with natural circulation, or **percolation**, which carries the lithium bromide/water solution from the generator (to which the activating heat is supplied) to the separator and condenser; there, the

reconcentrated LiBr is returned to the absorber while the water vapor goes to the condenser before being returned to the evaporator, where cooling occurs. Larger units use a centrifugal pump to transfer the fluid.

Design, Control, and Operation Guidelines

Absorption is the most popular heat-driven cooling technology, although different sorption technologies are also available (e.g., adsorption, see [Chapter 32 of the 2021 ASHRAE Handbook—Fundamentals](#)). Each technology has specific characteristics that match the building's HVAC design, loads, and local climatic conditions. A good design must first exploit all available solar radiation and then cover the remaining loads from conventional sources (Henning 2007).

Proper calculations for collector and storage size depend on the solar cooling technology used. A hot-water storage unit may be integrated between the solar collectors and the heat-driven chiller to dampen fluctuations in the return temperature of the hot water from the chiller. Storage size depends on the application: when cooling loads mainly occur during the day, a smaller storage is necessary than when the loads peak in the evening. Strictly avoid heating the hot-water storage by the backup heat source. The storage only exists to store excess heat of the solar system and to make it available when sufficient solar heat is not available.

The single-effect absorption machine gives best results with a heat supply temperature of 176 to 212°F. Double- and triple-effect machines require higher supply temperatures. Therefore, these machines require a higher-temperature collector. However, with a double-effect system, if the solar-supplied temperature drops below 212°F, the performance drops sharply, below that of a single-effect.

Most large-scale applications (85 ton and up) use LiBr/H₂O and produce chilled water at about 43 to 45°F; the COP is relatively higher than for H₂O/ammonia (NH₃). However, LiBr systems must be water-cooled and thus usually require a cooling tower, whereas NH₃ systems can have an air-cooled condenser. Because of the large vapor volume of the water refrigerant, LiBr/H₂O chillers usually have large physical dimensions. For small cooling loads and for applications where it is not possible to use water cooling, an H₂O/NH₃ system is preferred.

In hot and sunny climates, the required solar collector area is approximately 114 to 152 ft²/ton. Higher heat supply temperatures for multieffect chillers require higher-cost evacuated tube or concentrating collectors and may need a high-temperature (i.e., thermochemical) storage.

In LiBr/H₂O systems, the refrigerant freezes at 32°F, so care is necessary while the machine is idle, especially in winter. Another potential problem is the crystallization of the LiBr solution at high concentrations, which may result from high generator temperatures or inadequate temperature control at other parts of the machine. Thus, the heat supply temperature from the solar collectors or heat storage must be adequately controlled. The cooling water temperature, particularly to the absorber, must also be monitored. Chiller capacity may be controlled by increasing the heat supply temperature or decreasing the cooling water temperature; both techniques increase capacity as well as the COP.

A fuel-fired boiler usually covers the need for a back-up system to heat the desorber of the heat-driven chiller. However, use caution because, during periods of low solar radiation availability, collectors connected in series with a back-up boiler can turn into a heat sink instead of a heat source. Alternatively, one may use a back-up conventional chiller alongside the solar-assisted machine, but this requires an additional full-sized chiller, which would be idle for long periods. A viable design solution for a single-effect absorption cycle is to incorporate an auxiliary desorber powered by the back-up, whereas the original desorber is powered by solar heat. The weak solution goes first to the solar-powered desorber, where it is concentrated as much as possible with the available solar heat, and then proceeds to the auxiliary desorber, where it is concentrated further using heat from the back-up source. Vapor from both desorbers is then supplied to the condenser.

7. SIZING SOLAR HEATING AND COOLING SYSTEMS: ENERGY REQUIREMENTS

Methods used to determine solar heating and/or cooling energy requirements for both active and passive/hybrid systems are described by Feldman and Merriam (1979) and Hunn et al. (1987). Descriptions of public- and private-domain methods are included. The following simulation techniques are suitable for active heating and cooling systems analysis, and for passive/hybrid heating, cooling, and lighting analysis.

Performance Evaluation Methods

The performance of any solar energy system is directly related to the (1) heating load, (2) amount of solar radiation available, and (3) solar energy system characteristics. Various calculation methods use different procedures and data when considering the available solar radiation. Some simplified methods only consider average annual solar radiation; complex methods may use hourly data.

Solar energy system characteristics, as well as individual component characteristics, are required to evaluate performance. The degree of complexity with which these systems and components are described varies from system to system.

The cost effectiveness of a solar domestic and service hot-water heating system depends on the initial cost and energy cost savings. A major task is to determine how much energy is saved. The **annual solar fraction** (the annual solar contribution to the water-heating load divided by the total water-heating load) can be used to estimate these savings. It is expressed as a decimal or percentage and generally ranges from 0.3 to 0.8 (30 to 80%), although more extreme values are possible.

Simplified Analysis Methods

A very simplified way to initially estimate the size of a solar heating system is to divide the average daily load by the daily output of a particular collector based on its SRCC rating for the application and solar conditions. This requires knowledge of the average daily incident solar radiation for the site and the type of collector best suited to the application. See [Chapter 37 of the 2020 ASHRAE Handbook—HVAC Systems and Equipment](#) for more information.

Simplified analysis methods have the advantages of computational speed, low cost, rapid turnaround (especially important during iterative design phases), and ease of use by persons with little technical experience. Disadvantages include limited flexibility for design optimization, lack of control over assumptions, and a limited selection of systems that can be analyzed. Thus, if the application, configuration, or load characteristics under consideration are significantly nonstandard, a detailed computer simulation may be required to achieve accurate results. This section describes the f -Chart method for active solar heating and the solar load ratio method for passive solar heating (Dickinson and Cheremisinoff 1980; Klein and Beckman 1979; Lunde 1980).

Water-Heating Load

The amount of hot water required must be estimated accurately because it affects component selection. Oversized storage may result in low-temperature water that requires auxiliary heating to reach the desired supply temperature. Undersizing can prevent the collection and use of available solar energy. [Chapter 50](#) gives methods to determine the load.

Active Heating/Cooling

Beckman et al. (1977) developed the f -Chart method using an hourly simulation program (Klein et al. 1976) to evaluate space heating and service water heating in many climates and conditions. These analyses correlate the fraction f of the heat load met by solar energy. The correlations give the fraction f of the monthly heating load (for space heating and hot water) supplied by solar energy as a function of collector characteristics, heating loads, and weather. The standard error of the differences between detailed simulations in 14 locations in the United States and the f -Chart predictions was about 2.5%. Correlations also agree within the accuracy of measurements of long-term performance data. Beckman et al. (1977, 1981) and Duffie and Beckman (2006) discuss the method in detail.

The f -Chart method requires the following data:

- Monthly average daily radiation on a horizontal surface
- Monthly average ambient temperatures
- Collector thermal performance curve slope and intercept from standard collector tests; that is, $F_R U_L$ and $F_R (\tau\alpha)_n$ (see ISO *Standard* 9806-2017 and [Chapter 37 of the 2020 ASHRAE Handbook—HVAC Systems and Equipment](#))
- Monthly space- and water-heating loads

Standard Systems

The f -Chart assumes several standard systems and applies only to these liquid configurations. The standard **liquid heater** uses water, an antifreeze solution, or air as the heat transfer fluid in the collector loop and water as the storage medium ([Figure 27](#)). Energy is stored in the form of sensible heat in a water tank. A water-to-air heat exchanger transfers heat from the storage tank to the building. A liquid-to-liquid heat exchanger transfers energy from the main storage tank to a domestic hot-water preheat tank, which in turn supplies solar-heated water to a conventional water heater. A conventional furnace or heat pump is used to meet the space heating load when the thermal energy in the storage tank is depleted.

[Figure 28](#) shows the assumed configuration for a **solar air heater** with a pebble-bed storage unit. Energy for domestic hot water is provided by heat exchange from the air leaving the collector to a domestic water preheat tank, as in the liquid system. The hot water is further heated, if necessary, by a conventional water heater. During summer operation, a seasonal, manually operated storage bypass damper is used to avoid heat loss from the hot bed into the building.

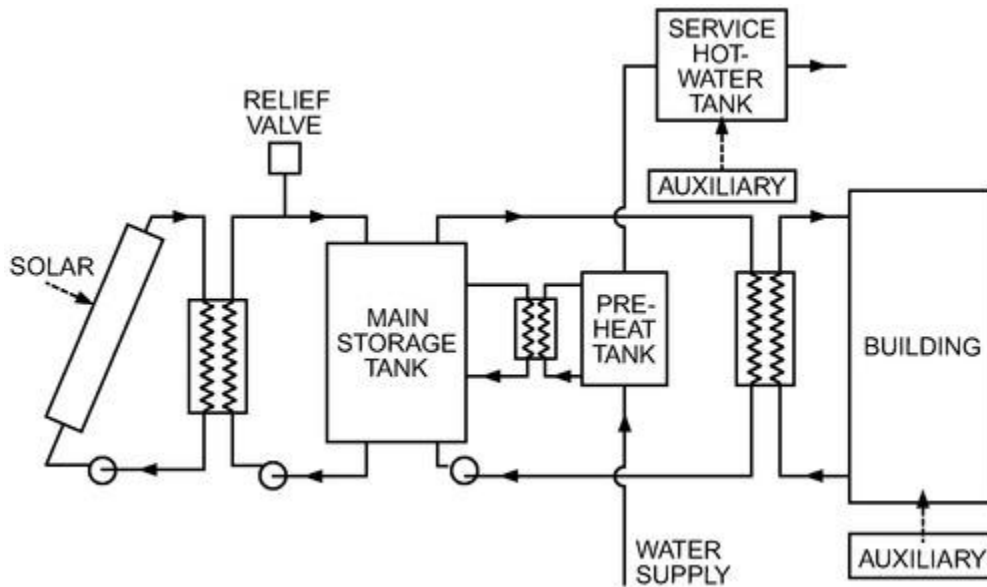


Figure 27. Liquid-Based Solar Heating System (Adapted from Beckman et al. 1977)

The standard **solar domestic water heater** collector heats either air or liquid. The collected energy is transferred by a heat exchanger to a domestic water preheat tank that supplies solar-heated water to a conventional water heater. The water is further heated to the desired temperature by conventional fuel if necessary.

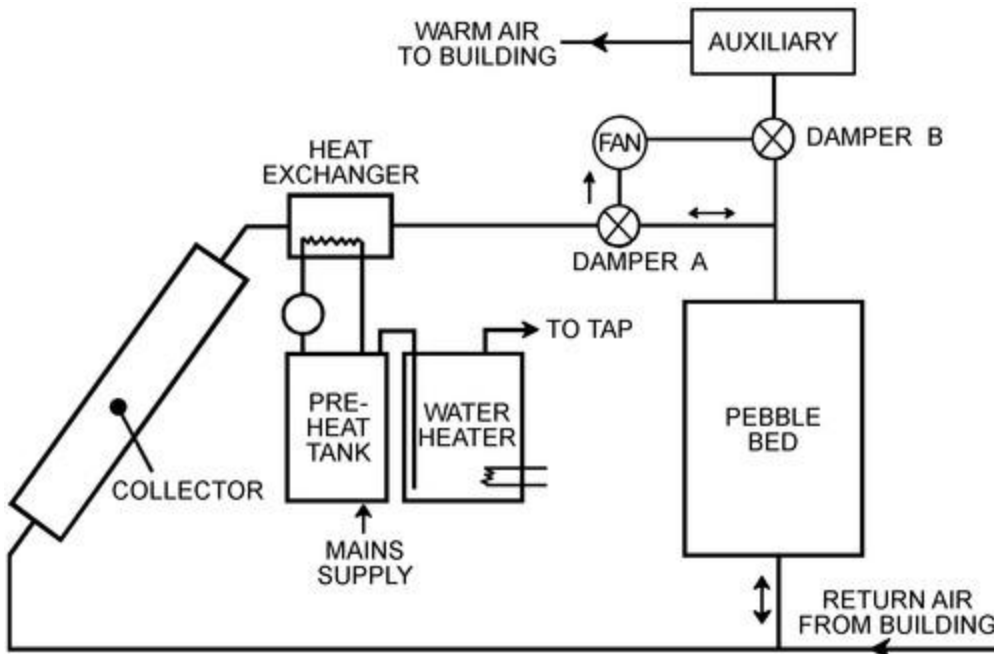


Figure 28. Solar Air Heating System (Adapted from Beckman et al. 1977)

***f*-Chart Method**

Computer simulations correlate dimensionless variables and the long-term performance of the systems. The fraction f of the monthly space- and water-heating loads supplied by solar energy is empirically related to two dimensionless groups. The first dimensionless group X is collector loss; the second Y is collector gain:

$$X = \frac{F_R U_L A_c \Delta \theta \left(\frac{F_r}{F_R} \right)}{L} (t_{ref} - \bar{t}_a) \quad (27)$$

$$Y = \frac{F_R (\tau \alpha)_n H_T N A_c \left(\frac{F_r}{F_R} \right) \left[\frac{(\tau \alpha)}{(\tau \alpha)_n} \right]}{L} \quad (28)$$

where

A_c = area of solar collector, ft²

F_r	=	collector heat exchanger efficiency factor
F_R	=	collector efficiency factor
U_L	=	collector overall energy loss coefficient, Btu/h · ft ² · °F
$\Delta\theta$	=	total number of hours in month
\bar{T}_a	=	monthly average ambient temperature, °F
L	=	monthly total heating load for space heating and hot water, Btu
\bar{H}_T	=	monthly averaged daily radiation incident on collector surface per unit area, Btu/day · ft ²
N	=	number of days in month
$(\tau\alpha)$	=	monthly average transmittance-absorptance product
$(\tau\alpha)_n$	=	normal transmittance-absorptance product
t_{ref}	=	reference temperature, 212°F

$F_R U_L$ and $F_R(\tau\alpha)_n$ are obtained from collector test results. The ratios F_r/F_R and $(\tau\alpha)/(\tau\alpha)_n$ are calculated using methods given by Beckman et al. (1977). The value of \bar{T}_a is obtained from meteorological records for the month and location desired. \bar{H}_T is calculated from the monthly averaged daily radiation on a horizontal surface by the methods previously discussed in this chapter or in Duffie and Beckman (2006). The monthly load L can be determined by any appropriate load-estimating method, including analytical techniques or measurements. Values of the collector area A_c are selected for the calculations. Thus, all the terms in these equations can be determined from available information.

The transmittance τ of the transparent collector cover and the absorptance α of the absorber plate depend on the angle of incidence of solar radiation on the collector surface. Collector tests are usually run with the radiation nearly perpendicularly incident on the collector. Thus, the value of $F_R(\tau\alpha)_n$ determined from these tests ordinarily corresponds to the transmittance and absorptance values for radiation at normal incidence. Depending on collector orientation and time of year, the monthly average values of transmittance and absorptance can be significantly lower. The f -Chart method requires knowledge of the ratio of the monthly average to normal incidence transmittance-absorptance.

The f -Chart method for liquid systems is similar to that for air systems. The fraction of the monthly total heating load supplied by the solar air heating system is correlated with the dimensionless groups X and Y , as shown in [Figure 29](#). To determine the fraction of the heating load supplied by solar energy for a month, values of X and Y are calculated for the collector and heating load in question. The value of f is determined at the intersection of X and Y on the f -Chart, or from the following equivalent equations.

Air system:

$$f = 1.04Y - 0.065X - 0.159Y^2 + 0.00187X^2 - 0.0095Y^3 \quad (29)$$

Liquid system:

$$f = 1.029Y - 0.065X - 0.245Y^2 + 0.0018X^2 - 0.025Y^3 \quad (30)$$

This is done for each month of the year. The solar energy contribution for the month is the product of f and the total heating load L for the month. Finally, the fraction F of the annual heating load supplied by solar energy is the sum of the monthly solar energy contributions divided by the annual load:

$$F = \frac{\sum fL}{\sum L} \quad (31)$$

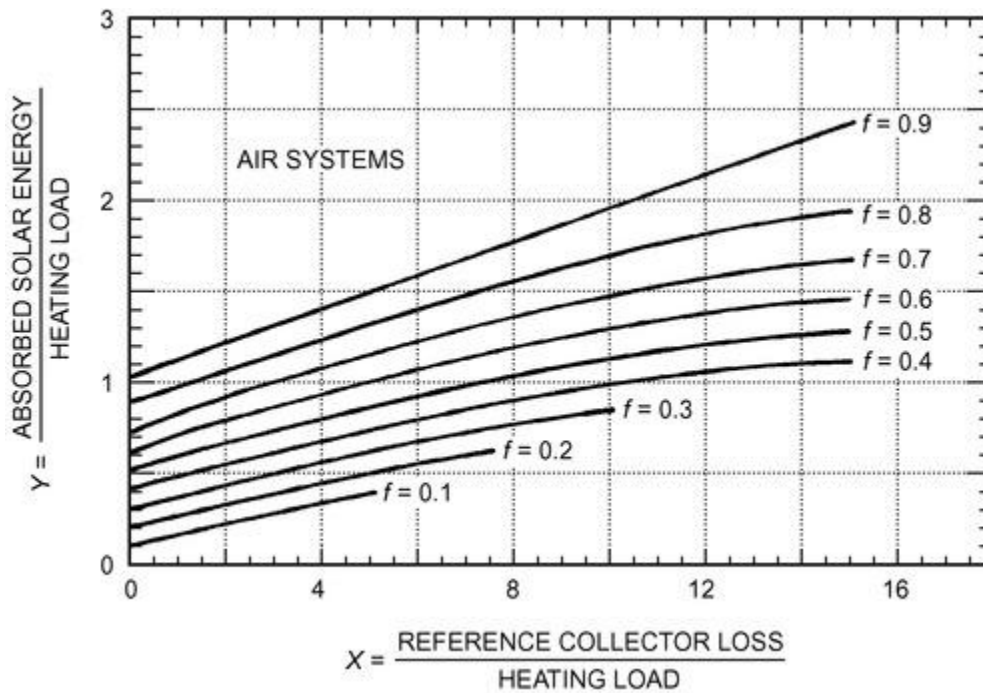


Figure 29. Chart for Air System (Adapted from Beckman et al. 1977)

Example 6. Calculating the heating performance of a residence, assume that a solar heating system is to be designed for use in Madison, WI, with two-cover collectors facing south, inclined 58° with respect to the horizontal. The air heating collectors have the characteristics $F_R U_L = 0.50 \text{ Btu/h} \cdot \text{ft}^2 \cdot ^\circ\text{F}$ and $F_R(\tau\alpha)_n = 0.49$. The \bar{T}_a is 19.4°F , the total space and water-heating load for January is $34.1 \times 10^6 \text{ Btu}$, and the solar radiation incident on the plane of the collector is $1.16 \times 10^3 \text{ Btu/day} \cdot \text{ft}^2$. Determine the fraction of the load supplied by solar energy with a system having a collector area of 538.2 ft^2 .

Solution: For air systems, there is no heat exchanger penalty factor and $F_r/F_R = 1$. The value of $(\bar{\tau\alpha})/(\tau\alpha)_n$ is 0.94 for a two-cover collector in January. Therefore, the values of X and Y are

$$X = 0.50(1)(212 - 19.4)(31)(24)(538.2)/(34.1 \times 10^6) = 1.13$$

$$Y = (0.49)(1)(0.94)(1.16 \times 10^3)(31)(538.2)/(34.1 \times 10^6) = 0.26$$

Then the fraction f of the energy supplied for January is 0.19. The total solar energy supplied by this system in January is

$$fL = (0.19)(34.1 \times 10^6) = 6.4 \times 10^6 \text{ Btu}$$

The annual system performance is obtained by summing the energy quantities for all months. The result is that 37% of the annual load is supplied by solar energy.

The collector heat removal factor F_R that appears in X and Y is a function of the collector fluid flow rate. Because of the higher cost of power for moving fluid through air collectors rather than through liquid collectors, the capacitance rate used in air heaters is ordinarily much lower than that in liquid heaters. As a result, air heaters generally have a lower F_R . Values of F_R corresponding to the expected airflow in the collector must be used to calculate X and Y .

Increased airflow rate tends to improve collector performance by increasing F_R , but it tends to decrease performance by reducing the degree of thermal stratification in the pebble bed (or water storage tank). The f -Chart for air systems is based on a collector airflow rate of 2 scfm per square foot of collector area. The performance with different collector airflow rates can be estimated by using the appropriate values of F_R in both X and Y . A further modification to the value of X is required to account for the change in degree of stratification in the pebble bed.

Air system performance is less sensitive to storage capacity than that of liquid systems for two reasons: (1) air systems can operate with air delivered directly to the building in which storage is not used, and (2) pebble beds are highly stratified and additional capacity is effectively added to the cold end of the bed, which is seldom heated and cooled to the same extent as the hot end. The f -Chart for air systems is for a nominal storage capacity. Performance of systems with other storage capacities can be determined by modifying the dimensionless group X as described in Beckman et al. (1977).

With modification, f -Charts can be used to estimate the performance of solar water heating operating in the range of 120 to 160°F . The main water supply temperature and minimum acceptable hot-water temperature (i.e., desired delivery

temperature) both affect the performance of solar water heating. The dimensionless group X , which is related to collector energy loss, can be redefined to include these effects. If monthly values of X are multiplied by a correction factor, the f -Chart for liquid-based solar space- and water-heating systems can be used to estimate monthly values of f for water heating. Experiments and analysis show that the load profile for a well-designed heater has little effect on long-term performance. Although the f -Chart was originally developed for two-tank systems, it may be applied to single- and double-tank domestic hot-water systems with and without collector tank heat exchangers. The standard f -Chart method is not designed to provide performance estimates of thermosiphon and ICS systems.

For industrial process heating, absorption air conditioning, or other processes for which the delivery temperature is outside the normal f -Chart range, modified f -Charts are applicable (Klein et al. 1976). The concept underlying these charts is solar usability: the fraction of the total solar energy that is useful in the given process. This fraction depends on the required delivery temperature as well as collector characteristics and solar radiation. The procedure allows the energy delivered to be calculated in a manner similar to that for f -Charts. An example of applying this method to solar-assisted heat pumps is presented in Svard et al. (1981).

Other Active Collector Methods

The **relative areas method**, based on correlations of the f -Chart method, predicts annual rather than monthly active heating performance (Barley and Winn 1978). An hourly simulation program was used to develop the **monthly solar-load ratio (SLR) method**, another simplified procedure for residential systems (Dickinson and Cheremisinoff 1980). Based on hour-by-hour simulations, a method was devised to estimate performance based on monthly values of horizontal solar radiation and heating degree-days. This SLR method has also been extended to nonresidential buildings for a range of design water temperatures (Dickinson and Cheremisinoff 1980; Schnurr et al. 1981).

Passive Heating

A widely accepted simplified passive space heating design tool is the solar-load ratio (SLR) method (Balcomb et al. 1984; DOE 1980/1982). It can be applied manually, although, like the f -Chart, software is also available. The SLR method for passive systems is based on correlating results of multiple hour-by-hour computer simulations, the algorithms of which have been validated against test cell data for the following generic passive heating types: direct gain, thermal storage wall, and attached sunspace. Monthly and annual performance, as expressed by the auxiliary heating requirement, is predicted by this method. The method applies to single-zone, envelope-dominated buildings. A simplified, annual-basis distillation of SLR results, the **load collector ratio (LCR) method**, and several simple-to-use rules have grown out of the SLR method. Several hand-held calculator and microcomputer programs have been written using the method (Nordham 1981).

The SLR method uses a single dimensionless correlating parameter (SLR), which Balcomb et al. (1982) define as a particular ratio of solar energy gains to building heating load:

$$\text{SLR} = \frac{\text{Solar energy absorbed}}{\text{Building heating load}} \quad (32)$$

A correlation period of 1 month is used; thus the quantities in the SLR are calculated for a 1 month period.

The parameter that is correlated to the SLR, the **solar savings fraction (SSF)**, is defined as

$$\text{SSF} = 1 - \frac{\text{Auxiliary heat}}{\text{Net reference load}} \quad (33)$$

The SSF measures the energy savings expected from the passive solar building, relative to a reference nonpassive solar building.

In [Equation \(33\)](#), the net reference load is equal to the degree-day load DD of the nonsolar elements of the building:

$$\text{Net reference load} = (\text{NLC})(\text{DD}) \quad (34)$$

where NLC is the net load coefficient, which is a modified UA coefficient computed by leaving out the solar elements of the building. The nominal units are $\text{Btu}/^\circ\text{F} \cdot \text{day}$. The term DD is the temperature departure in degree-days computed for an appropriate base temperature. A building energy analysis based on the SLR correlations begins with a calculation of the monthly SSF values. The monthly auxiliary heating requirement is then calculated by

$$\text{Auxiliary heat} = (\text{NLC})(\text{DD})(1 - \text{SSF}) \quad (35)$$

Annual auxiliary heat is calculated by summing the monthly values.

By definition, SSF is the fraction of the heat load of the nonsolar portions of the building met by the solar element. If the solar elements of the building (south-facing walls and windows in the northern hemisphere) were replaced by other elements so that the net annual flow of heat through these elements was zero, the building's annual heat consumption would be the net reference load. The savings achieved by the solar elements would therefore be the net reference load in [Equation \(34\)](#) minus the auxiliary heat in [Equation \(35\)](#), which gives

$$\text{Solar savings} = (\text{NLC})(\text{DD})(\text{SSF}) \quad (36)$$

Although simple, in many situations and climates, Equation (36) is only approximately true because a normal solar-facing wall with a normal complement of opaque walls and windows has a near-zero effect over the entire heating season. In any case, the auxiliary heat estimate is the primary result and does not depend on this assumption.

The hour-by-hour simulations used as the basis for the SLR correlations are done with a detailed model of the building in which all the design parameters are specified. The only parameter that remains a variable is the solar collector area, which can be expressed in terms of the load collector ratio (LCR):

$$\text{LCR} = \frac{\text{NLC}}{A_p} = \frac{\text{Net load coefficient}}{\text{Projected collector area}} \quad (37)$$

Performance variations are estimated from the correlations, which allow the user to account directly for thermostat set point, internal heat generation, glazing orientation, and configuration, shading, and other solar radiation modifiers. Major solar system characteristics are accounted for by selecting one of 94 reference designs. Other design parameters, such as thermal storage thickness and conductivity, and the spacing between glazings, are included in a series of sensitivity calculations obtained using hour-by-hour simulations. The results are generally presented in graphic form so that the designer can see the effect of changing a particular parameter.

Solar radiation correlations for the collector area have been determined using hour-by-hour simulation and typical meteorological year (TMY) weather data. These correlations are expressed as ratios of incident-to-horizontal radiation, transmitted-to-incident radiation, and absorbed-to-transmitted radiation as a function of the latitude minus mid-month solar declination and the atmospheric clearness index (i.e., the ratio between the actual clear-day direct irradiation intensity at a specific location and the intensity calculated for the standard atmosphere for the same location and date).

Performance predictions of the SLR method have been compared to predictions made by the detailed hour-by-hour simulations for various climates in the United States. The standard error in the prediction of the annual SSF, compared to the hour-by-hour simulation, is typically 2 to 4%.

The annual solar savings fraction calculation involves summing the results of 12 monthly calculations. For a particular city, the resulting SSF depends only on the LCR of Equation (37), system type, and the temperature base used in calculating the temperature departure. Thus, tables that relate SSF to LCR for various systems and for various degree-day base temperatures may be generated for a particular city. Such tables are easier for hand analysis than are the SLR correlations.

Annual SSF versus LCR tables have been developed for 209 locations in the United States and 14 cities in southern Canada for 94 reference designs and 12 base temperatures (Balcomb et al. 1984). Fernandez-Gonzalez (2007) evaluates the thermal performance of five passive solar strategies (direct gain, Trombe wall, water wall, sunspace, and roof pond) under severe winter climates with predominant overcast sky conditions.

Example 7. (Abstracted from the detailed version in Balcomb et al. [1982].) Consider a small office building located in Denver, Colorado, with 3000 ft² of usable space and a sunspace entry foyer that faces due south; the vertically projected collector area A_p is 420 ft². A sketch and preliminary plan are shown in Figure 30. Distribution of solar heat to the offices is primarily by convection through the doorways from the sunspace. The principal thermal mass is in the common wall that separates the sunspace from the offices and in the sunspace floor. Even though lighting and cooling are likely to have the greatest energy costs for this building, heating is a significant energy item and should be addressed by a design that integrates passive solar heating, cooling, and lighting.

Solution: Table 3 shows calculations of the net load coefficient. Then,

$$\text{NLC} = 24 \times 525 = 12,600 \text{ Btu/}^\circ\text{F} \cdot \text{day}$$

and the total load coefficient includes the solar aperture

$$\text{TLC} = 24 \times 676 = 16,224 \text{ Btu/}^\circ\text{F} \cdot \text{day}$$

From Equation (37), the load collector ratio is

$$\text{LCR} = 12,600/420 = 30 \text{ Btu/ft}^2 \cdot ^\circ\text{F} \cdot \text{day}$$

If the daily internal heat is 130,000 Btu/day, and the average thermostat setting is 68°F, then

$$T_{\text{base}} = 68 - 130,000/16,224 = 60^\circ\text{F}$$

(Note that solar gains to the indoor space are not included in the internal gain term as they customarily are for nonsolar buildings.)

In this example, the solar system is type SSD1, defined in Balcomb et al. (1982, 1984). It is a semiclosed sunspace with a 12 in. masonry common wall between it and the heated space (offices). The aperture is double-glazed, with a 50° tilt and no night insulation. To achieve a vertically projected area of 420 ft², a sloped glazed area of $420/\sin 50^\circ = 548 \text{ ft}^2$ is required.

The SLR correlation for solar system type SSD1 is shown in [Figure 31](#). Values of the absorbed solar energy S and heating degree-days DD to base temperature 60°F are determined monthly. For S , the solar radiation correlation presented in Balcomb et al. (1984) for tabulated Denver, CO, weather data is used. For January, the horizontal surface incident radiation is 840 Btu/ft² · day. The 60°F base degree-days are 933. Using the tabulated incident-to-absorbed coefficients found in Balcomb et al. (1984), $S = 43,681 \text{ Btu/ft}^2$. Thus $S/DD = 46.8 \text{ Btu/ft}^2 \cdot ^\circ\text{F} \cdot \text{day}$. From [Figure 31](#), at an LCR = 30 Btu/ft² · °F · day, the SSF = 0.51. Therefore, for January,

$$\text{Net reference load} = (933)(12,600) = 11.76 \times 10^6 \text{ Btu}$$

$$\text{Solar savings} = (11.76 \times 10^6)(0.51) = 6.00 \times 10^6 \text{ Btu}$$

$$\text{Auxiliary heat} = (11.76 \times 10^6) - (6.00 \times 10^6) = 5.76 \times 10^6 \text{ Btu}$$

Repeating this calculation for each month and adding the results for the year yields an annual auxiliary heat of $19.94 \times 10^6 \text{ Btu}$.

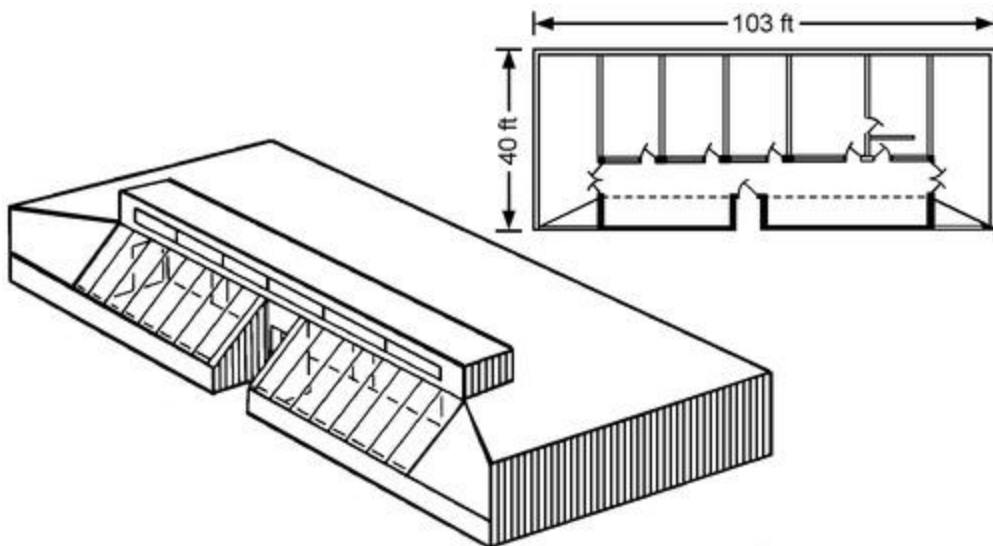


Figure 30. Commercial Building in Example 7

Table 3 Calculations for Example 7

	Area A , ft ²	U-Factor, Btu/h · ft ² · °F	UA , Btu/h · °F
Opaque wall	2000	0.04	80
Ceiling	3000	0.03	90
Floor (over crawl space)	3000	0.04	120
Windows (E, W, N)	100	0.55	55
		Subtotal	345
Infiltration			180
		Subtotal	525
Sunspace (treated as unheated space)			151
		Total	676

ASHRAE procedures are approximated with V = volume, ft³; c = heat capacity of Denver air, Btu/ft³ · °F; ACH = air changes/h; equivalent UA for infiltration = $VcACH$. In this case, $V = 24,000 \text{ ft}^3$, $c = 0.015 \text{ Btu/ft}^3 \cdot ^\circ\text{F}$, and $ACH = 0.5$.

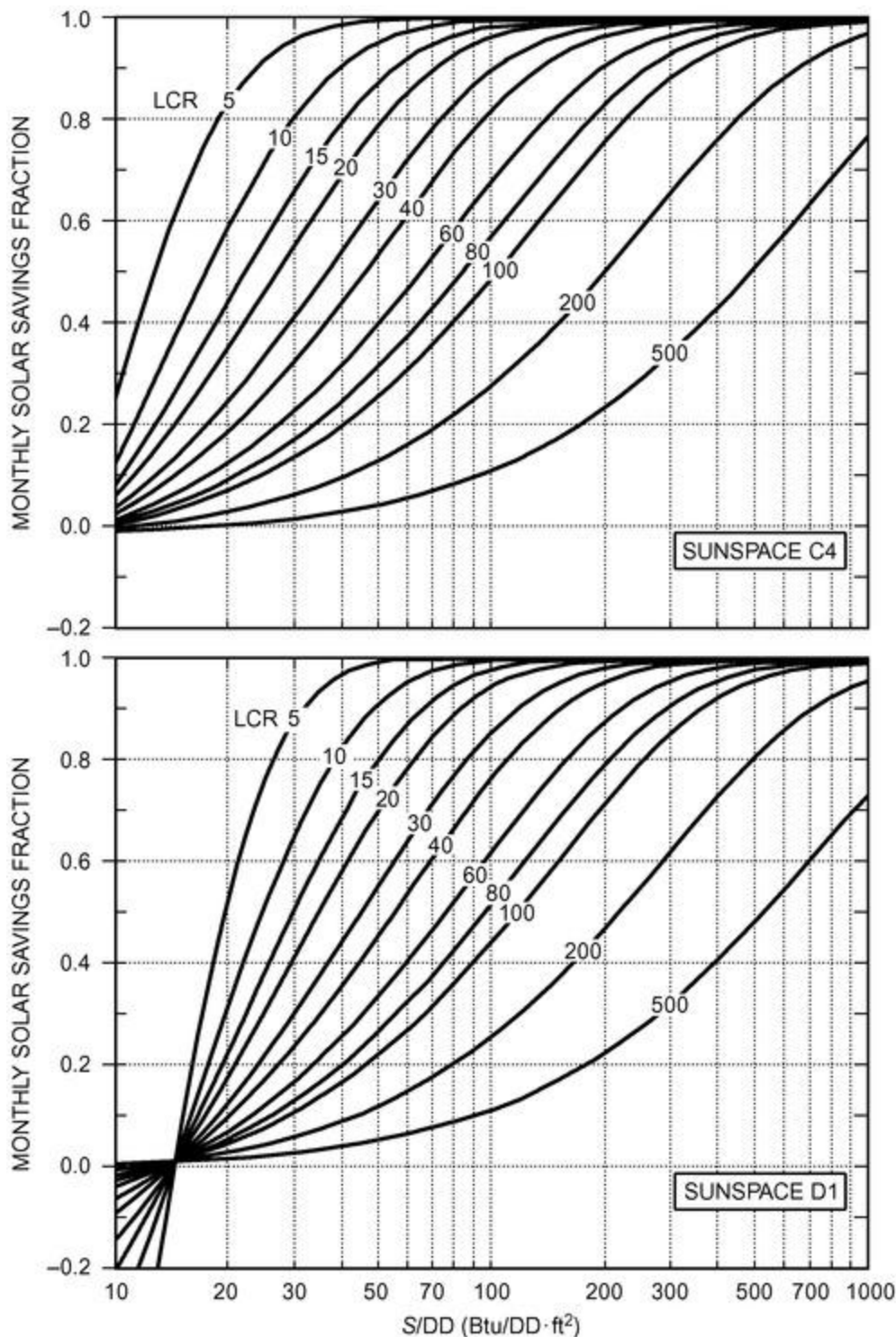


Figure 31. Monthly SSF Versus Monthly S/DD for Various LCR Values

Other Passive Heating Methods

The concept of usability has been applied to passive buildings. In this approach, the energy requirements of zero- and infinite-capacity buildings are calculated. The amount of solar energy that enters the building and exceeds the instantaneous load of the zero-capacity building is then calculated. This excess energy must be dumped in the zero-capacity building, but it can be stored to offset heating loads in a finite-capacity building. Methods are provided to interpolate between the zero- and infinite-capacity limits for finite-capacity buildings. Equations and graphs for direct gain and collector-storage wall systems are given in Mosen et al. (1981, 1982).

8. INSTALLATION GUIDELINES OF SOLAR THERMAL COLLECTORS

Most solar components are the same as those in HVAC and hot-water systems (pumps, piping, valves, and controls), and their installation is not much different from a conventional installation. Solar collectors are the most unfamiliar component in a solar heater. They are located outdoors, which requires penetration of the building envelope. They also require a structural element to support them at the proper tilt and orientation toward the sun.

The site must be taken into account. Collectors should be (1) located so that shading is minimized and (2) installed to be attractive both on and off site. They should also be located to minimize vandalism and to avoid a safety hazard.

Collectors should be placed near the storage tank to reduce piping cost and heat loss. The collector and piping must be installed so that they can be drained without trapping fluid in the system.

For best annual performance, collectors should be installed at a tilt angle above the horizontal that is appropriate for the local latitude. In the northern hemisphere they should be oriented toward true south, not magnetic south. Small variations in tilt ($\pm 10^\circ$) and orientation ($\pm 20^\circ$) do not reduce performance significantly.

Collector Mounting

Solar thermal collectors are usually mounted on the ground or on flat or pitched roofs. A roof location necessitates penetration of the building envelope by mounting hardware, piping, and control wiring. Ground or flat-roof-mounted collectors are generally rack mounted.

Pitched-roof mounting can be done several ways. Collectors can be mounted on structural **standoffs**, which support them at an angle other than that of the roof to optimize solar tilt. In another pitched-roof-mounting technique known as **direct mounting**, collectors are placed on a waterproof membrane on top of the roof sheeting. The finished roof surface, together with the necessary collector structural attachments and flashing, is then built up around the collector. A weatherproof seal between the collector and the roof must be maintained to prevent leakage, mildew, and rotting.

Integral mounting can be done for new pitched-roof or curtain-wall construction. The collector is attached to and supported by the structural framing members. The top of the collector then serves as the finished roof surface. Weathertightness is crucial to avoid damage and mildew. This building-integrated approach is often incorporated in green building design and generally is used for photovoltaic modules rather than thermal collectors.

Collectors should support snow loads that occur on the roof area they cover. The collector tilt usually expedites snow sliding with only a small loss in efficiency. The roof structure should be free of objects that could impede snow sliding, and the collectors should be raised high enough to prevent snow buildup over them.

The mounting structure should be built to withstand winds of at least 100 mph, which impose a wind load of 40 lb/ft² on a vertical surface or an average of 25 lb/ft² on a tilted roof (HUD 1977). Wind load requirements may be higher, depending on local building codes, especially in coastal areas exposed to hurricanes. Flat-plate collectors mounted flush with the roof surface should be constructed to withstand the same wind loads. See [Chapter 55](#) for additional information.

The collector array becomes more vulnerable to wind gusts as the angle of the mount increases. This wind load, in addition to the equivalent roof area wind loads, should be determined according to accepted engineering procedures (ASCE *Standards* 7, 8, and 9).

Expansion and contraction of system components, material compatibility, and use of dissimilar metals must be considered. Collector arrays and mounting hardware (bolts, screws, washers, and angles) must be well protected from corrosion. Steel mounting hardware in contact with aluminum and copper piping in contact with aluminum hardware are both examples of metal combinations that have a high potential for corrosion. Dissimilar metals can be separated by washers made of fluorocarbon polymer, phenolic, or neoprene rubber.

Freeze Protection

Freeze protection is extremely important and is often the determining factor when selecting a system in the United States. Freezing can occur at ambient temperatures as high as 42°F because of radiation to the night sky. Manual freeze protection should not be used for commercial installations.

One simple way of protecting against freezing is to drain fluid from the collector array and interior piping when potential freezing conditions exist. Drainage may be automatic, as in draindown and drainback systems, or manual, as in direct thermosiphon systems. Automatic systems should be capable of fail-safe drainage operation, even in the event of pump failure or power outage. In some cases water may be designed to drain back through the pump, so the design must allow refilling without causing cavitation.

In areas where freezing is infrequent, recirculating water from storage to the collector array can be used as freeze protection. Freeze protection can also be provided by using fluids that resist freezing. Fluids such as water/glycol solutions, silicone oils, and hydrocarbon oils are circulated by pumps through the collector array and double-wall heat exchanger. Draining the collector fluid is not required, because these fluids have freezing points well below the coldest anticipated outdoor temperature.

In mild climates where recirculation freeze protection is used, a second level of freeze protection should be provided by flushing the collector with cold supply water when the collector approaches near-freezing temperatures. This can be accomplished with a temperature-controlled valve that will automatically open a small port at a near-freezing temperature of about 40°F and then close at a slightly higher temperature.

Overheat Protection

During periods of high insolation and low hot-water demand, overheating can occur in the collectors or storage tanks. Protection against overheating must be considered for all portions of the solar hot-water system. Liquid expansion or excessive pressure can burst piping or storage tanks. Steam or other gases within a system can restrict liquid flow, making the system inoperable.

The most common methods of overheat protection stop circulation in the collection loop until the storage temperature decreases, discharge the overheated water and replace it with cold makeup water, or use a heat exchanger as a means of heat rejection. Some freeze protection methods can also provide overheat protection by circulating the collector fluid at night to radiate excess heat.

For nonfreezing fluids such as glycol antifreezing agents, overheat protection is needed to limit fluid degradation at high temperatures during collector stagnation.

Safety

Safety precautions required for installing, operating, and servicing a solar domestic hot-water heater are essentially the same as those for a conventional domestic hot-water heater. One major exception is that some solar systems use nonpotable heat transfer fluids. Local codes may require a double-wall heat exchanger for potable water installations.

Pressure relief must be provided by valves in all parts of the collector array that can be isolated. The outlet of these relief valves should be piped to a container or drain, and not where people could be affected.

Start-Up Commissioning Procedure

After completing the installation, tests must be performed before charging or filling the system. The system must be checked for leakage, and pumps, fans, valves, and sensors must be checked to see that they function. Testing procedures vary with system type.

Closed-loop systems should be hydrostatically tested. The system is filled and pressurized to 1.5 times the operating pressure for one hour and inspected for leaks and any appreciable pressure drop.

Draindown systems should be tested to be sure that all water drains from the collectors and piping located outdoors. All lines should be checked for proper pitch so that gravity drains them completely. All valves should be verified to be in working order.

Drainback systems should be tested to ensure that collector fluid drains back to the reservoir tank when circulation stops and that the system refills properly.

Air systems should be tested for leaks before insulation is applied by starting the fans and checking the ductwork for leaks.

Pumps and sensors should be inspected to verify that they are in proper working order. Proper cycling of the pumps can be checked by a running time meter. A sensor that is suspected of being faulty can be dipped in hot and cold water alternately to see if the pump starts or stops.

After system testing and before filling or charging it with heat transfer fluid, the system should be flushed to remove debris.

Maintenance

All systems should be checked at least once a year in addition to any periodic maintenance that may be required for specific components. A log of all maintenance performed should be kept. System designers and installers should provide building owners with operating manuals that describe maintenance procedures and operating modes in sufficient detail to support ongoing performance.

The collectors' outer glazing should be hosed down periodically. Leaves, seeds, dirt, and other debris should be carefully swept from the collectors. Take care not to damage plastic covers.

Without opening a sealed collector panel, check the absorber plate for surface coating damage caused by peeling, crazing, or scratching. Also, inspect the collector tubing to ensure that it contacts the absorber. If the tubing is loose, consult the manufacturer for repair instructions.

Heat transfer fluids should be tested and replaced at intervals suggested by the manufacturer. Also, the solar energy storage tank should be drained about every six months to remove sediment.

Performance Monitoring/Minimum Instrumentation

Temperature sensors and temperature differential controllers are required to operate most solar systems. However, additional instruments should be installed for monitoring, checking, and troubleshooting.

Thermometers should be located on the collector supply and return lines so that the temperature difference in the lines can be determined visually.

A pressure gage should be inserted on the discharge side of the pump. The gage can be used to monitor the pressure that the pump must work against and to indicate if the flow passages are blocked.

Running time meters on pumps and fans may be installed to determine if the system is cycling properly.

9. DESIGN, INSTALLATION, AND OPERATION CHECKLIST OF SOLAR HEATING AND COOLING SYSTEMS

The following checklist is for designers of solar heating and cooling systems. Specific values have not been included because these vary for each application. The designer must decide whether design figures are within acceptable limits for any particular project (see DOE [1978b] for further information). The review order listed does not reflect their precedence or importance during design.

Collectors

- Check flow rate for compliance with manufacturer's recommendation.
- Check that the collector area matches the application and claimed solar fraction of the load.
- Review collector instantaneous efficiency curve and check the match between collector and system requirements.
- Relate collector construction to end use; two cover plates are not required for low-temperature collection in warm climates and may, in fact, be detrimental. Two cover plates are more efficient when the temperature difference between the absorber plate and outdoor air is high, such as in severe winter climates or when collecting at high temperatures for cooling. Radiation loss only becomes significant at relatively high absorber plate temperatures. Selective surfaces should be used in these cases. Flat-black surfaces are acceptable and sometimes more desirable for low collection temperatures.
- Check match between collector tilt angle, latitude, and collector end use.
- Check collector azimuth.
- Check collector location for potential shading and exposure to vandalism or accidental damage.
- Review provisions for high stagnation temperature. If not used, are liquid collectors drained or left filled in summer?
- Check for snow hang-up and ice formation. Will casing vents become blocked?
- Review precautions, if any, against outgassing.
- Check access for cleaning covers.
- Check the mounting for stability in high winds.
- Check for architectural integration. Do collectors on the roof present rainwater drainage or condensation problems? Do roof penetrations present potential leak problems?
- Check collector construction for structural integrity and durability. Will materials deteriorate under operating conditions? Will any pieces fall off?
- Are liquid collector passages organized in such a way as to allow natural fill and drain? Does mounting configuration affect this?
- Does air collector duct connection promote balanced airflow and uniform heat transfer? Are connections potentially leaky?

Heat Transfer Fluid

- Check that the flow rate through the collector array matches system parameters.
- If antifreeze is used, check that flow rate has been modified to allow for the viscosity and specific heat.
- Review properties of proposed antifreeze. Some fluids are highly flammable. Check toxicity, vapor pressure, flash point, and boiling and freezing temperatures at atmospheric pressure.
- Check means of makeup into the antifreeze system. An automatic water makeup system can result in freezing.
- Check that provisions are made for draining and filling the system (air vents at high points, drains at low points, pipes correctly graded in-between, drainback vented to storage or expansion tank).
- If the system uses drainback freeze protection, check that

- Provision is made for drainback volume and back venting
- Pipes are graded for drainback
- Solar primary pump is sized for lift head
- Pump is self-priming if the tank is below the pump
- Check that collector pressure drop for drainback is slightly higher than static pressure between supply and return headers.
- The optimum pipe arrangement is reverse-return with collectors in parallel. Series collectors reduce the flow rate and increase the head. A combination of parallel/series can sometimes be beneficial, but check that equipment has been sized and selected properly.
- Cross-connections under different operating modes sometimes result in pumps operating in opposition or tandem, causing severe hydraulic problems.
- If heat exchangers are used, check that the approach temperature differential has been recognized in the calculations.
- Check that adequate provisions are made for water expansion and contraction. Use specific volume/temperature tables for calculation. Each unique circuit must have its own provision for expansion and contraction.
- Three-port valves tend to leak through the closed port. This, together with reversed flows in some modes, can cause potential hydraulic problems. As a general rule, simple circuits and controls are better.

Airflow

- Check that the flow rate through the collector array matches system design values.
- Check temperature rise across collectors using air mass flow and specific heat.
- Check that duct velocities are within design limits.
- Check that cold air or water cannot flow from collectors by gravity under “no-sun” conditions.
- Verify duct material and construction methods. Ductwork must be sealed to reduce loss.
- Check duct configuration for balanced flow through collector array.
- Check number of collectors in series. More than two collectors in series can reduce collection efficiency.

Thermal Storage

- Check that thermal storage capacity matches values of collector area, collection temperature, use temperature, and load.
- Verify that thermal inertia does not impede effective operation.
- Check provisions for promoting temperature stratification during both collection and use.
- Check that pipe and duct connections to storage are compatible with the control, ensuring that only the coolest air goes to the collectors and connections.
- If liquid storage is used for high-temperature (above 200°F) applications, check that tank material and construction can withstand the temperature and pressure.
- Check that the storage location does not promote unwanted heat loss or gain and that adequate insulation is provided.
- Verify that liquid storage tanks are treated to resist corrosion. This is particularly important in tanks that are partially filled.
- Check that provision is made to protect liquid tanks from exposure to either overpressure or vacuum.

Uses

Domestic Hot Water

- Characteristics of domestic hot-water loads include short periods of high draw interspersed with long dormant periods. Check that domestic hot-water storage matches solar heat input.
- Check that provisions have been made to prevent reverse heating of the solar thermal storage by the domestic hot-water back-up heater.
- Check that the design allows cold makeup water preheating on days of low solar input.
- Verify that the antiscald valve limits domestic hot-water supply to a safe temperature during periods of high solar input.
- Depending on total dissolved solids, city water heated above 150°F may precipitate a calcium carbonate scale. If collectors are used to heat water directly, check provisions for preventing scale formation in absorber plate waterways.
- Check whether the heater is required to have a double-wall heat exchanger and that it conforms to appropriate codes if the collector uses nonpotable fluids.

Heating

- Low-temperature heating and high-temperature cooling are ideal applications for solar heat and power, and are becoming widely used (REHVA 2013).
- Warm-air heating systems can use solar energy directly at moderate temperatures. Check that air volume is sufficient to meet the heating load at low supply temperatures and that the limit thermostat has been reset.
- At times of low solar insolation, solar heat can still be used to meet part of the load by preheating return air. Check the location of the solar heating coil in the system.
- Baseboard heaters require relatively high supply temperatures for satisfactory operation. Their output varies as the 1.5 power of the log mean temperature difference and falls off drastically at low temperatures. If solar is combined with baseboard heating, check that the supply temperature is compatible with the heating load. Equipment oversizing and/or temperature peaking is required with most current technology. However, new heating and cooling terminal units that operate at low temperatures for heating and at high temperatures for cooling are becoming available (Kilkis et al. 2021). Chilled beams are another option (REHVA 2004), along with radiant panels (see [Chapter 6 in the 2020 ASHRAE Handbook—HVAC Systems and Equipment](#)).
- Heat exchangers imply an approach temperature difference that must be added to the system operating temperature to derive the minimum collection temperature. Verify calculations.
- Water-to-air heat pumps rely on a constant solar water heat source for operation. When the heat source is depleted, the back-up system must be used. Check that storage is adequate.

Cooling

- Solar-activated absorption or adsorption cooling machines (with or without fossil fuel backup for PV electricity) is a commercially available active cooling option. Be assured of all design criteria and a large amount of solar participation. Verify calculations.
- Storing both hot and chilled water may make better use of available storage capacity.
- New innovations are becoming available such as thermoelectric generator (TEG) cooling operated by solar power.

Controls

- Check that the control design matches desired modes of operation.
- Verify that collector loop controls recognize solar input, collector temperature, and storage temperature.
- Verify that controls allow both the collector and usage loops to operate independently.
- Check that control sequences are reversible and always revert to the most economical mode.
- Check that controls are as simple as possible within the system requirements. Complex controls increase the frequency and possibility of breakdowns.

- Check that all controls are fail-safe.

Performance

- Check the heating, cooling, and domestic hot-water loads of the building as applicable. Verify that the building thermal characteristics are acceptable.
- Check solar energy collected on a monthly basis. Compare with loads and verify solar participation.

10. PHOTOVOLTAIC APPLICATIONS

Photovoltaic (PV) systems are used for electricity generation and can be either standalone or connected to a grid. Previously, photovoltaics were mainly used to generate electrical power for remotely located communication equipment, remote monitoring, lighting, water pumping, battery charging, and cathodic protection. Currently, due to their lower cost and higher efficiency, PV systems are widely used in the built environment, farmland, transportation, and solar farms for large-scale power generation. PV systems are designed to reduce non-renewable energy consumption, reduce peak power demand, and/or enhance energy resiliency. Before considering implementation of a PV system, the first step is to analyze the electric loads it will be powering and minimize them wherever possible. For a building application, the size of a PV array can be reduced substantially with an energy-conserving design and by implementing energy efficiency measures such as high-efficiency HVAC equipment, appliances, motors, and plug loads.

Grid-Connected Systems

This section describes PV system applications that are connected to the electric utility and allow for bidirectional flow of electricity between the client (e.g., a building with a grid-connected PV system) and the power grid ([Figure 32](#)).

Grid-Connected Systems. Grid-connected (also known as **grid-tied**) PV systems use string inverters or microinverters that convert DC power from the PV array to AC. The AC output power is then fed to the AC load circuit. The inverters are designed to synchronize their AC output (phase, frequency, and voltage) with the electric utility.

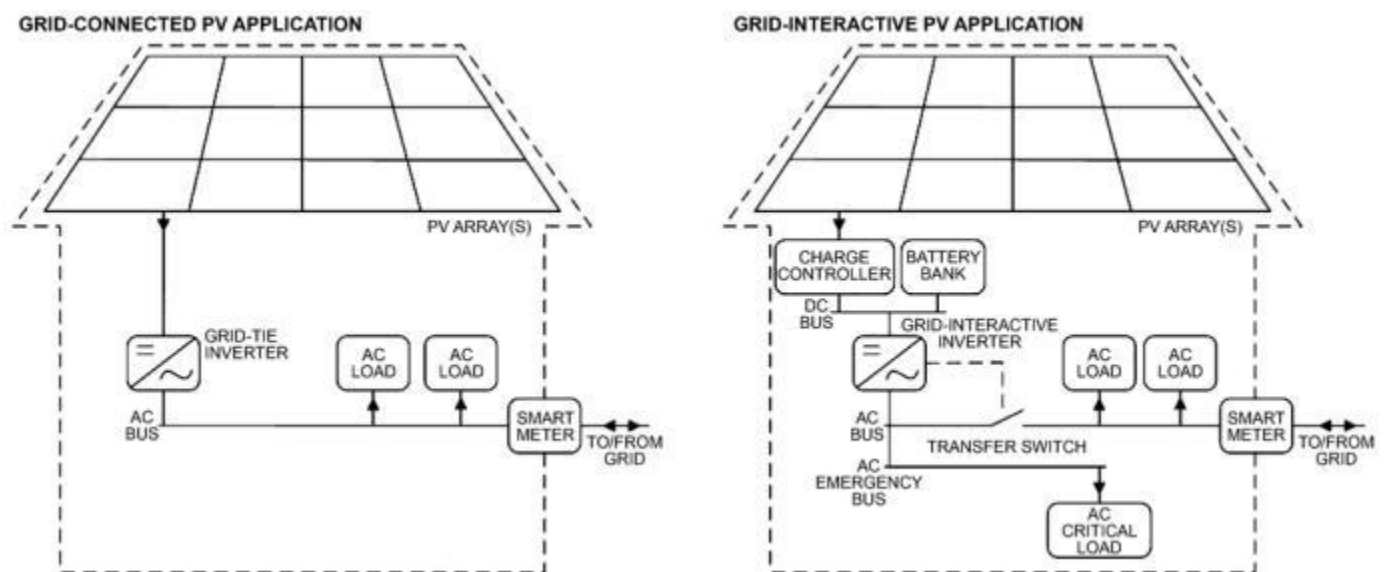


Figure 32. Grid-Connected (Left) and Grid-Interactive (Right) Photovoltaic Applications for Buildings (Natural Resources Canada 2018)

A typical grid-connected PV system uses no battery storage. Excess power generated during the day is fed back to the utility grid. Grid power is used when the PV system does not generate enough energy to fulfill the building's electricity requirements. During a power outage, a grid-tie inverter automatically disconnects, so no solar power is fed to the AC load circuit or to the grid until grid power is restored.

Without storage, a building's grid-connected PV system is mainly used to reduce the amount of electricity supplied by the grid. When storage is added, it can provide additional benefits such as increasing the building's resiliency, reducing its peak power demand, or providing flexibility to the grid.

Grid-Interactive Systems. These are advanced configurations of a grid-connected system that can also function in isolated mode (when the grid is down) or in a parallel-to-the-grid mode by using **grid-interactive inverters** ([Figure 32](#)). A grid-interactive inverter can regulate or form its own local grid, thus allowing the PV system to feed the AC load circuit with power for emergency loads even when the grid is down. It may also be able to perform advanced inverter

functions at the request of the utility, such as improving voltage or reactive power characteristics. In areas where energy resiliency and emergency operation are of importance (e.g., areas vulnerable to earthquakes, hurricanes, heat waves, ice storms, etc.), the use of grid-interactive inverters is recommended. A typical grid-interactive system incorporates battery storage and aims to reduce end-use utility energy consumption, reduce peak power demand, and enhance energy resiliency.

PV for Buildings

Photovoltaic modules can be installed on flat roofs, sloped roofs, facades, and shading elements. In all cases, the PV system should be designed and installed without compromising any requirements or functions of the building envelope.

Building-Applied PV. In building-applied PV (BAPV) applications, the PV modules are mounted on the building to generate solar electricity. If the BAPV system is removed, the building envelope will still perform as designed. Rack-mounted photovoltaic systems on roofs or facades are typical examples of BAPV systems. In these applications, the PV modules are mounted either parallel to the building surface or at optimal tilt and azimuth angles to maximize energy yield.

Building-Integrated PV. In building-integrated PV (BIPV) applications, the PV modules act as a building envelope product or system in addition to generating solar electricity. If a BIPV system is removed, the building envelope performance is compromised and the BIPV will need to be replaced by an appropriate envelope product or system. Typical applications include flat or inclined BIPV roofing and skylights, opaque and transparent BIPV curtain walls, double-skin BIPV facades, and exterior BIPV shading elements. Depending on the application, a BIPV system might influence daylighting, passive solar gains, and visual as well as thermal and acoustic comfort. As a result, the building heating, cooling, and electric lighting loads are also affected ([Figure 33](#)). Ideally, design of a BIPV system should take place in conjunction with the design of the HVAC system and the building envelope.

Other Photovoltaic Applications

Photovoltaic and photovoltaic-battery systems can be implemented in virtually any application where a supply of AC or DC power is required. A list of other popular PV applications, many of which are off-grid (not connected to the larger utility grid), follows. In off-grid systems, the accurate estimate of electrical load consumption and PV system losses is critical.

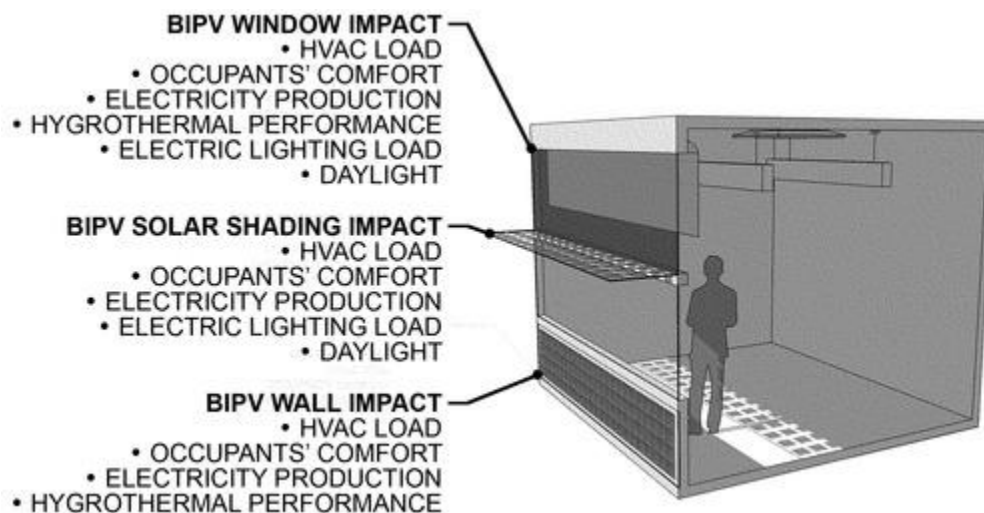


Figure 33. Representation of Major Interactions Between BIPV Application, Building Systems, and Occupants (Natural Resources Canada 2018)

Remote Site Electrification. Photovoltaics are used to provide power to rural residences, visitor centers in parks, vacation cabins, islands and villages, remote research facilities, and military test areas that are not connected to an electric utility (off-grid). The loads include lighting, small appliances, water pumps (including circulators on solar water-heating systems), and communications equipment. Load demand varies from a few watts to tens of kilowatts. A deep-cycle battery is most often used in these applications for nighttime power, and is typically sized to meet the load for two to three days' autonomy (without PV input). Hybrid systems are also common, using wind, small hydro, or diesel/propane generation equipment. Systems may be DC only, or include an **off-grid inverter** for AC loads.

Communications. Photovoltaics can provide reliable power with little maintenance for communications systems, especially those in remote areas (away from the power grid) with extreme weather conditions (e.g., high winds, heavy snow, ice). Examples include communication relay towers, travelers' information transmitters, cellular phones, mobile radio systems, emergency call boxes, and military test equipment. These systems range in size from a few watts for call boxes to several kilowatts for microwave repeater stations. For larger systems at remote sites, an engine generator is

often combined with the photovoltaic-battery system. These hybrid systems with two or more generators can achieve nearly 100% availability.

Remote Monitoring. Photovoltaics provide power at remote sites to sensors, data loggers, and associated transmitters for meteorological monitoring, structural condition measurement, seismic recording, irrigation control, highway/traffic monitoring, security monitoring, and scientific research. Most of these applications require less than 200 W, and many can be powered by a single photovoltaic module. Vandalism may be a problem in some areas, so non-glass-covered modules are sometimes used. Mounting the modules on a tall pole or in an inaccessible manner may also help avoid damage or theft. The batteries are often located in the same weather-resistant enclosure as the data acquisition/monitoring equipment. This enclosure is sometimes camouflaged or buried for protection. Some data loggers come with their own battery and charge regulator.

Signs and Signals. A popular application for photovoltaics is warning signs. Typical devices include navigational beacons, audible signals such as sirens, highway warning signs, railroad signals, and aircraft warning beacons. Because these signals are critical to public safety, they must be operative at all times, and thus the reliability of the photovoltaic system is extremely important. High reliability can be achieved by using large-capacity batteries. Many of these systems operate in harsh environments. Maritime applications use special PV modules that are resistant to corrosion from salt water.

Water Pumping and Control. Photovoltaics are typically used for intermediate-sized water pumping applications (those larger than hand pumps and smaller than large engine-powered pumps). The range of sizes for photovoltaic-powered pumps is a few hundred watts to a few kilowatts. Applications include domestic use, water for campgrounds, irrigation, village water supplies, and livestock watering. Photovoltaics for livestock watering can be more economical than maintaining a distribution line to a remote pump on a ranch. Most pumping systems do not use batteries but instead pump water into holding tanks for storage. For this application, photovoltaic modules may be mounted on tracking frames that maximize energy production by tracking sun position on a continuous basis.

Rest Room Facilities. Highway rest stops, public beach facilities, outdoor recreation parks, and public campgrounds may have photovoltaics to operate air circulation and ventilation fans, interior and exterior lights, and auxiliary water pumps for sinks and showers. For most of these applications, the initial cost for photovoltaic power is the least expensive option.

Charging Auto, Boat, and RV Batteries. Batteries self discharge over time if they are not used. This is a problem for organizations that maintain a fleet of vehicles such as fire-fighting or snow removal equipment, some of which are infrequently used. Photovoltaic battery chargers can solve this problem by providing a trickle charging current that keeps the battery highly charged. A small PV module, not rated for prolonged outdoor exposure, can be placed inside the windshield and plugged into the vehicle's power socket, thus using existing wiring and protection circuits and providing a quick disconnect for the module. Modules are installed on the roof or engine hood of larger vehicles. Another application is using PV modules to charge the batteries in electric vehicles, although large PV arrays are typically needed in this case. Charging stations for electric vehicles in off-road and remote areas is another new application of PV power.

11. SOLAR PVT SYSTEMS

PV with Thermal Energy Recovery. PV modules typically convert 5 to 22% of the incident solar radiation into electricity; a small fraction is reflected while the rest is absorbed and converted into thermal energy (in some cases where the PV module is transparent, a portion of the incident solar radiation is also transmitted). In a **photovoltaic module with thermal energy recovery (PVT)**, a fraction of this thermal energy is recovered either actively or passively by a heat recovery fluid (air, a liquid, or a refrigerant). As a result, PVT collectors produce both thermal and electrical energy using the same surface area.

Thermal energy can also be recovered from BIPV systems. Such systems are called **building-integrated photovoltaics with thermal energy recovery (BIPVT)**. Air-based PVT or BIPVT systems have an open-loop configuration and use air as the heat recovery fluid. A ventilation cavity is created by installing the photovoltaic modules at a certain distance from the facade or roof on which they are mounted. A fan located downstream of the ventilation cavity draws ambient air through the cavity from one or multiple inlets. The air circulates behind the photovoltaic array to recover some of the heat generated by the modules before entering the building through one or multiple ducts in a plenum. In most PVT or BIPVT systems, air flows from bottom to top to avoid going against natural buoyancy and increasing the system pressure drop. Other airflow patterns are possible, however, such as double-pass flow. Perforated baffles increase the efficiency in terms of both solar energy quantity and quality (Kim et al. 2021).

The thermal energy collected can be used directly, as preheated fresh air, or for space or domestic hot-water heating through an air-to-water heat exchanger or heat pump (Figure 34). For all applications, however, the thermal energy generated is not useable at all times. Thus, a well-designed BIPVT roof or facade should have a venting system for air to escape the cavity naturally when thermal energy is not required and the BIPVT mechanical ventilation system is off. The same design approach also applies to PVT systems. This natural ventilation prevents the cells from overheating. Both forced and natural ventilation operating modes should be considered when selecting the ventilation cavity thickness. Under natural convection, the Nusselt number inside the cavity increases with cavity thickness, enhancing the cooling of the modules. Under mechanical ventilation conditions, however, the convective heat transfer coefficient

between the air and the back surface of the module decreases as the cavity thickness increases due to reduced air velocity.

Note that, by operating a PVT or BIPVT roof system during the night, the outdoor air can be precooled by nocturnal radiation and introduced into the building for night cooling.

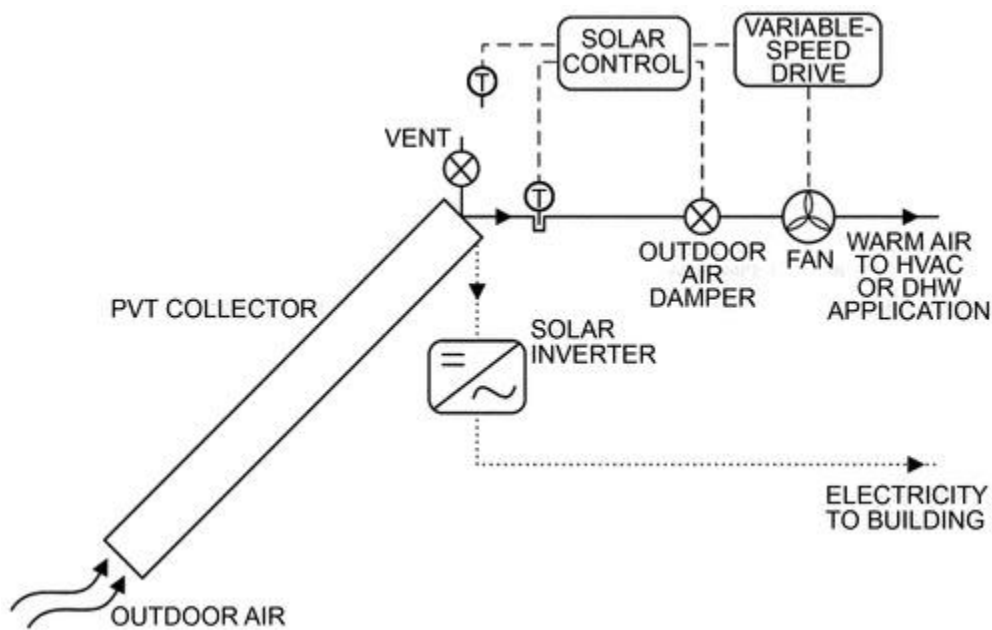


Figure 34. Air-Based PVT System (Natural Resources Canada 2018)

12. DESIGN AND PERFORMANCE OF PV AND PVT SYSTEMS

General design considerations are similar to solar thermal collectors, with orientation in the northern hemisphere generally facing south at a similar tilt to the latitude ($\text{LAT} \pm 15^\circ$), for latitudes below 65° . PV systems with other orientations and tilt angles will still generate solar electricity, but with lower energy yield. This is due to reduced irradiance (e.g., an east- or west-facing BIPV facade receives significantly less solar radiation than an equatorial-facing one, on an annual basis), soiling, or snow accumulation. However, nonoptimal angles may be desired for aesthetic, economic, or generation profile tuning reasons.

PV Design Considerations

An on-site visit and site survey are essential for the proper design, installation and performance of a PV system. The final system design should be performed by a certified professional. The design must comply with local electrical codes. Local building codes may also apply, as well as fire safety regulation and other legislation.

Shading. During the design of any PV system, attention should be given to routine shading (e.g., self-shading, shading due to surrounding buildings, vegetation, topography) or temporary shading (e.g., shading due to vegetation, snow, soiling). A shadow cast on a PV system has higher impact on its energy yield than it would for a solar thermal system because PV is reliant on direct photon energy. Ideally, a PV array should be installed in a shadow-free environment to avoid impact on yield and damage to the PV modules. In reality, shading losses are hard to avoid in an urban or suburban environment. A shading analysis should be carried out to minimize these losses. In the case of a building, a shading analysis also indicates the surfaces with the highest solar potential. Several tools and techniques are available to assist with a shading analysis, including existing building or PV performance simulation tools. For BIPV curtain wall applications, the mounting hardware (mullions) might introduce some shading. Thus, low-profile (or flushed) mullions are recommended.

Shading from neighboring buildings, constructions, trees, and public installations (e.g., skyways, bridges, transforming stations) must be taken into account for potential solar obstructions, which limit the utilization rate of the solar quality and may also compromise performance of the PV array (Salih and Taha 2013). PV systems should be carefully installed in critical locations like airports to avoid glare towards pilots and the control tower. The same also applies to highways, shipping docks, sea terminals, traffic control terminals, and helipads. Solar glint and glare assessment simulation packages are available to properly locate PV systems in or near airports (Zehndorfer Eng. 2021). Another potential risk is radar interference (FAA 2018). In urban areas, the heat island effect also must be analyzed, especially since larger solar power plants increase local temperatures (Barron-Gafford et al. 2016).

For crystalline silicon (c-Si) PV systems, mounting in landscape orientation helps to minimize shading losses due to the location of the bypass diodes on the module circuit. The diodes protect the PV cells from damaging reverse-current flow when a PV cell is shaded. However the diodes are prone to failure, and attempts should be made to minimize routine shading. PV-module level inverters or maximum power point trackers can help reducing power losses by

optimizing the power output of each PV module individually, so that a low-performing PV module does not impact others in the system.

Soiling and Snow. The amount, type, and characteristics of soiling depend on location. Soiling can cause a reduction in power output between 2% and, in extreme cases, 25%. In most locations, losses due to soiling represent less than 5%, because most soiling is removed by rainfall. Tilt angles of 12° or higher also allow for more self cleaning with rain. Uniform shading reduces power output. It does not typically damage the PV modules, however, because all cells are uniformly affected. Sometimes, a “dirt dam,” which can shade a row of PV cells, may form at the lower edge of a framed PV module. Bird droppings and leaves are frequent causes of localized shading. Localized shading can damage a PV module, especially if the protective bypass diode is malfunctioning. In areas where snow accumulation might be a concern, tilt angles of 45° and higher are recommended. In this case, precautions should be taken to ensure pedestrian safety in case of sliding snow.

PV Mounting. General mounting considerations are similar to solar thermal collectors (see the section on Collector Mounting). Mounting tilt, azimuth angle, and module layout influence the maximum electricity production potential. The layout should avoid routine inter-row racking shading and other known shading obstacles. The building and racking system must be able to handle increased loads from the PV system as well as resulting wind and snow loading. Seismic calculations may be needed for earthquake-prone areas. The roof/building condition should have an estimated lifetime at least as long as the PV system (20 years or more).

Care must be taken to ensure that any roof penetration for BAPV and BIPV installations is sealed to prevent water ingress. For ballasted systems, the roofing membrane must be protected from damage due to the weight and possible movement of the system. In addition, adequate rear ventilation is required for most PV modules to ensure product safety and performance. This is typically 4 in. minimum clearance at the rear side of the PV module. An exception is PV modules rated for building integrated installations. Care should be taken when racking and/or module-level electronics may impede ventilation. In all cases, refer to the temperature rating and installation recommendations given by the equipment manufacturer. Clearance should also be given to allow for water drainage and leaf/debris clearing.

Seasonal and daily expansion and contraction of metal components, PV modules, and cabling should be accounted for. Direct contact between dissimilar metals (e.g., steel and aluminum) should be avoided due to galvanic corrosion; stainless steel is often used as an intermediary, especially between aluminum PV module frames and copper grounding/bonding wires.

Ideally, there are access paths to allow servicing of equipment. In some jurisdictions, fire codes require certain setbacks. For sloped-roof installations and carport/canopy applications, sliding snow may present a hazard to pedestrians.

PV equipment staging before installation and structural calculations should also be considered at the design stage.

Wiring Management. PV systems are often comprised of both AC and DC wiring. In AC circuits, electron flow changes direction multiple times every second at a given frequency. However, with DC electricity, electrons flow in one direction only, similar to air moving from higher to lower pressure. Therefore, because the current never crosses zero in a DC circuit, electrical arcing from DC faults can last longer than AC arcs. For this reason, AC switchgear and protection devices cannot be substituted for DC purpose. Special care must also be provided to avoid degraded contact resistance in wiring components due to mechanical stress or corrosion. Ratings for outdoor cables are different than for indoor applications. Cable selection must account for their exposure to the elements, service and installation temperature, and exposure to sunlight. Means must be provided to secure the wiring, avoid abrasion from sharp corners and movement due to wind or other vibrations, and withstand load from snow or freezing rain. Similarly, connectors should be supported and provided with drip loops to avoid water ingress. In some locations, mechanical screening methods are used to protect the DC wiring from rodents.

For BIPV. Depending on the BIPV application, performance and design considerations extend beyond solar electricity generation. Design considerations related to common envelope assemblies ([Chapter 45](#)) also apply to BIPV systems.

For BIPV roof applications (the use of typical PV modules), PV shingles or lightweight flexible PV modules can serve as a waterproofing membrane. The design should consider thermal expansion of both modules and cabling.

For BIPV curtain wall applications, BIPV arrays can serve as a face-sealed or rain screen system. A drained/vented air cavity behind the BIPV module should be designed to (1) minimize rain entry in the wall and outward drainage of the cavity and (2) prevent module overheating by allowing natural ventilation in the cavity.

For BIPV fenestration applications, BIPV modules should always be the outermost layer of the glazing unit to maximize solar electricity generation and minimize overheating. The selection of optical, thermal, and electrical properties of the BIPV fenestration product should be the result of an integrated design approach where solar gains, solar electricity generation, visual and thermal comfort, and acoustic and thermal insulation are assessed through building performance simulations. [Chapter 60](#) discusses the integrated design approach that should be followed in the design and realization of BIPV system applications.

For BIPV shading applications, BIPV modules should be oriented to provide the building or building facade with the desired shading while limiting routine or temporary shading on the modules.

When BIPV systems are located in areas prone to hurricanes, cyclones, or earthquakes or the application requires blast or impact live load protection, they should be designed to satisfy the relevant safety and performance standards.

Depending on building size, “blanks” are sometimes used to mimic the visual aesthetics of PV modules to fill gaps in the PV system and achieve the electrical wiring configuration required. Because these are typically not exact replicas, they should be symmetrically positioned to maintain aesthetics.

For BIPVT. In PVT or BIPVT systems, the thermal yield influences the electrical yield and vice versa. Most PV technologies operate with higher efficiency at lower temperature. Therefore, a more efficient thermal system removing more heat allows the PV to generate more electricity. In a BIPVT air system, performance is affected not only by the cavity thickness, but also by its configuration and the solar cell technology used. In addition, the thermal and electrical yield of BIPVT air systems depends on the weather and operating conditions that typically affect both air solar thermal collectors and photovoltaic modules. These variables include incident solar radiation, ambient air temperature, wind speed, air flowrate, and second-order effects, such as solar angle of incidence and air mass. Generally, useful performance metrics for BIPVT air systems consist of thermal efficiency, air temperature rise, and electrical efficiency. The effects of irradiance and wind speed on the thermal efficiency, air temperature rise, and PV modules back-surface temperature of a nearly 15 ft long BIPVT system with a 1.6 in. cavity thickness are shown in [Figures 35](#) and [36](#).

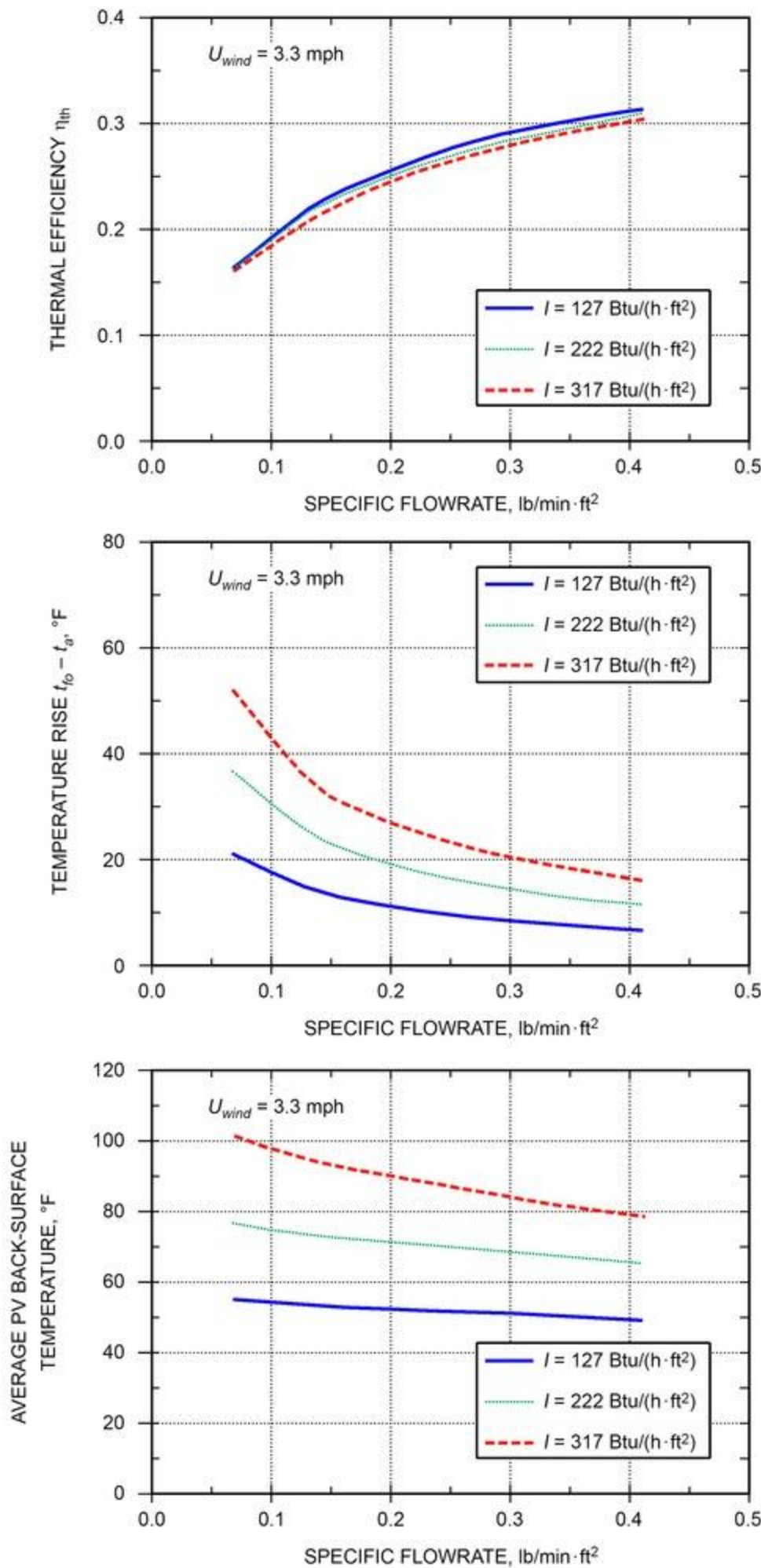


Figure 35. Air-Based BIPVT Thermal Efficiency, Temperature Rise, and Back-Surface Temperature as Function of Specific Flowrate and Incident Irradiance (Natural Resources Canada 2018)

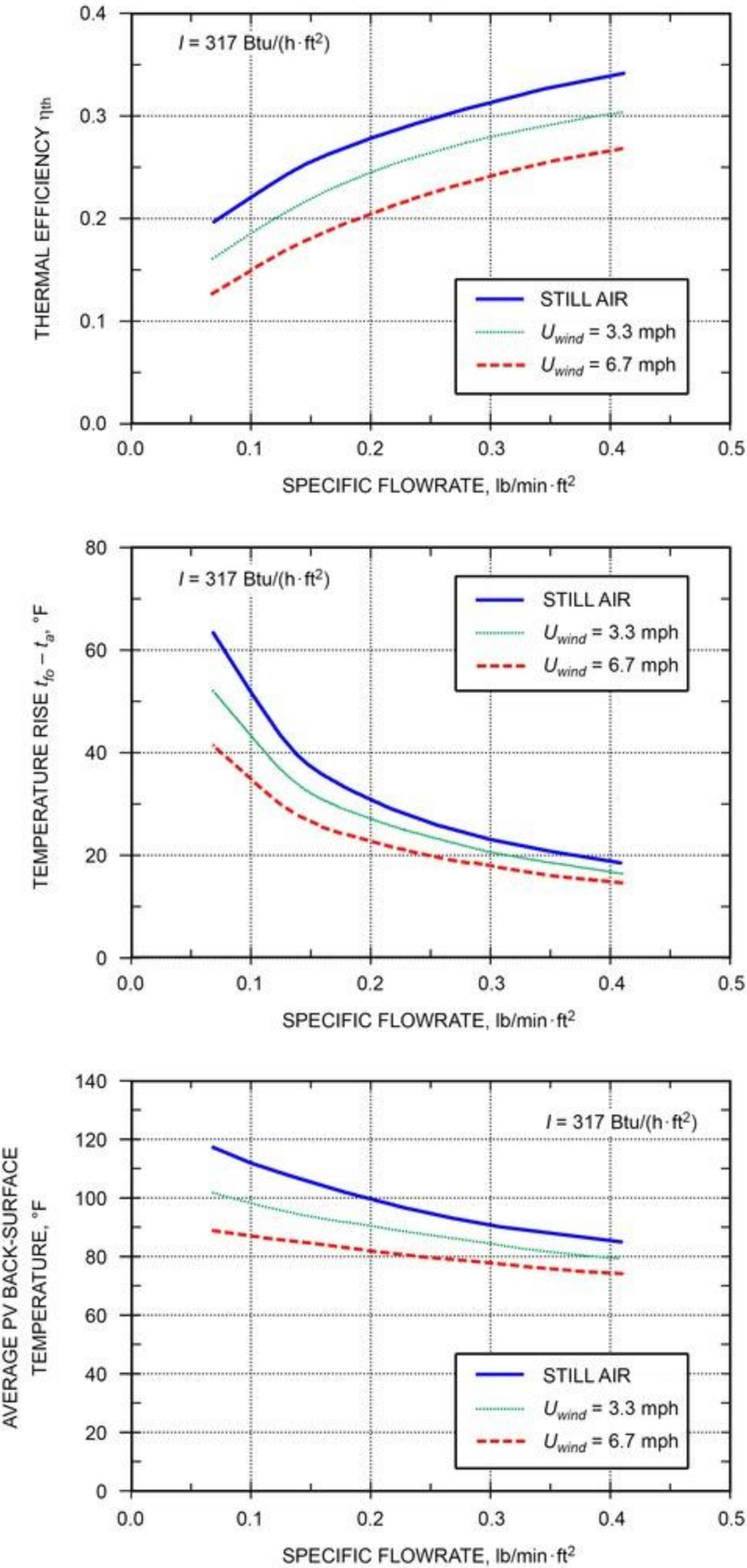


Figure 36. Air-Based BIPVT Thermal Efficiency, Temperature Rise, and Back-Surface Temperature as Function of Specific Flowrate and Wind Speed (Natural Resources Canada 2018)

Heat recovery in BIPVT systems can be improved with heat enhancement strategies such as fins and roughness elements. Fins create a larger surface area for heat transfer, but usually increase pressure drop inside the cavity and, as a result, the fan power requirements. The purpose of roughness elements is to generate local turbulence to increase the heat transfer coefficient locally, limiting the impact on the pressure losses. The design of such roughness elements is challenging, however, because the operating flowrate strongly affects their efficiency. The addition of **thermal boosters** is also an option to achieve higher temperatures in a BIPVT system. These boosters are similar to glazed air solar thermal collectors and are generally added at the top section of a BIPVT roof or facade to increase the air temperature prior to entering the building.

Fan Power Requirements. To estimate the total pressure drop in a BIPVT system, consider the pressure losses associated with the following components of the system: (1) the actual BIPVT roof or facade, (2) the dampers, (3) the plenum, and (4) the ducts and fittings required to bring the preheated air to its final end usage.

Pressure losses associated with the BIPVT roof or facade are generally much less than those of the other components, especially the ducts and fittings bringing the preheated air in the plenum. However, this depends on the BIPVT configuration. For example, a small cavity thickness or the presence of heat transfer enhancement strategies such as fins can significantly increase the pressure drop of the actual BIPVT roof or facade. [Chapter 21 of the 2021 ASHRAE Handbook—Fundamentals](#) examines this subject in greater detail.

Batteries. Off-grid and grid-connected systems may contain batteries. The design, size, and ratings depend on the application. Deep-cycle batteries can be discharged to a higher capacity, and the number of cycles indicates how often this can occur. Racking must be robust and appropriate for the battery type. Ventilation or insulation requirements and temperature ratings depend on the battery technology and installation location. Hazardous DC voltages and significant short-circuit capacity may be present. Initial charging may be necessary before first use, and routine maintenance for some technologies may be impractical for certain applications.

PV, BAPV, and BIPV Electrical Performance

A number of methods can predict the performance of PV and BIPV systems. Though distinct in complexity and accuracy of prediction offered, all have something in common: all require the incident solar radiation and the PV cell operating temperature as minimum inputs. For additional information on calculating incident solar radiation from first principles, see [Chapter 14 of the 2021 ASHRAE Handbook—Fundamentals](#).

PV Modules. The simplified model presented provides an estimate of the electrical yield of PV modules (excluding inverter and balance of system), based on typical meteorological data. Note that PV specifications are typically given in international SI units; care should be taken when using I-P conversions. The solar power generation is calculated based on Evan's model (reported in watts):

$$P_{mod} = c \eta_{ref} [1 + \mu_{P,mp} (t_{cell} - t_{ref})] I A_g \quad (38)$$

where

c = unit correction coefficient, 0.293 W · h/Btu

I = incident total irradiance, Btu/h · ft²

P_{mod} = electrical output of PV modules, W

t_{cell} = operating cell temperature, °F

t_{ref} = reference temperature, usually at 77°F

η_{ref} = electrical efficiency under reference conditions (typically to 317 Btu/h·ft², PV module temperature of 77°F and solar spectrum of air mass 1.5), available through manufacturer's data sheet of solar module

$\mu_{P,mp}$ = temperature coefficient at maximum power point, available through manufacturer's data sheet of solar module, °F⁻¹

Module reference efficiency and power temperature coefficient are usually provided in the PV manufacturer's data sheet. [Table 4](#) provides typical values for various photovoltaic module technologies available on the market. These values may vary depending on solar cell technology, module assembly, and manufacturer.

Table 4 Typical Values and Range of Module Electrical Efficiency (η_{ref}) and Temperature Coefficient at Maximum Power Point ($\mu_{P,mp}$), for Various Photovoltaic Technologies

Photovoltaic Technology	η_{ref}		$\mu_{P,mp}$ %/°F ⁻¹	
	Typical	Range	Typical	Range
Monocrystalline silicon	0.157	0.084 to 0.221	-0.252	-0.499 to -0.126
Polycrystalline silicon	0.149	0.062 to 0.204	-0.253	-0.377 to -0.191

Silicon heterostructures (HIT)	0.173	0.126 to 0.197	-0.185	-0.261 to +0.001
Amorphous silicon (a-Si)	0.064	0.053 to 0.088	-0.145	-0.195 to -0.119
Micromorphous silicon (a-Si/ μ c-Si)	0.082	0.063 to 0.104	-0.178	-0.219 to -0.101
Cadmium telluride (CdTe)	0.139	0.094 to 0.170	-0.159	-0.234 to -0.092
Copper indium (gallium) selenide (CI[G]S)	0.117	0.055 to 0.167	-0.198	-0.288 to -0.120

The calculation of the PV power generation also requires the PV operating cell temperature $t_{t,cell}$ as an input. King's model (King et al. 2004) uses an implicit correlation between the measured back-surface temperature $t_{t,back}$ and operating cell temperature:

$$t_{t,cell} = t_{t,back} + (I/I_{ref})\Delta t \quad (39)$$

In a typical PV module, the back-surface temperature refers to the rear side of the module. In a BIPV window, the back-surface temperature refers to the rear side of the BIPV window, which is the surface of the insulated glazing unit facing the indoor environment (e.g., surface 4 on a double glazing window). When the back-surface temperature is unknown or cannot be measured directly, the following empirical model can be used:

$$t_{t,back} = c_1 I e^{(a + b U_{met})} + t_a \quad (40)$$

where

a = empirically determined coefficient indicating upper temperature limit under low wind speeds and high solar irradiance

b = empirically determined coefficient indicating rate at which back-surface temperature drops with wind speed, mph^{-1}

c_1 = unit correction coefficient, $5.68 \text{ h} \cdot ^\circ\text{F} \cdot \text{ft}^2/\text{Btu}$

I_{ref} = reference solar irradiance, typically $317 \text{ Btu/h} \cdot \text{ft}^2$

$t_{t,back}$ = back-surface PV module temperature, $^\circ\text{F}$

t_a = ambient air temperature, $^\circ\text{F}$

U_{met} = wind speed measured at standard 33 ft height, mph

$\Delta t = t_{cell} - t_{back}$, temperature difference between cell and module back surface at irradiance level of $317 \text{ Btu/h} \cdot \text{ft}^2$

Table 5 provides representative coefficient values for PV and BIPV systems, using crystalline silicon PV cells. The empirically determined coefficients may vary depending on PV module assembly, mounting arrangement, and location.

Example 8. Estimate (1) the average operating cell temperature and (2) the PV modules' power generation for a 100 ft^2 micromorphous double glazing BIPV curtain wall system under $I = 250 \text{ Btu/h} \cdot \text{ft}^2$, $t_a = 70^\circ\text{F}$, and $U_{met} = 3 \text{ mph}$.

Solution. Using Tables 4 and 5, the average back-surface temperature of a micromorphous double glazing BIPV window system can be calculated with Equation (40):

$$t_{back} = 5.68 \times 250 e^{(-2.85 - 0.0157 \times 3)} + 70 = 148.3^\circ\text{F}$$

(1) From Equation (39) and Table 5, the average operating cell temperature of the BIPV window system is:

$$t_{cell} = 148.3 + (250/317)16.2 = 161.1^\circ\text{F}$$

(2) From Equation (38) and Table 4, the estimated solar power generation is:

$$P_{mod} = 0.293 \times 0.082[1 - 0.178\%(161.1 - 77)]250 \times 100 = 511 \text{ W}$$

Table 5 Typical Values for Coefficients a , b , and Δt in Prediction of PV or BIPV Electrical Yield

Type of PV Application	a	b , mph^{-1}	Δt , $^\circ\text{F}$
Open rack PV, BAPV or BIPV with good rear ventilation	-3.47	-0.0266	5.4
BAPV or BIPV with medium rear ventilation	-2.98	-0.0211	1.8
BAPV or BIPV with poor rear ventilation	-2.81	-0.0203	0
Double glazing BIPV window with low emissivity coating (surface 2 or 3)	-2.85	-0.0157	16.2
Triple glazing BIPV window with low emissivity coatings (surfaces 2 and 4 or 3 and 5)	-2.88	-0.0143	19.8

Sources: Adapted from Kapsis (2016) and King et al. (2004).

Table 6 Typical Values and Range of PV System Electric Losses Due to Various Factors

Electric Loss Factor, EL_i	Typical	Range
Shading	0.00	0.00–1.00
Soiling	0.05	0.02–0.25
PV module nameplate DC rating	0.00	0.00–0.15
Initial light-induced degradation	0.02	0.01–0.10
Inverter	0.04	0.04–0.07
Transformers	0.03	0.02–0.04
Mismatch	0.02	0.02–0.03
DC wiring	0.02	0.01–0.03
AC wiring	0.01	0.01–0.02
Diodes and connections	0.005	0.00–0.01

Source: Adapted from Marion et al. (2005).

PV Systems. Besides PV modules, photovoltaic systems are comprised of a number of supporting equipment, which serves to make them operational. Depending on the system configuration, the **balance of system (BoS)** may include inverters, DC and AC wiring, relays, transformers, charge/load controllers, and a battery bank. When compared to the PV module power output, the total output of a PV system is reduced due to losses related to BoS components, mismatch, wiring, and more. [Table 6](#) provides a range of PV system losses for AC power rating due to various factors. Nevertheless, losses are specific to each installation and location. Loss factors influenced by meteorological conditions also vary daily, seasonally, and annually. Taking into account the various losses, the PV system solar power generation is estimated as follows (reported in watts):

$$P_{el} = EL_{total} P_{mod} \quad (41)$$

where

$EL_{total} = (1 - EL_1)(1 - EL_2) \dots (1 - EL_i)$, total electric loss factor

P_{el} = electrical output of PV system, W

EL_i = electric losses due to factor i

Example 9. Considering the PV installation from Example 8, calculate the PV system's power generation assuming total wiring losses of 3%, inverter losses of 4%, mismatch losses of 2%, losses due to soiling of 5%, and losses due to shading of 5%.

Solution. Considering the above loss factors, the PV system's power generation is calculated using [Equation \(41\)](#):

$$P_{el} = (1 - 0.03)(1 - 0.04)(1 - 0.02)(1 - 0.05)(1 - 0.05)511 = 421 \text{ W}$$

Preliminary PV Sizing and Design. The simplified approach presented here can be used to inform the preliminary design stages of a PV system, which consist of the following steps:

- Estimating the annual electrical load to be offset by the PV system (E_{annual}).
- Calculating the average daily electricity E_{daily} to be generated by the PV system.

$$E_{daily} = E_{annual}/365 \quad (42)$$

- Estimating the **sun hours** (i.e., equivalent number of hours which a particular location would be exposed to, if the sun was shining at $I_{STC} = 317 \text{ Btu/h} \cdot \text{ft}^2$) per day available for the location of interest. For the United States, this information is available through NREL's website at [nsrdb.nrel.gov/](https://nrel.gov/nsrdb), and for Canada, through NRCAN's website at www.nrcan.gc.ca/18366.

$$SHD = E_{sun}/I_{STC} \quad (43)$$

- Calculating the PV array installed capacity required.

$$P_{mod} = E_{daily} / SHD / EL_{total} \quad (44)$$

- Calculating the number of PV modules required.

$$N_{mod} = P_{mod} / P_{STC} \quad (45)$$

where

E_{annual} = annual electrical load to be offset by PV system, kWh

E_{daily} = daily average electricity to be generated by PV system, kWh

E_{sun} = daily average solar energy that strikes surface per unit area, for given location, Btu/day

I_{STC} = solar irradiance under standard testing conditions, 317 Btu/h · ft²

N_{mod} = number of PV panels required

P_{STC} = power rating of module under standard testing conditions, W

SHD = sun hours per day, h

Example 10. A two-story apartment building (8 apartments) in Phoenix, AZ, has an annual energy consumption of 112,000 kWh. The building owner would like to have 40% of the annual energy requirement delivered by a flat roof-mounted solar PV system. Calculate the number of PV panels required to generate 40% of the building's annual energy requirement.

Site Specifications:

- Array orientation (solar azimuth ϕ): south (180°)
- Array tilt angle (Σ): 18°
- Site latitude (LAT): 33.43°N

Selected PV System Characteristics:

- Rated power of PV module under standard testing conditions: 310 W
- Module length: 61.4 in.
- Module width: 41.2 in.
- Module depth: 1.81 in.
- PV electric loss factor: 0.86

Solution

Step 1: Calculate the annual electrical load that needs to be offset by the PV system:

$$E_{annual} = 112,000 \times 40\% = 44,800 \text{ kWh}$$

Step 2: Estimate daily average energy usage:

$$E_{daily} = 44,800 / 365 = 123 \text{ kWh/day}$$

Step 3: For Phoenix, AZ, the SHD \approx 6.4 h. The SHD is approximated by using the value for LAT-15° (redc.nrel.gov/solar/pubs/redbook/).

The PV array installed capacity required is

$$P_{mod} = (123 / 6.4) / 0.86 \approx 22 \text{ kW}$$

Step 4: Calculate number of PV panels required:

$$N_{mod} = 22,000 / 310 \approx 75 \text{ modules of 310 W rated power each}$$

Example 11. Based on PV module characteristics listed in Example 10, calculate the minimum spacing required between rows to avoid inter-row shading on December 21 (during the winter season).

Solution. Assuming six hours of sunlight on December 21 (from 9:00 am to 3:00 pm), the solar altitude and solar azimuth at 9:00 am on December 21 are $\beta = 19^\circ$ and $\psi = 139^\circ$ respectively, as calculated using [Equations \(6\)](#) and [\(7\)](#). From [Figure 37](#), the PV array height h can be calculated by simple trigonometry as follows:

$$h = \sin(\Sigma)w = 12.73 \text{ in.}$$

Similarly, the PV shadow SH is calculated as follows:

$$SH = h/\tan(\beta) \approx 37 \text{ in.}$$

Thus, the minimum inter-row spacing IS is

$$IS = SH \times \cos(180^\circ - \psi) \approx 27 \text{ in.}$$

Note that the last calculation takes into account the correction of the solar azimuth.

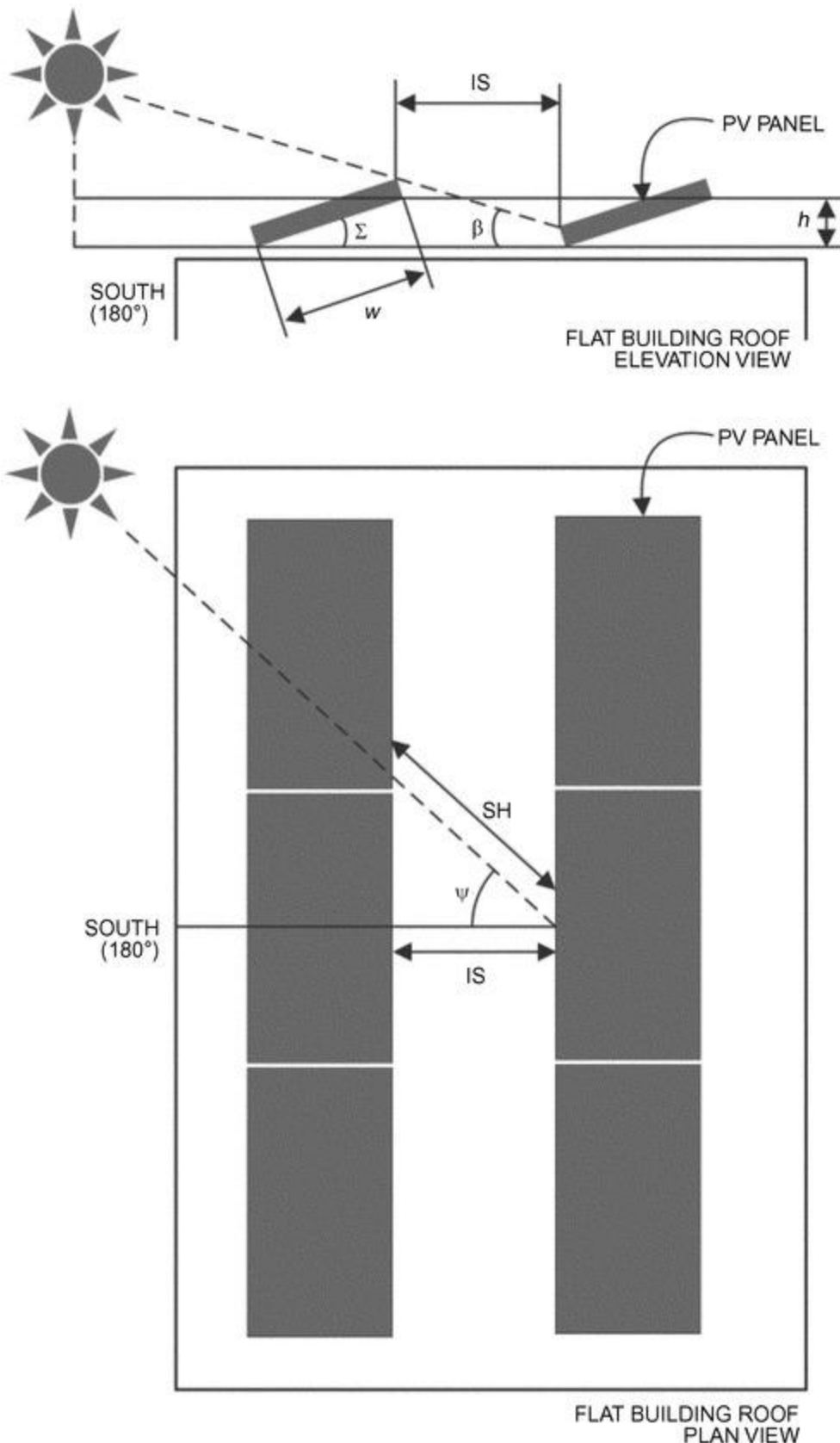


Figure 37. Side View and Top View of Tilted PV Array Mounted on Flat Building Roof

13. INSTALLATION AND OPERATION GUIDELINES FOR PHOTOVOLTAIC SYSTEMS

PV modules are generally smaller and lighter than solar thermal collectors. Nevertheless, they should be handled carefully due to their thin rear-insulating layer. Damage to the delicate PV cells may not be visible, but can reduce system performance significantly.

Proper installation is critical to the long-term reliability and performance of a PV system. Even with an appropriate design, a system's safety and power production can be negatively impacted by inadequate installation procedures. The

crew performing the installation should, at minimum, be led by someone trained, qualified, and experienced in PV installation and system design. Depending on the jurisdiction, a certified electrician may be required for all or portions of the installation. A proper installation should not compromise any building envelope warranties.

Safety

The installation must comply with local electrical, fire, and building codes. Other legislation, as well as local zoning and urbanism restrictions, may also impact installation activities. Site-specific permitting or environmental studies may also be required. For grid-connected systems, the interconnection is subject to the local utility technical and administrative requirements. Interconnection permission should be obtained before project initiation, because in some cases electrical feeders may not be capable of hosting additional generation.

PV systems also pose unique hazards that must be understood, and mitigation procedures should be in place before undertaking an installation. These include hazardous DC voltages and currents whenever the sun is out (even if the system not on), AC voltages, cut/drop hazards, exposure to environmental elements, and fall hazards, especially if working at heights.

Documentation

All site and project documentation should be provided by the installer. This includes general system information, such as project identification and location, designer and installer contact information, DC ratings, and major equipment ratings, as well as detailed system information (i.e., single-line wiring diagrams, array layouts and string information, electrical equipment ratings, PV module and inverter datasheets, racking documentation, and installation manuals, warranty information). Photos of major pieces of equipment are useful, and any important information for O&M (e.g., location of emergency equipment and access/egress routes) should be included. All commissioning measurements, findings, and results, including weather conditions, should be in the documentation package provided to the customer.

On-site documentation should indicate presence of the PV system at the utility's entrance to the home and/or other visible place for emergency responders, and the equipment should be labeled and identified on a nearby single line diagram.

Start-Up Commissioning

During commissioning, the proper implementation of PV system design is confirmed, and any changes or site-specific conditions/concerns are noted and approved. Commissioning is done through a combination of visual inspections and performance verification. It is therefore important that the PV system documentation is complete and accurate.

Visual inspections examine all aspects of the PV array, mounting, wiring, electrical equipment, connections, and general site conditions. The PV system should be installed in a safe manner, following best practices and code requirements. Separate roof/building/electrical inspections may be necessary to maintain warranties and meet local requirements.

Damage to PV modules and system components can result if modules or strings are improperly wired. DC string polarity is therefore confirmed both visually and with an appropriately rated voltmeter, taking extreme care with the + or – sign. String voltages should be equal to the number of modules in a string times the open circuit voltage (V_{oc}), adjusted by the temperature coefficient. Deviations from this, especially when compared to adjacent and similarly configured strings, can indicate a problem with the string, an individual module, or the wiring.

Example 12: String Voltage Calculation. A module having $V_{oc} = 36$ V DC at STC (standard test conditions of 317 Btu/h·ft², 77°F cell temperature) and a voltage temperature coefficient of 0.33%/°F will have a voltage of 41.4 V DC at 32°F. A string of 12 modules is therefore expected to have an open circuit voltage of 497 V DC at 32°F.

Ideally, current and power measurements are taken under clear blue sky, bright sunlight, low wind, and uniform conditions. This allows for more accurate measurements that can be compared between strings or used as an important baseline for future measurements. After confirming correct polarity and voltages at the DC side, and performing any verification of DC current, system grounding, and racking bonding, activating the inverter allows validation of the PV array power output. Many jurisdictions require the local electrical authority to conduct their safety inspection before allowing the inverter's operation/connection to the grid. Performance validation can be a simple confirmation of operation, a side-by-side comparison of output with another similarly configured array, or a detailed performance validation using simultaneous environmental monitoring under bright, blue sky and calm conditions.

Optionally, I - V curve measurements of each DC string can provide useful diagnostic and reference information. These are ideally taken above 190 Btu/h·ft² under clear-sky conditions. Also, IR imaging of electronics and switches to identify hotspots is possible when the system is active (generating AC power). These are ideally taken above 190 Btu/h·ft² but even a minimum irradiance of 95 Btu/(h·ft²) (which will generate 30% of rated closed-circuit current [I_{sc}] in the components) may assist in identifying extreme equipment malfunctions.

Off-Grid Systems. Due to the variability in design parameters for off-grid systems, commissioning includes verification of software settings within the inverter, battery charge controller (if applicable), and any other critical piece

of equipment. The initial battery stabilization procedure should have already been performed (if applicable), the batteries should be housed in a suitable location for the technology type, and the battery monitor's voltage readings should be confirmed using an independent meter.

Maintenance

With no moving parts, PV systems are low maintenance (but not no-maintenance), with tasks typically limited to visual inspection, monitoring, and occasional maintenance. Recommended tasks and frequency depend on the location, mounting type, and performance requirements. A standard frequency for small systems with no performance guarantee is annually. Many systems are monitored remotely, with on-site inspections limited to important stages of the project cycle, such as commissioning, warranty expiration, and asset transfer, or when remote monitoring indicates a concern. Many issues with PV systems can be remotely detected via careful system performance monitoring. A complete system documentation package is extremely useful for performing maintenance, and detailed maintenance records should be kept. This is especially important, because owners and maintenance personnel may change, and PV system typically have expected lifetimes in excess of 20 years.

Visual inspection typically starts with verification that all electronic equipment is operational and that no faults are indicated. An arc-fault alarm or a ground-fault trip can indicate hazardous conditions. In this case, the cause should be carefully investigated and addressed by a trained professional to avoid shock and fire hazards. All personnel on site typically wear personal protective equipment, are specially trained, and are aware of the hazards.

The PV array can be visually inspected for any PV module breakage or misaligned parts. To facilitate inspection and maintenance, the area should be designed for accessibility. Confirm that original design assumptions have not changed. Evidence of any fire hazards, (e.g., presence of leaves, debris, birds, rodents) should be immediately addressed. In some cases, mechanical barriers between PV modules and the roof are used to deter build-up of debris and chewing of cables by animals. A cleaning schedule may be desired. Wiring and connectors should remain securely fastened and have no indications of water ingress, abrasion, or arcing.

PV module racking structures often recommend checking bolt torques, particularly after the first year of operation, to ensure no movement due to seasonal effects or improper initial tightening. To confirm no water leakage into the building, roof/building penetration should be examined. Likewise, ballasted systems should be examined to ensure absence of movement and damage to roofing surface. Depending on the location, cleaning of the PV modules or snow removal may be cost effective.

Inverters and other electronic equipment may require annual filter cleaning. Electrical and mechanical connections should remain secure, with no signs of arcing or loosening. If they are located outdoors, water damage can cause corrosion, resulting in fire or underperformance. Spare parts may be required in case of equipment malfunction. Infrared cameras may help to identify faulty components. To maintain accuracy, monitoring equipment should be cleaned and calibrated as required.

Performance Monitoring/Minimum Instrumentation

PV electronic equipment, such as inverters and solar battery charge controllers, often contain integrated displays for real-time and cumulative performance of the PV system. Typical parameters include instantaneous DC voltages, DC current, AC power, AC frequency, and year-to-date cumulative kilowatt-hour energy generation. Note that accuracy of the integrated monitoring displays varies. Many inverter manufacturers offer remote monitoring capabilities, either free or on a paid subscription basis. The web-based information availability and format depend on the manufacturer. External third-party meters may be attached to both the DC and AC side of the system to ensure correct operation, and these may also be remotely monitored. They typically offer better accuracy and can be configured based on the user's requirements.

To determine whether the system is performing optimally, environmental information is also required. Key pieces of environmental monitoring equipment are an in-plane irradiance sensor (spectrally matched reference cell or calibrated pyranometer), ambient temperature sensor (shielded), several PV module back-sheet temperature sensors (carefully affixed), and optional wind speed and direction sensors and snow/rain gages. Larger systems in dusty environments may use soiling sensors. These are connected to a data logger, and ideally take instantaneous measurements synchronized with the PV system monitoring equipment. This allows calculation of ideal versus actual power output, and visualization of any seasonal or annual performance losses. An alternative to an on-site environmental station is using satellite data or data from local meteorological stations (often near local airports), although care needs to be taken that the local topography, microclimate, and time interval are appropriate. It is best to corroborate satellite or meteorological station data with on-site data.

For systems with remote monitoring enabled, more frequent performance monitoring and fault detection is possible with little time required (often less than 5 minutes to log in and verify operation). This allows issues to be detected quickly and addressed as needed. Often, a third-party solar expert is engaged to perform these checks, sometimes using automated alert generation.

Solar Energy and Green Hydrogen

Solar and wind energy are becoming strong assets for green hydrogen production and use in the built environment against climate warming. One of the main methods to generate green hydrogen is water electrolysis with solar PV and PVT electricity. Hydrogen is then converted to electricity and heat in fuel cells, cogeneration engines, or turbines at central plants or demand points (see [Chapter 7 of the 2020 ASHRAE Handbook—HVAC Systems and Equipment](#)). Hydrogen storage is a suitable medium to store variable solar energy. In fuel cells, current technology may reach up to 65% power efficiency; cogeneration units may have an efficiency of up to 40%, below that of fuel cells but providing higher thermal energy temperatures, which may be used in absorption engines for cooling (tri-generation). The waste is water. Thus, a closed water cycle may also be established.

Hydrogen is a clean medium for storing and transporting energy, but care must be paid in the value chain to minimize leaks: hydrogen has small but nonzero global warming potential, with an indirect greenhouse effect. Furthermore, storing hydrogen in the form of compressed gas or liquid at cryogenic temperatures is energy intensive, and all these processes must also be carried out by green energy.

14. SYMBOLS

a	= empirically determined coefficient indicating the upper temperature limit under low wind speeds and high solar irradiance
A	= surface area, ft^2
A_{abs}, A_{ap}	= areas of absorber surface and of aperture that admit or receive radiation, ft^2
A_c	= area of solar collector, ft^2
ACH	= air changes per hour, ach
A_g	= gross collector area, ft^2
A_p	= projected collector area, ft^2
AST	= apparent solar time, decimal h
b	= empirically determined coefficient indicating rate at which back-surface temperature drops with wind speed mph^{-1}
c	= unit correction coefficient, $0.293 \text{ W} \cdot \text{h/Btu}$
c_1	= unit correction coefficient, $5.68 \text{ h} \cdot ^\circ\text{F} \cdot \text{ft}^2/\text{Btu}$
c_p	= specific heat of fluid, $\text{Btu/lb} \cdot ^\circ\text{F}$
DD	= temperature departure in degree-days computed for an appropriate base temperature
DST	= daylight saving time, decimal h
e_{at}	= sky emittance
E_{annual}	= annual electrical load to be offset by PV system, kWh
E_{daily}	= daily average electricity to be generated by PV system, kWh
EL	= electric loss factor
e_s	= surface emittance
E_{sun}	= daily average solar energy that strikes a surface per unit area, for a given location, $\text{Btu/ft}^2 \cdot \text{day}$
ET	= equation of time, min
f	= fraction of monthly space- and water-heating loads supplied by solar energy
F	= fraction of the annual heating load supplied by solar energy
F_r	= collector heat exchanger efficiency factor
F_R	= collector heat removal factor; ratio of heat actually delivered by collector to heat that would be delivered if absorber were at t_{fi}
H	= hour angle, degrees
h	= PV array height, ft
H_T	= monthly averaged daily radiation incident on collector surface per unit area, $\text{Btu/day} \cdot \text{ft}^2$
I	= incident total irradiance, $\text{Btu/h} \cdot \text{ft}^2$
I_{DN}	= direct normal irradiation, $\text{Btu/h} \cdot \text{ft}^2$
$I_{d\theta}$	= diffuse component of solar radiation from sky, $\text{Btu/h} \cdot \text{ft}^2$
I_r	= reflected shortwave radiation, $\text{Btu/h} \cdot \text{ft}^2$
I_{ref}	= reference solar irradiance, typically $317 \text{ Btu/h} \cdot \text{ft}^2$
IS	= minimum inter-row spacing, ft
I_{STC}	= solar irradiance under standard testing conditions, $317 \text{ Btu/h} \cdot \text{ft}^2$
$I_{t\theta}$	= total solar irradiation of terrestrial surface or collector, $\text{Btu/h} \cdot \text{ft}^2$
L	= monthly total heating load for space heating and hot water, Btu

LCR	=	load collector ratio; net load coefficient divided by projected collector area, $\text{Btu/ft}^2 \cdot ^\circ\text{F} \cdot \text{day}$
LST	=	local standard time, decimal h
m	=	air mass; $= 1.0/\sin \beta$ at sea level and 0 outside earth's atmosphere; also fluid flow rate, lb/h
\dot{m}	=	fluid flow rate, lb/h
N	=	day of year, with January 1 = 1; also number of days in month
NLC	=	net load coefficient, $\text{Btu/}^\circ\text{F} \cdot \text{day}$
N_{mod}	=	number of PV panels required
P_{el}	=	electrical output of the PV system, W
P_{mod}	=	electrical output of the PV modules, W
P_{STC}	=	power rating of module under standard testing conditions, W
q_{Rat}	=	downward radiation from atmosphere, $\text{Btu/h} \cdot \text{ft}^2$
q_{Rs}	=	longwave radiation emitted by surface on earth, $\text{Btu/h} \cdot \text{ft}^2$
q_u	=	useful heat gained by collector per unit of aperture area, $\text{Btu/h} \cdot \text{ft}^2$
R_{net}	=	net radiative cooling rate of horizontal surface, $\text{Btu/h} \cdot \text{ft}^2$
S	=	total downward radiant heat flux from atmosphere, $\text{Btu/h} \cdot \text{ft}^2$
SH	=	PV shadow length, ft
SHD	=	sun hours per day, h
SLR	=	solar energy absorbed divided by building heating load
SSF	=	solar savings fraction
t_a	=	temperature of atmosphere, dry-bulb temperature, or average ambient temperature, $^\circ\text{F}$
\bar{T}_a	=	monthly average ambient temperature, $^\circ\text{F}$
t_{abs}	=	temperature of absorber, $^\circ\text{F}$
T_{at}	=	ground-level dry-bulb temperature, $^\circ\text{R}$
T_{back}	=	back-surface PV module temperature, $^\circ\text{F}$
T_{base}	=	base temperature, $^\circ\text{F}$
T_{cell}	=	operating cell temperature, $^\circ\text{F}$
t_{fe}, t_{fi}	=	temperatures of fluid leaving and entering collector, respectively, $^\circ\text{F}$
TLC	=	total load coefficient, $\text{Btu/}^\circ\text{F} \cdot \text{day}$
t_p	=	temperature of absorber plate, $^\circ\text{F}$
T_{rad}	=	absolute temperature of horizontal surface, $^\circ\text{R}$
t_{ref}	=	reference temperature, $^\circ\text{F}$
T_s	=	absolute temperature of surface, $^\circ\text{R}$
T_{sky}	=	apparent sky temperature, $^\circ\text{R}$
U_L	=	overall heat loss coefficient, $\text{Btu/h} \cdot \text{ft}^2 \cdot ^\circ\text{F}$
U_{met}	=	wind speed measured at standard 33 ft height, mph
U_{wind}	=	wind speed measured near collector's surface, mph
X	=	reference collector loss divided by heating load
Y	=	absorbed solar energy divided by heating load

Greek

α	=	absorptance
β	=	sun's altitude above horizon, degrees
γ	=	surface-solar azimuth, degrees
δ	=	solar declination, degrees
$\Delta\theta$	=	total number of hours in month
ΔT	=	temperature difference between the cell and the module back-surface at an irradiance level of 317 $\text{Btu/h} \cdot \text{ft}^2$
ε	=	nonspectral emittance of horizontal surface; about 0.9 for most nonmetallic construction materials
η	=	collector's electrical or thermal efficiency as specified
η_{ref}	=	electrical efficiency under reference conditions, available through manufacturer's data sheet for solar module
θ	=	solar incident angle, degrees
$\mu_{p,mp}$	=	temperature coefficient at maximum power point, $^\circ\text{F}^{-1}$
$\rho\Gamma$	=	reflectance of concentrator surface times fraction of reflected or refracted radiation that reaches absorber

σ	=	Stefan-Boltzmann constant, $0.1712 \times 10^{-8} \text{ Btu/h} \cdot \text{ft}^2 \cdot ^\circ\text{R}^4$
Σ	=	tilt angle of surface, measured from horizontal, degrees
τ	=	transmittance
$(\tau\alpha)$	=	monthly average transmittance-absorptance product
$(\tau\alpha)_n$	=	normal transmittance-absorptance product
$(\tau\alpha)_\theta$	=	transmittance τ of cover times absorptance α of plate at prevailing incident angle θ
ϕ	=	solar azimuth, degrees
ψ	=	surface azimuth, degrees

REFERENCES

- ASHRAE members can access *ASHRAE Journal* articles and ASHRAE research project final reports at technologyportal.ashrae.org. Articles and reports are also available for purchase by nonmembers in the online ASHRAE Bookstore at www.ashrae.org/bookstore.
- Argiriou, A., M. Santamouris, C.A. Balaras, and S. Jeter. 1993. Potential of radiative cooling in southern Europe. *International Journal of Solar Energy* 13(3):189-203.
- ASCE. 2003. Minimum design loads for buildings and other structures. *ANSI/ASCE Standard 7-2003*. American Society of Civil Engineers, Reston, VA.
- ASCE. 1991. Specification for the design of cold-formed stainless steel structural members. *ANSI/ASCE Standard 8-91*. American Society of Civil Engineers, Reston, VA.
- ASCE. 1994. Standard practice for construction and inspection of composite slabs. *ANSI/ASCE Standard 9-94*. American Society of Civil Engineers, Reston, VA.
- ASHRAE. 1983. *Solar domestic and service hot water manual*.
- Athienitis, A.K., and M. Santamouris, eds. 2002. *Thermal analysis and design of passive solar buildings*. James and James, London.
- Bai, Y., G. Fraisse, F. Wurtz, A. Foggia, Y. Deless, and F. Domain. 2011. Experimental and numerical study of a directly PV-assisted domestic hot water system. *Solar Energy* 85(9):1979-1991.
- Balaras, C.A., E. Dascalaki, P. Tsekouras, and A. Aidonis. 2010. High solar combi systems in Europe. *ASHRAE Transactions* 116(1):408-415.
- Balcomb, J.D., J.C. Hedstrom, and R.D. McFarland. 1977. Thermal storage walls in New Mexico. *Solar Age* 2(8):20-23.
- Balcomb, J.D., R.W. Jones, R.D. McFarland, and W.O. Wray. 1982. Expanding the SLR method. *Passive Solar Journal* 1(2):67-90.
- Balcomb, J.D., R.W. Jones, R.D. McFarland, and W.O. Wray. 1984. *Passive solar heating analysis: A design manual*. ASHRAE.
- Barley, C.D., and C.B. Winn. 1978. Optimal sizing of solar collectors by the method of relative areas. *Solar Energy* 21(4):279-289.
- Barron-Gafford, G.A., R.L. Minor, N.A. Allen, A.D. Cronin, A.E. Brooks, and M.A. Pavao-Zuckerman. 2016. The photovoltaic heat island effect: Larger solar power plants increase local temperatures. *Nature: Scientific Reports* 35070. [dx.doi.org/10.1038/srep35070](https://doi.org/10.1038/srep35070).
- Beckman, W.A., S.A. Klein, and J.A. Duffie. 1977. *Solar heating design by the f-Chart method*. John Wiley, New York.
- Beckman, W.A., S.A. Klein, and J.A. Duffie. 1981. Performance predictions for solar heating systems. In *Solar energy handbook*, J.F. Kreider and F. Kreith, eds. McGraw Hill, New York.
- Bliss, R.W. 1961. Atmospheric radiation near the surface of the earth. *Solar Energy* 59(3):103.
- Clark, G. 1981. Passive/hybrid comfort cooling by thermal radiation. *Proceedings of the International Passive and Hybrid Cooling Conference*. American Section of the International Solar Energy Society, Miami Beach, FL.
- Cole, R.L., A.J. Gorski, R.M. Graven, W.R. McIntire, W.W. Schertz, R. Winston, and S. Zwerdling. 1977. Applications of compound parabolic concentrators to solar energy conversion. *Report AMLw42*. Argonne National Laboratory, Chicago.
- CPUC. 2020. *California solar initiative, annual program assessment*. California Public Utilities Commission. tinyurl.com/CPUC2020.
- Cromer, C.J. 1984. *Design of a DC-pump, photovoltaic-powered circulation system for a solar domestic hot water system*. Florida Solar Energy Center, Cocoa.
- Dickinson, W.C., and P.N. Cheremisinoff, eds. 1980. *Solar energy technology handbook, Part B: Application, systems design and economics*. Marcel Dekker, New York.
- DOE. 1978a. *SOLCOST—Solar hot water handbook; A simplified design method for sizing and costing residential and commercial solar service hot water systems*, 3rd ed. DOE/CS-0042/2. U.S. Department of Energy.
- DOE. 1978b. *DOE facilities solar design handbook*. DOE/AD-0006/1. U.S. Department of Energy.
- DOE. 1980/1982. *Passive solar design handbooks*, vols. 2 and 3, *Passive solar design analysis*. DOE Reports/CS-0127/2 and CS-0127/3. January, July. U.S. Department of Energy.

- Duffie, J.A., and W.A. Beckman. 2006. *Solar thermal energy processes*, 3rd ed. Wiley Interscience, New York.
- Erell, E., and Y. Etzion. 2000. Radiative cooling of buildings with flat-plate solar collectors. *Building and Environment* 35(4):297-305.
- Evans, D.L. 1981. Simplified method for predicting photovoltaic array output. *Solar Energy* 27:555-560.
- FAA. 2018. *Technical guidance for evaluating selected solar technologies on airports*. Washington, D.C. www.faa.gov/sites/faa.gov/files/airports/environmental/FAA-Airport-Solar-Guide-2018.pdf.
- Feldman, S.J., and R.L. Merriam. 1979. Building energy analysis computer programs with solar heating and cooling system capabilities. Arthur D. Little, Inc. Report EPRIER-1146 (August) to the Electric Power Research Institute.
- Fernandez-Gonzalez, A. 2007. Analysis of the thermal performance and comfort conditions produced by five different passive solar heating strategies in the United States midwest. *Solar Energy* 81:581-593.
- Freeman, T.L., J.W. Mitchell, and T.E. Audit. 1979. Performance of combined solar-heat pump systems. *Solar Energy* 22(2):125-135.
- Gates, D.M. 1966. Spectral distribution of solar radiation at the earth's surface. *Science* 151(3710):523-529.
- Givoni, B. 1981. Experimental studies on radiant and evaporative cooling of roofs. *Proceedings of the International Passive and Hybrid Cooling Conference*. American Section of the International Solar Energy Society, Miami Beach, FL.
- Gueymard, C., and D. Thevenard. 2013. Revising ASHRAE climatic data for design and standards—Part 2: Clear-sky solar radiation model. *ASHRAE Transactions* 119(2).
- Hay, H.R., and J.I. Yellott. 1969. Natural air conditioning with roof ponds and movable insulation. *ASHRAE Transactions* 75(1):165-177.
- Henning, H.-M. 2007. *Solar assisted air-conditioning in buildings—A handbook for planners*, 2nd ed. Springer-Verlag, Vienna.
- Hottel, H.C., and B.B. Woertz. 1942. The performance of flat-plate solar collectors. *Transactions of ASME* 64:91-103.
- Howard, B.D. 1986. Air core systems for passive and hybrid energy-conserving buildings. *ASHRAE Transactions* 92(2B):815-830.
- Howard, B.D., and E.O. Pollock. 1982. *Comparative report—Performance of passive solar heating systems*. Vitro Corp. U.S. DOE National Solar Data Program, Oak Ridge, TN.
- Howard, B.D., and D.H. Saunders. 1989. Building performance monitoring—The thermal envelope perspective—Past, present, and future. Thermal Performance of the Exterior Envelopes of Buildings IV, ASHRAE.
- HUD. 1977. *Intermediate minimum property standards supplement for solar heating and domestic hot water systems*. SD Cat. No. 0-236-648. U.S. Department of Housing and Urban Development.
- Hunn, B.D., N. Carlisle, G. Franta, and W. Kolar. 1987. *Engineering principles and concepts for active solar systems*. SERI/SP-271-2892. Solar Energy Research Institute, Golden, CO.
- Hunt, J.D., B. Zakeri, A. Nascimento, B. Garnier, M.G. Pereira, R.A. Bellezoni, N. de Assis Brasil Weber, P. Smith Schneider, P.P. Bezerra Machado, and D. Soares Ramos. 2020. High velocity seawater air-conditioning with thermal energy storage and its operation with intermittent renewable energies. *Energy Efficiency* 13:1825-1840. [dx.doi.org/10.1007/s12053-020-09905-0](https://doi.org/10.1007/s12053-020-09905-0).
- IEA. 2002. *Solar combisystems*. International Energy Agency Task 26. task26.iea-shc.org/.
- IEA. 2010. *Solar air-conditioning and refrigeration. Solar heating and cooling programme*. International Energy Agency Task 38. task38.iea-shc.org/.
- IEA. 2022. *Market reports*. International Energy Agency PVPS. iea-pvps.org/publications/market-reports/.
- IEA. 2022. *Solar heat worldwide*. International Energy Agency SHC. www.iea-shc.org/solar-heat-worldwide.
- IPCC. 2012. *Renewable energy sources and climate change mitigation*. Special Report of the Intergovernmental Panel on Climate Change: Summary for Policymakers and Technical Summary. Cambridge University Press.
- ISO. 2017. Solar energy—Solar thermal collectors—Test methods. *Standard* 9806:2017. International Organization for Standardization, Geneva.
- Jordan, R.C., and B.Y.H. Liu, eds. 1977. Applications of solar energy for heating and cooling of buildings. ASHRAE Publication GRP 170.
- Kapsis, K. 2016. *Modelling, design and experimental study of semi-transparent photovoltaic windows for commercial building applications*. Concordia University, Montreal.
- Kilkis, B., M. Çaglar, and M. Sengul. 2021. Energy benefits of heat pipe technology for achieving 100% renewable heating and cooling for fifth-generation, low-temperature district heating systems. *Energies* 14(17):5398.
- Kim, J.-H., J.-S. Yu, and J.-T. Kim. 2021. An experimental study on the energy and exergy performance of an air-type pvt collector with perforated baffle. *Energies* 14 (10): 2919.
- King, D.L., W.E. Boyson, and J.A. Kratochvil. 2004. Photovoltaic array performance model. Report SAND2004-3535. Sandia National Laboratories, Albuquerque, NM, and Livermore, CA.
- Klein, S.A., and W.A. Beckman. 1979. A general design method for closed-loop solar energy systems. *Solar Energy* 22(3):269-282.
- Klein, S.A., and D.T. Reindl. 2005. Solar refrigeration. *ASHRAE Journal* 47(9):S26-S30.
- Klein, S.A., W.A. Beckman, and J.A. Duffie. 1976. TRNSYS—A transient simulation program. *ASHRAE Transactions* 82(1):623-633.

- Kutscher, C.F. 1996. *Proceedings of the 19th World Energy Engineering Congress*, Atlanta.
- LBL. 1981. *DOE-2 reference manual version 2.1A*. Los Alamos Scientific Laboratory, LA-7689-M, Version 2.1A. Lawrence Berkeley Laboratory, LBL-8706 Rev. 2.
- Lister, L., and T. Newell. 1989. *Expansion tank characteristics of closed loop, active solar energy collection systems; Solar engineering—1989*. American Society of Mechanical Engineers, New York.
- Lund, H. 2014. *Renewable energy systems: A smart energy systems approach to the choice and modeling of 100% renewable solutions*, 2nd ed. Elsevier.
- Lunde, P.J. 1980. *Thermal engineering*. John Wiley & Sons, New York.
- Marion, B., J. Adelstein, K. Boyle, H. Hayden, B. Hammond, T. Fletcher, B. Canada, D. Narang, A. Kimber, L. Mitchell, and G. Rich. 2005. Performance parameters for grid-connected PV systems. *Proceedings 31st IEEE Photovoltaics Specialists Conference*, pp. 1601-1606.
- Marlatt, W., C. Murray, and S. Squire. 1984. Roofpond systems energy technology engineering center. Rockwell International, *Report ETEC6*.
- Martin, M., and P. Berdahl. 1984. Characteristics of infrared sky radiation in the United States. *Solar Energy* 33(3/4):321-336.
- Mazria, E. 1979. *The passive solar energy book*. Rodale, Emmaus, PA.
- Mitchell, D., and K.L. Biggs. 1979. Radiative cooling of buildings at night. *Applied Energy* 5:263-275.
- Monsen, W.A., S.A. Klein, and W.A. Beckman. 1981. Prediction of direct gain solar heating system performance. *Solar Energy* 27(2):143-147.
- Monsen, W.A., S.A. Klein, and W.A. Beckman. 1982. The un-utilizability design method for collector-storage walls. *Solar Energy* 29(5):421-429.
- Morehouse, J.H., and P.J. Hughes. 1979. Residential solar-heat pump systems: Thermal and economic performance. *Paper 79-WA/SOL-25*, ASME Winter Annual Meeting, New York.
- NASA. 2022. *Solar irradiance*. www.earthdata.nasa.gov/topics/atmosphere/atmospheric-radiation/solar-irradiance.
- NOAA. 2010. U.S. climate atlas. www.ncdc.noaa.gov/climateatlas/.
- Nordham, D. 1981. *Microcomputer methods for solar design and analysis*. Solar Energy Research Institute, SERI-SP-722-1127.
- NREL. 1990. Solar radiation data manual for flat-plate and concentrating collectors. redc.nrel.gov/solar/pubs/redbook/.
- Pittenger, A.L., W.R. White, and J.I. Yellott. 1978. A new method of passive solar heating and cooling. *Proceedings of the Second National Passive Systems Conference*, Philadelphia, ISES and DOE.
- REHVA. 2004. Chilled beam application guidebook. *Guidebook 5*. Federation of European Heating, Ventilation and Air Conditioning Associations.
- REHVA. 2010. Solar shading. *Guidebook 12*. Federation of European Heating, Ventilation and Air Conditioning Associations.
- REHVA. 2013. Low temperature heating and high temperature cooling—Embedded water based surface heating and cooling systems. *Guidebook 7*. Federation of European Heating, Ventilation and Air Conditioning Associations.
- Reitan, C.H. 1963. Surface dew point and water vapor aloft. *Journal of Applied Meteorology* 2(6):776-779.
- Root, D.E., S. Chandra, C. Cromer, J. Harrison, D. LaHart, T. Merrigan, and J.G. Ventre. 1985. *Solar water and pool heating course manual*, 2 vols. Florida Solar Energy Center, Cocoa.
- Salih, S.M., and M.Q. Taha. 2013. Analysis of shading impact factor for photovoltaic modules. *Center of Desert Conference Proceedings, University of Anbar, Iraq*, 2.
- Scharmer, K., and J. Grief. 2000. *The European solar radiation atlas*. Les Presses de l'École des Mines, Paris.
- Schnurr, N.M., B.D. Hunn, and K.D. Williamson. 1981. The solar load ratio method applied to commercial buildings active solar system sizing. *Proceedings of the ASME Solar Energy Division Third Annual Conference on System Simulation*, Economic Analysis/Solar Heating and Cooling Operational Results, Reno, NV.
- Shukla, A., D.N. Nkwetta, Y.J. Cho, V. Stevenson, and P. Jones. 2012. A state of art review on the performance of transpired solar collector. *Renewable and Sustainable Energy Reviews* 16(6):3975-3985.
- Simon, F.F. 1976. Flat-plate solar collector performance evaluation with a solar simulator as a basis for collector selection and performance prediction. *Solar Energy* 18(5):451-466.
- Svard, C.D., J.W. Mitchell, and W.A. Beckman. 1981. Design procedure and applications of solar-assisted series heat pump systems. *Journal of Solar Energy Engineering* 103(5):135-143.
- Swartman, R.K., V. Ha, and A.J. Newton. 1974. Review of solar-powered refrigeration. *Paper 73-WA/SOL-6*. American Society of Mechanical Engineers, New York.
- Swift, J.M., and T. Lawrence, eds. 2013. *ASHRAE greenguide: Design, construction, and operation of sustainable buildings*, 4th ed.
- Thekaekara, M.P. 1973. Solar energy outside the earth's atmosphere. *Solar Energy* 14(2):109-127.
- Thevenard, D., and C. Gueymard. 2010. Updating the ASHRAE climatic data for design and standards (RP-1453). *ASHRAE Transactions* 116(2): 444-459.
- Threlkeld, J.L., and R.C. Jordan. 1958. Direct radiation available on clear days. *ASHRAE Transactions* 64:45-68.
- Torcellini, P., and S. Pless. 2004. Trombe walls in low-energy buildings: Practical experiences. *Report NREL/CP-550-36277*.

- Trombe, F., J.F. Robert, M. Caloanet, and B. Sesolis. 1977. Concrete walls for heat. *Solar Age* 2(8):13.
- Weiss, W., and M. Spork-Dur. 2017. *Solar heat worldwide: Global market development and trend in 2017*. IEA Solar Heating and Cooling Programme.
- Whillier, A. 1964. Thermal resistance of the tube-plate bond in solar heat collectors. *Solar Energy* 8(3):95.
- Wilson, A.T. 1979. *Thermal storage wall design manual*. New Mexico Solar Energy Association, Albuquerque.
- Yellott, J.I. 1977. Passive solar heating and cooling systems. *ASHRAE Transactions* 83(2):429-445.
- Yellott, J.I., D. Aiello, G. Rand, and M.Y. Kung. 1976. *Solar-oriented architecture*. Arizona State University Architecture Foundation, Tempe.
- Zehndorfer Eng. 2021. *Solar glare analysis at Vienna Airport helps avoid glaring hazard for the tower*, www.zehndorfer.at/en/news-en/14-news/71-news-glare-viennaairport-en.

BIBLIOGRAPHY

- Abdulla, S.H., S.A. Klein, and W.A. Beckman. 2000. *A new correlation for the prediction of the frequency distribution of daily solar radiation*. American Solar Energy Society, Boulder, CO.
- ASHRAE. 2011. Standard for the design of high-performance green buildings except low-rise residential buildings. ANSI/ASHRAE/USGBC/IES *Standard* 189.1.
- ASTM. 2014. Standard solar constant and zero air mass solar spectral irradiance tables. *Standard* E490-00a. American Society for Testing and Materials, West Conshohocken, PA.
- ASTM. 2012. Standard guide for fire prevention for photovoltaic panels, modules, and systems. *Standard* E2908-12. American Society for Testing and Materials, West Conshohocken, PA.
- ASTM. 2013. Standard practice for determining reporting conditions and expected capacity for photovoltaic non-concentrator systems. *Standard* E2939-13. American Society for Testing and Materials, West Conshohocken, PA.
- ASTM. 2013. Standard practice for installation of roof mounted photovoltaic arrays on steep-slope roofs. *Standard* E2766-13. American Society for Testing and Materials, West Conshohocken, PA.
- ASTM. 2013. Standard test method for reporting photovoltaic non-concentrator system performance. *Standard* E2848-13. American Society for Testing and Materials, West Conshohocken, PA.
- ASTM. 2015. Standard practice for installation, commissioning, operation, and maintenance process (ICOMP) of photovoltaic arrays. *Standard* E3010-15. American Society for Testing and Materials, West Conshohocken, PA.
- Athienitis, A., and W. O'Brien, eds. 2015. *Modeling, design, and optimization of net-zero energy buildings*. John Wiley & Sons, Hoboken, NJ.
- Badescu, V., C.A. Gueymard, S. Cheval, C. Oprea, M. Baci, A. Dumitrescu, F. Iacobescu, I. Milos, and C. Rada. 2012. Computing global and diffuse solar hourly irradiation on clear sky. Review and testing of 54 models. *Renewable and Sustainable Energy Reviews* 16(3):1636-1656.
- Brook, W., and J. Dunlop. 2013. *Photovoltaic (PV) installation professional resource guide*. North American Board of Certified Energy Practitioners, New York, NY.
- Candanedo, L., A. Athienitis, and K. Park. 2011. Convective heat transfer coefficients in a building-integrated photovoltaic/thermal system. *Journal of Solar Energy Engineering* 133(2).
- Cook, J., ed. 2000. *Passive cooling*, 2nd ed. MIT, Cambridge, MA.
- CSA. 2012. Solar photovoltaic rooftop-installation best practices guideline. *Standard* SPE-900-13. Canadian Standards Association, Mississauga, ON.
- Cunningham, J., P. Hernday, and J. Mokri. 2014. Commissioning for PV performance. *Report* D42039-1. SunSpec Alliance, San Jose, CA.
- Cunningham, J., P. Hernday, and J. Mokri. 2014. *PV system performance assessment*. SunSpec Alliance, San Jose, CA.
- Delisle, V., and M. Kummert. 2016. Cost-benefit analysis of integrating BIPV-T air systems into energy-efficient homes. *Solar Energy* 136:385-400.
- Dierauf, T., A. Growitz, S. Kurtz, J.L.B. Cruz, E. Riley, and C. Hansen. 2013. Weather-corrected performance ratio. *Report* NREL/TP-5200-57991. National Renewable Energy Laboratory (NREL), Golden, CO.
- Doyle, C., A. Truitt, D. Inda, R. Lawrence, Lockhard, R., and M. Golden. 2015. SAPC best practices in PV system installation. *Report* NREL/LGG-5-42199-01. National Renewable Energy Laboratory, Golden, CO.
- Drosou, V.N., P.D. Tsekouras, T.I. Oikonomou, P. I. Kosmopoulos, C.S. Karytsas. 2014. The HIGH-COMBI project: High solar fraction heating and cooling systems with combination of innovative components and methods. *Renewable and Sustainable Energy Reviews* 29:463-472. doi.org/10.1016/j.rser.2013.08.019.
- Eicker, U. 2014. *Energy efficient buildings with solar and geothermal resources*. John Wiley & Sons, Hoboken, NJ.
- Endecon Engineering. 2001. A guide to photovoltaic (PV) system design and installation. *Report* 500-01-020. California Energy Commission, Sacramento, CA.
- Eyzaguirre, C., and J. Mankey, eds. 2014. *California solar permitting guidebook*. The Governor's Office of Planning and Research, Sacramento, CA.
- Häberlin, H. 2012. *Photovoltaics: System design and practice*. John Wiley & Sons, Hoboken, NJ.

- Hwang, Y., R. Radermacher, A. Alalili, and I. Kubo. 2008. Review of solar cooling technologies. *HVAC&R Research* (now *Science and Technology for the Build Environment*) 14(3):507-525.
- Grossman, G. 2002. Solar-powered systems for cooling, dehumidification and air conditioning. *Solar Energy* 72(1):53-62.
- IEA. 2004. *Solar assisted air conditioning of buildings*. International Energy Agency Task 25. task25.iea-shc.org/.
- IEA. 2013. *Solar and heat pump systems*. International Energy Agency Task 44. task44.iea-shc.org/.
- IEC. 2004. Photovoltaic (PV) stand alone systems—Design verification. *Standard* 62124:2004. International Electrotechnical Commission, Geneva.
- IEC. 2015. Photovoltaic (PV) array—On-site measurement of current-voltage characteristics. *Standard* 61829:2015. International Electrotechnical Commission, Geneva.
- IEC. 2016. Photovoltaic (PV) arrays—Design requirements. *Standard* 62548:2016. International Electrotechnical Commission, Geneva.
- IEC. 2016. Photovoltaic (PV) systems—Requirements for testing, documentation and maintenance—Part 1, 2 and 3. *Standard* 62446:2016. International Electrotechnical Commission, Geneva.
- IEC. 2016. Low-voltage electrical installations—Part 6: Verification. *Standard* 60364-6:2016. International Electrotechnical Commission, Geneva.
- IEC. 2017. Photovoltaic system performance—Part 1, 2 and 3. *Standard* IEC 61724:2017. International Electrotechnical Commission, Geneva, CH.
- JRC. 2016. *Photovoltaic geographical information system (PVGIS)*. Joint Research Centre, European Commission. ec.europa.eu/jrc/en/scientific-tool/pvgis.
- Kaplanis, S.N. 2006. New methodologies to estimate the hourly global solar radiation: Comparisons with existing models. *Renewable Energy* 31(6): 781-790.
- Klein, S.A., and W.A. Beckman. 2001. *PV f-chart: Photovoltaic system analysis software; User's manual*. F-Chart Software, Middleton, WI.
- Lawrence, T., A.K. Darwich, and J.K. Means, eds. 2013. *ASHRAE greenguide: Design, construction, and operation of sustainable buildings*, 4th ed.
- NREL. 2018. Solar resource data and tools. National Renewable Energy Laboratory. www.nrel.gov/grid/solar-resource/renewable-resource-data.html.
- OAFC and CANSIA. 2014. *Solar electricity safety handbook for firefighters*. Canadian Solar Industry Association Ottawa, ON.
- Palyvos, J. 2008. A survey of wind convection coefficient correlations for building envelope energy systems' modeling. *Applied Thermal Engineering* 28:801-808.
- Solarcombi+. 2010. Identification of most promising markets and promotion of standardised system configurations for the market entry of small scale combined solar heating & cooling applications. *Final Report*. Intelligent Energy Europe programme, European Commission, Brussels. ec.europa.eu/energy/intelligent/projects/en/projects/solar-combi.
- Solar Energy Research Institute. 1981. Solar radiation energy resource atlas of the United States. *Report* SERI/SP642-1037. Golden, CO.
- Theologitis, I.T. 2016. *O&M best practices guidelines*. Solar Power Europe, Brussels, BE.
- Thevenard, D., and S. Pelland. 2013. Estimating the uncertainty in long-term photovoltaic yield predictions. *Solar energy*, 91:432-445.
- Weiss, W., ed. 2003. *Solar heating for houses: A design handbook for solar combisystems*. International Energy Agency, James & James, Ltd., London.
- Whaley, C. 2016. Best practices in photovoltaic system operations and maintenance. *Report* NREL/TP-7A40-67553. National Renewable Energy Laboratory, Golden, CO.
- WMO. 2014. *Home page*. World Meteorological Organization, Geneva, Switzerland. www.wmo.int.

The preparation of this chapter is assigned to TC 6.7, Solar Energy Utilization.